AN INVESTIGATION OF THE STRUCTURAL PROPERTIES OF STABILIZED LAYERS IN FLEXIBLE PAVEMENT SYSTEMS

W. R. Barker, et al

Army Engineer Waterways Experiment Station
Vicksburg, Massachusetts

October 1973

DISCLAIMER NOTICE

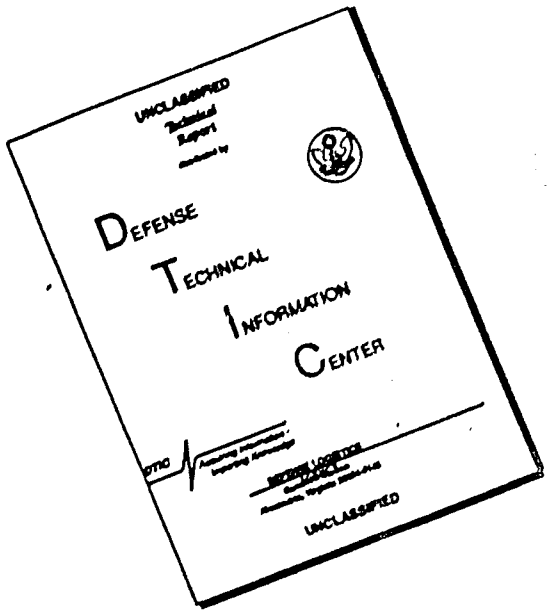

THIS DOCUMENT IS BEST QUALITY AVAILABLE. THE COPY FURNISHED TO DTIC CONTAINED A SIGNIFICANT NUMBER OF PAGES WHICH DO NOT REPRODUCE LEGIBLY.

UNCLASSIFIED
Security Classification

AD-769 292

DOCUMENT CONTROL DATA - R & D

(Security classification of title, body of abstract and indexing annotation must be entered when the overall report is classified)

1. ORIGINATING ACTIVITY (Corporate author)
US Army Engineers Waterways Experiment Station
Vicksburg, Mississippi 39181

2a. REPORT SECURITY CLASSIFICATION
UNCLASSIFIED

2b. GROUP

3. REPORT TITLE
AN INVESTIGATION OF THE STRUCTURAL PROPERTIES OF STABILIZED LAYERS IN FLEXIBLE PAVEMENT SYSTEMS

4. DESCRIPTIVE NOTES (Type of report and inclusive dates)
February 1971-August 1973

5. AUTHOR(S) (First name, middle initial, last name)
W. R. Barker; W. N. Brabston; F. C. Townsend

6. REPORT DATE	7a. TOTAL NO. OF PAGES	7b. NO OF REFS
October 1973	166	29

8a. CONTRACT OR GRANT NO.	F29601-71-X-0008	9a. ORIGINATOR'S REPORT NUMBER(S)	
b. PROJECT NO.	683M		AFWL-TR-73-21
c. Task No.	4	9b. OTHER REPORT NO(S) (Any other numbers that may be assigned this report)	
d.			

10. DISTRIBUTION STATEMENT
Approved for public release; distribution Unlimited.

11. SUPPLEMENTARY NOTES	12. SPONSORING MILITARY ACTIVITY
	AFWL (DEZ) Kirtland AFB, NM 87117

13. ABSTRACT

(Distribution Limitation Statement A)

In recent years mechanistic models have been advocated as a tool for predicting the performance of pavement systems under aircraft traffic. In the investigation reported herein, layered elastic and nonlinear finite element models were used to determine the benefit of stabilized layers within a pavement system. The performance of several types of pavement structures that were constructed and trafficked under controlled conditions at the US Army Engineer Waterways Experiment Station were analyzed with respect to predicted response, measured response, and manifestation of traffic distress in the pavement systems. From the analysis, relationships were developed between pavement life and predicted response such that the benefit of the use of stabilized materials within a pavement system could be examined based on the influence which the material would have on the predicted life of the pavement system.

DD FORM 1 NOV 68 1473

UNCLASSIFIED
Security Classification

14. KEY WORDS	LINK A		LINK B		LINK C	
	ROLE	WT	ROLE	WT	ROLE	WT
Civil engineering Airfields Soil mechanics Flexible pavement Soil stabilizations						

AFWL-TR-73-21

AIR FORCE WEAPONS LABORATORY
Air Force Systems Command
Kirtland Air Force Base
New Mexico 87117

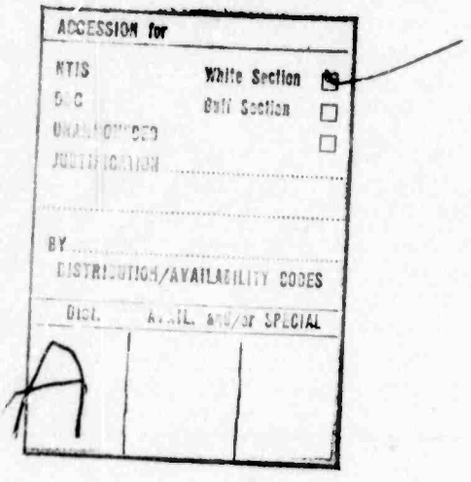

AN INVESTIGATION OF THE STRUCTURAL PROPERTIES OF STABILIZED LAYERS IN FLEXIBLE PAVEMENT SYSTEMS

W. R. Barker
W. N. Brabston
F. C. Townsend
US Army Engineer Waterways Experiment Station
Vicksburg, MS 39181

TECHNICAL REPORT NO. AFWL-TR-73-21

FOREWORD

This report was prepared by the US Army Engineer Waterways Experiment Station, Vicksburg, Mississippi, under Project Order F29601-71-X-0008. The research was performed under Program Element 63723F, Project 683M, Task 4.

Inclusive dates of research were Feburary 1971 through August 1973. The report was submitted 19 September 1973 by the Air Force Weapons Laboratory Project Officer, Captain Richard A. Weismiller (DEZ).

The investigation reported herein was conducted under the overall supervision of Messers. J. P. Sale, R. G. Ahlvin, and R. L. Hutchinson. The principal investigators in research were Dr. W. R. Barker, Mr. W. N. Brabston, and Dr. F. C. Townsend. Mr. R. H. Ledbetter was responsible for collection and interpreting the instrumentation data utilized in the investigation. The data from the soil stabilization test section was interpreted by Mr. Ledbetter.

This technical report has been reviewed and is approved.

Richard A. Weismiller

RICHARD A. WEISMILLER
Captain, USAF
Project Officer

OREN G. STROM
Lt Colonel, USAF
Chief, Aerospace Facilities Branch

William B. Liddicoet

WILLIAM B. LIDDICOET
Colonel, USAF
Chief, Civil Engineering Research Division

ABSTRACT

(Distribution Limitation Statement A)

In recent years mechanistic models have been advocated as a tool for predicting the performance of pavement systems under aircraft traffic. In the investigation reported herein, layered elastic and nonlinear finite element models were used to determine the benefit of stabilized layers within a pavement system. The performances of several types of pavement structures that were constructed and trafficked under controlled conditions at the U. S. Army Engineer Waterways Experiment Station were analyzed with respect to predicted response, measured response, and manifestation of traffic distress in the pavement systems.

From the analysis, relationships were developed between pavement life and predicted response such that the benefit of the use of stabilized materials within a pavement system could be examined based on the influence which the material would have on the predicted life of the pavement system.

CONTENTS

CONTENTS (Cont'd)

ILLUSTRATIONS

ILLUSTRATIONS (Cont'd)

ILLUSTRATIONS (Cont'd)

ILLUSTRATIONS (Cont'd)

ILLUSTRATIONS (Cont'd)

ILLUSTRAITONS (Cont'd)

TABLES

TABLES (Cont'd)

SECTION I

INTRODUCTION

1. OBJECTIVES

The initial objectives of this investigation were to compare known responses of full-scale flexible pavements of various composition with responses predicted by a layered elastic analytical model and to investigate possible correlations of pavement performance under traffic with actual or predicted critical response values. The objectives were later expanded to include analysis of pavement response predicted by other analytical models.

2. SCOPE

The objectives were accomplished by:

a. Examining data available from past pavement field tests conducted at the U. S. Army Engineer Waterways Experiment Station (WES) and selecting for analysis in the study those performance and response data that appeared to include information that would fulfill the objective of this study within established funding and time limitation.

b. Selecting and modifying the CHEVRON computer program as the layered elastic analytical model for initial analysis.

c. Determining or adopting expressions for modulus of elasticity E and Poisson's ratio ν of the materials included in the pavements under consideration.

d. Examining the predicted responses as determined by the CHEVRON program with known values, such as surface deflection and internal stress and strain, measured by sensors installed in the pavements.

e. Repeating the initial analysis for selected test pavements using two additional analytical models: the FEPAV II and AFPAV programs.

f. Defining critical response values and examining their relationships to pavement life.

3. BACKGROUND

Most current pavement design procedures involve one common feature: a degree of empiricism applied either totally or at some stage of the design procedure to compensate for inaccuracies or unknowns. In the past few years, however, many investigations have worked toward moving pavement design and analysis to the theoretical end of the spectrum. Development of a system based on a theoretically correct and totally reliable mechanistic concept would obviously be justified by providing the ultimate in economic design. Important advances in this area include the Shell and the Chevron methods that are based on the concept of a pavement being represented by multiple layers of linearly elastic material (references 1 and 2, respectively). Other investigators have approached pavement analysis using nonlinear elastic and viscoelastic theories. Much of the previous work, however, has been centered around laboratory characterization of the structural properties of component materials followed by assumptions of pavement response when the various materials are coupled in an actual pavement structure. In the investigation reported herein, the performances of several types of pavement structure that were constructed and trafficked under controlled conditions at the WES were analyzed. In this study the known responses of the pavement structures were examined with respect to predicted values determined from established mechanistic models.

A significant feature of this investigation was the availability of a broad data base of pavement response measurements, such as surface deflection and internal stress and strain values, of a wide variety of flexible pavements. These pavements were constructed and trafficked under several pavement

and stabilization investigation programs conducted earlier by the WES. During the conduct of these tests, voluminous data were collected on material strength, surface roughness and deflection, and internal stress and strain values, etc., for a variety of landing gear configurations and loadings. Complete tabulations of these data are contained in the reports covering the respective tests (references 3-5). Although all applicable response data were considered in conducting this analysis, generally only those considered pertinent are shown herein. The exception is Appendix I, which contains tabulations of strain values obtained from one of the test sections.

SECTION II

DESCRIPTION OF PAVEMENTS, LOADING, AND INSTRUMENTATION

1. GENERAL

The pavements analyzed in this study were constructed and trafficked at the WES as part of three separate field pavement studies: the multiple-wheel heavy gear load (MWHGL) pavement tests (reference 3), the bituminous-stabilized base course study (reference 4), and the evaluation of structural layers in flexible pavements (reference 5). All were studies of flexible pavements that were constructed on a low-strength, heavy clay subgrade. Of the 13 different pavement configurations involved in these tests, 11 are considered in this analysis. The individual pavements and their material composition are described in the following paragraphs. The test pavements were equipped with stress and strain sensors from which some of the field response values discussed in this analysis were obtained. All response values used in this report were obtained under static wheel loadings of the indicated landing gear assembly. Surface deflections used in this analysis were obtained using engineer levels, first with the load off the pavement and then with the test cart at a prearranged position on the pavement.

2. MWHGL TESTS

a. Pavements.

Pavements involved in these tests were of similar construction but varied in the thickness of the subbase course. Material composition of each pavement consisted of a 3-in.-thick wearing course of asphaltic concrete, a 6-in.-thick base course of crushed limestone, and a gravelly sand subbase course. Gradation and classification data for the base, subbase, and subgrade materials and for the aggregate component of the asphaltic concrete are shown

in figure 1. Of the five test items included in the original study, three were considered in this analysis. A longitudinal section of these items is shown in figure 2. As can be seen, items 1, 2, and 3 had total thicknesses of 15, 24, and 33 in., respectively, above the subgrade. Mix design data for the asphaltic concrete are shown in figure 3. A summary of field in-place CBR, water content, and dry density data for the granular materials and subgrade immediately after construction is given in table I. Properties of the asphaltic concrete wearing course as determined from field cores are shown in table II. The asphaltic concrete, base course, and subbase course materials were designed to conform to the requirements set forth in references 6-8.

b. Test Loads

Wheel and assembly loadings involved in the analysis of the MWHGL test section that were considered in the study reported herein are given below:

Configuration	Assembly Load, kips	Tire Pressure, psi	Contact Area, $in.^2$
12 wheel (C-5A)	360	100	285
Single-wheel	30	100	285
	50	165	285
	75	290	270

3. BITUMINOUS-STABILIZED BASE COURSE STUDY

a. Pavements

Four types of pavements were involved in this study (figure 4). Items 1 and 2 each had a total thickness of 15 in., and items 3 and 4 each were 24 in. thick. Item 1 consisted of a 3-in.-thick asphaltic concrete wearing course over a 12-in.-thick bituminous-stabilized base course. The asphaltic concrete wearing course was designed to conform to the specifications in reference 6. The base course consisted of a gravelly sand treated with

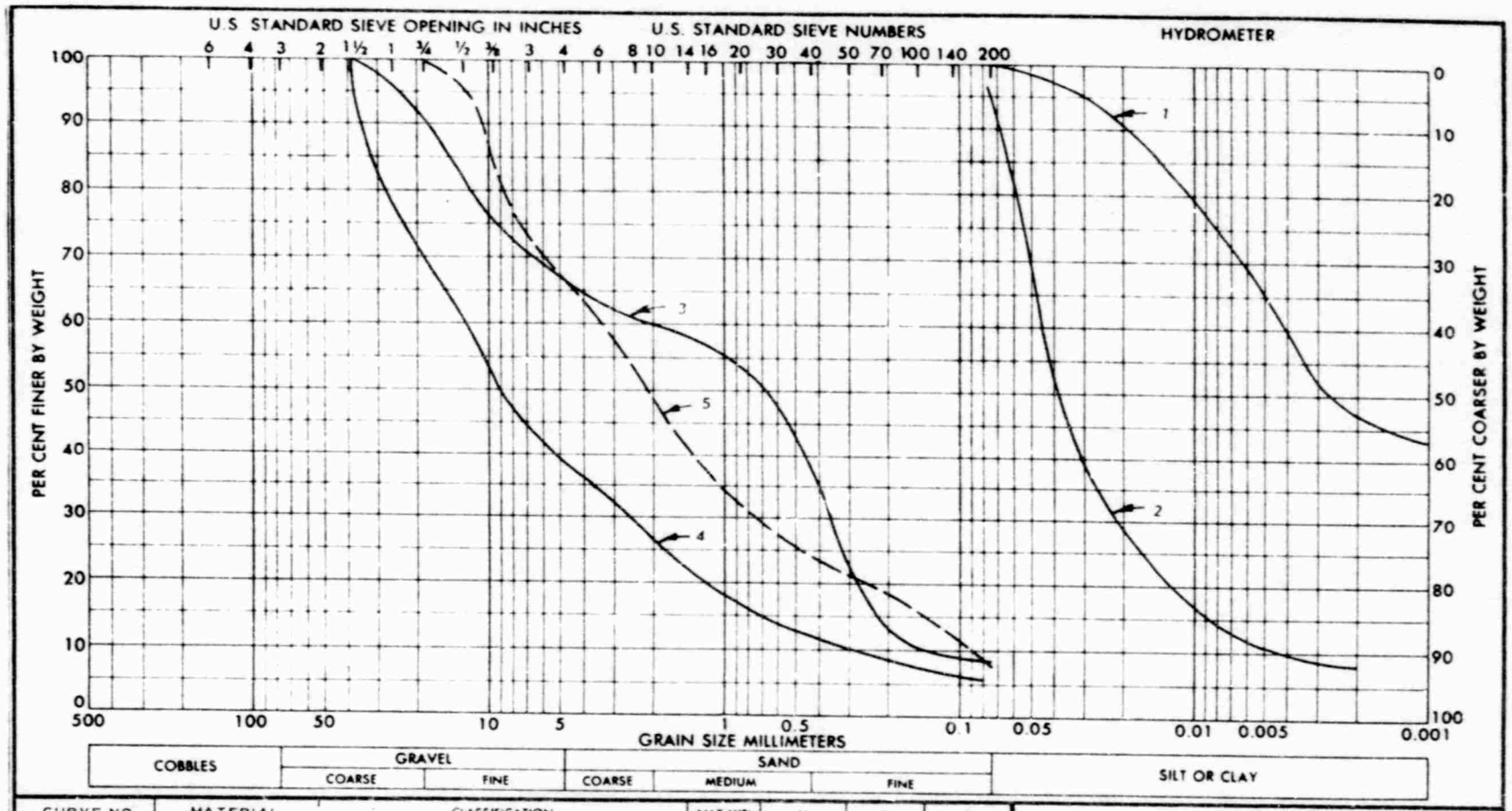

CURVE NO.	MATERIAL	CLASSIFICATION	NAT W%	LL	PL	PI
1	SUBGRADE	HEAVY CLAY (CH)		73	25	48
2	SUBBASE	LEAN CLAY (CL)		34	22	12
3	BASE	CLAYEY GRAVELLY SAND (SP-SC)		23	12	11
4	BASE	CRUSHED STONE (GW)		NONPLASTIC		
5	WEARING COURSE BLENDED STOCKPILE AGGREGATES			NONPLASTIC		

Figure 1. Gradation and classification data for base, subbase, and subgrade materials and for the aggregate component of the asphaltic concrete of the MWHGL test section.

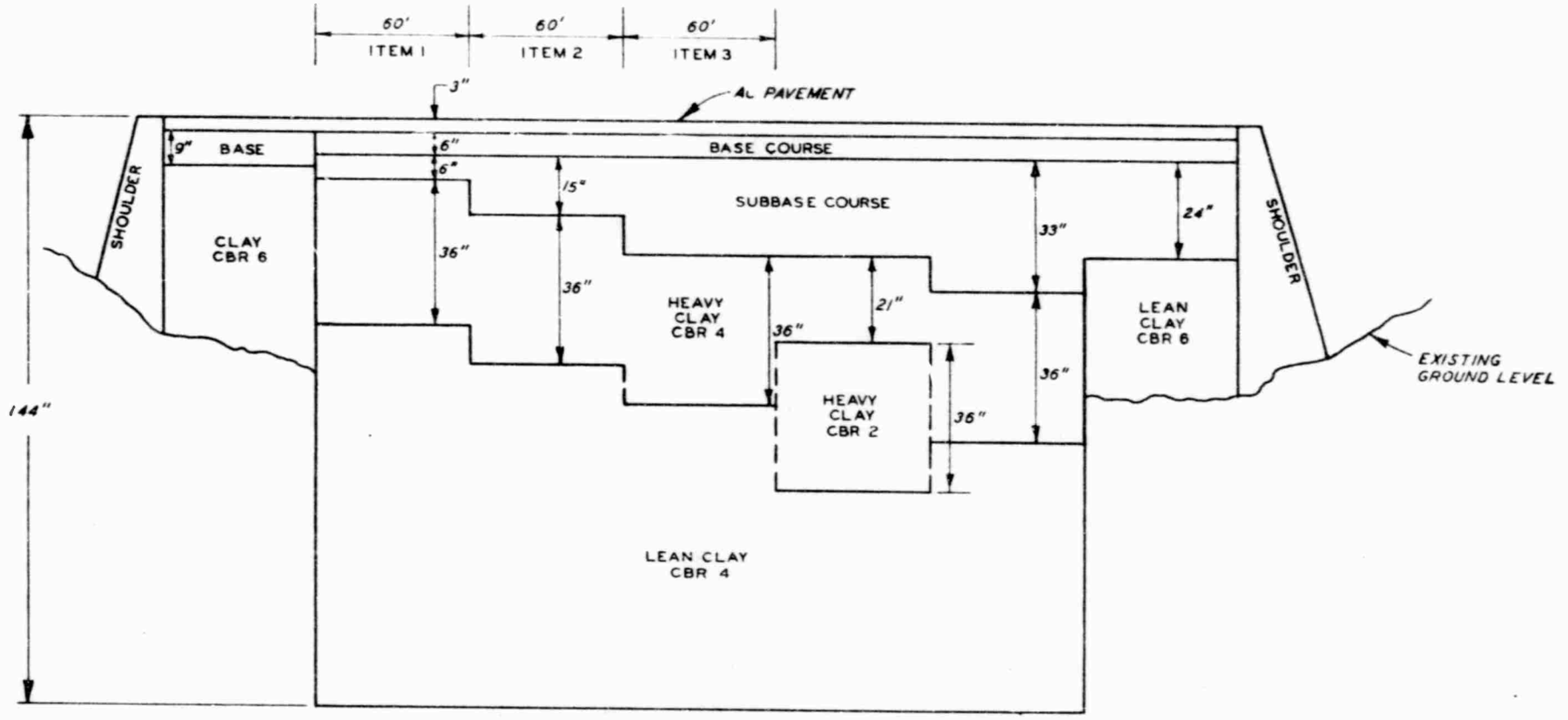

Figure 2. Longitudinal section of MWHGL test section.

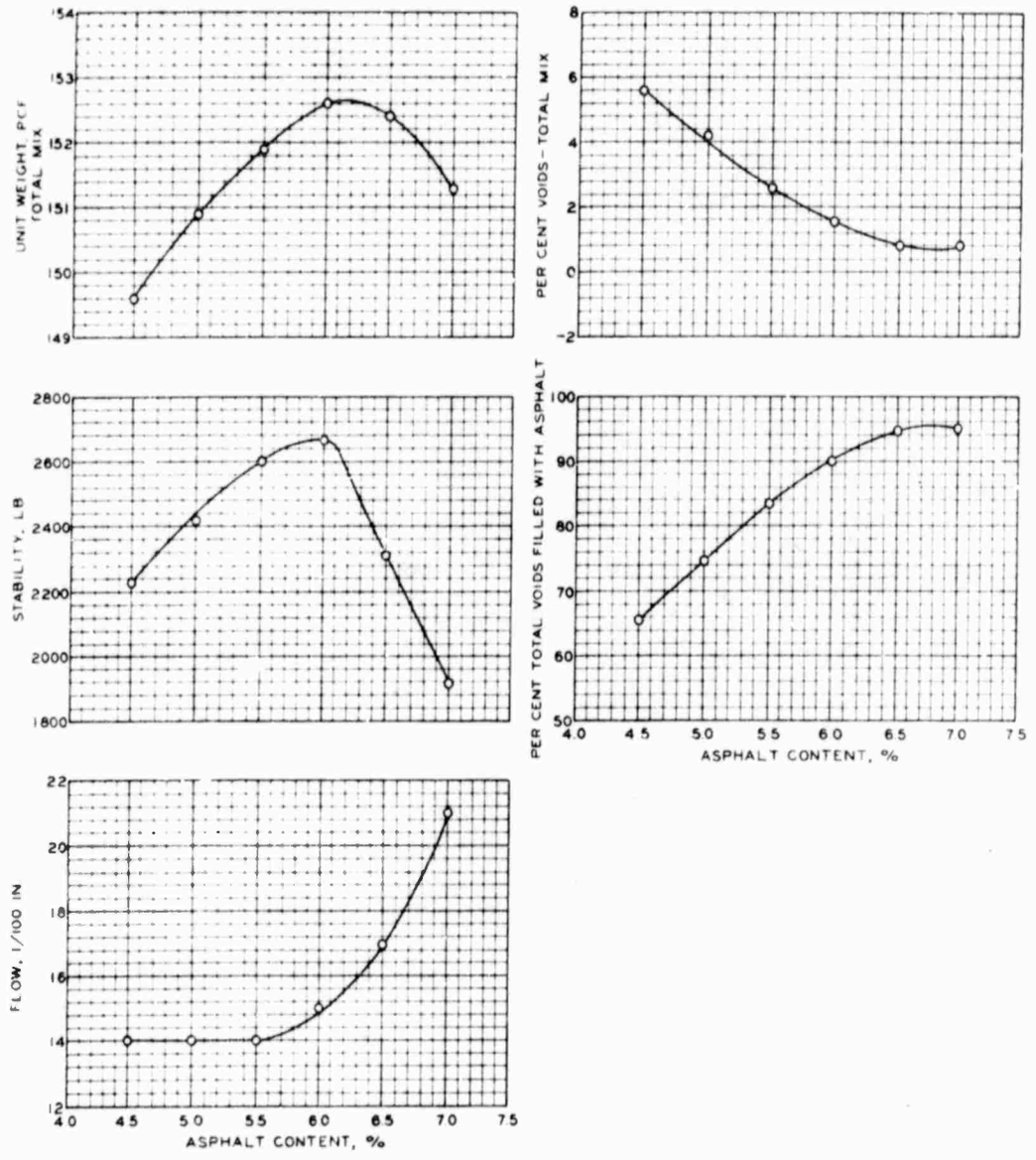

Figure 3. Laboratory mix design properties of asphaltic concrete wearing course for MWHGL test section.

Table 1

As-Constructed Thickness, CBR, Water Content and Density Data for MWHGL Test Section

Test Item	Material		Station	Elev ft	Layer Thickness ft	Layer Thickness in.	Total Thickness in. Design	Total Thickness in. Actual	CBR	Water Content %	Dry Density, pcf in Place (A)	Dry Density, pcf CE 55* (B)	Percent CE 55 Density (A/B)
West maneuver area	Cr stone base		3+90	194.05	0.90	10.8	12	13	34	1.4	135.2	140	97
	Subgrade			193.15					11	19.0	105.8	106	100
1	Cr stone		3+30	193.67	0.30	3.6	15	15	51	1.9	136.6	140	98
	Subbase			193.37	0.89	10.7			13	5.0	124.1	126	98
	Subgrade	(CH)		192.48					3.0	33.2	86.0	85	101
		(CH)		191.64					3.7	31.8	86.0	88	98
		(CH)		190.79					3.4	32.5	83.3	87	96
		(CL)		189.82					2.2	23.8	97.0	97	100
		(CL)		188.88					4.0	23.5	98.9	97	102
2	Cr stone		2+70	193.42	0.60	7.2	24	24	81	1.8	141.3	140	101
	Subbase			192.82	1.26	15.1			12	5.0	129.4	126	103
	Subgrade	(CH)		191.56					4.5	30.9	88.6	89	100
		(CH)		190.44					3.6	33.4	82.9	85	98
		(CH)		189.70					3.4	33.9	87.6	84	103
		(CL)		188.45					3.6	24.8	97.3	95	102
		(CL)		187.56					3.8	21.4	92.0	101	92
3	Cr stone		2+10	193.15	0.69	8.1	33	33	61	2.0	142.2	140	102
	Subbase			192.46	2.0	24.0			13	3.4	121.6	126	96
	Subgrade	(CH)		190.46					3.4	30.9	87.6	89	99
		(CH)		189.55					2.4	32.5	85.4	86	99
		(CH)		188.54					3.3	34.8	84.0	83	101
		(CL)		187.74					4.5	20.9	[illegible].8	102	101
		(CL)		186.59					3.7	20.6	101.9	102	100
		(CL)		185.61					3.9	23.0	99.7	98	101
		(CL)		184.81					1.8	22.1	99.0	100	99
		(CL)		184.00					1.1	23.2	98.6	98	101
		(CL)		182.65					1.9	21.7	98.1	99	99
		(CL)		181.78					2.2	22.2	96.7	99	98

* Laboratory densities shown in this column are the CE 55 maximum densities at optimum water content for the crushed-stone base and the gravelly sand subbase material and the CE 55 density corresponding to the field in-place water contents for the subgrade material.

Table II

Physical Properties of Asphaltic Concrete Wearing Course of MWHGL Test Section

Test Item	Coverages	Asphalt Content % Total Wt	Stability lb	Flow 1/100 in.	Percent Voids Total Mix	Percent Voids Filled/AC	Unit Wt Total Mix pcf	Percent Plant Laboratory Density
			Laboratory Mix Design*					
--	--	5.0	2420	14	4.1	74.0	150.9	--
			Plant-Mixed, Laboratory-Compacted Samples*					
--	--	5.0	2200	10	4.5	73.0	150.3	100.0
			Field Cores**					
1-5	0	5.0	650	9	7.5	60.5	145.4	96.8
1	12	5.0	1310	18	6.6	63.6	147.0	97.5
2	200	5.0	1362	18	6.0	65.9	147.8	98.0
3	3334	5.0	1593	15	4.3	73.3	150.6	100.2
4	3343	5.0	1455	16	4.5	70.6	149.7	99.3
5	3848	5.0	1700	16	3.7	76.8	151.5	100.8

* Specimens compacted by gyratory compaction, 200-psi pressure, 1-deg pitch, and 30 revolutions.

** Field cores obtained from traffic lane 1, 360,000-lb, 12-wheel gear assembly.

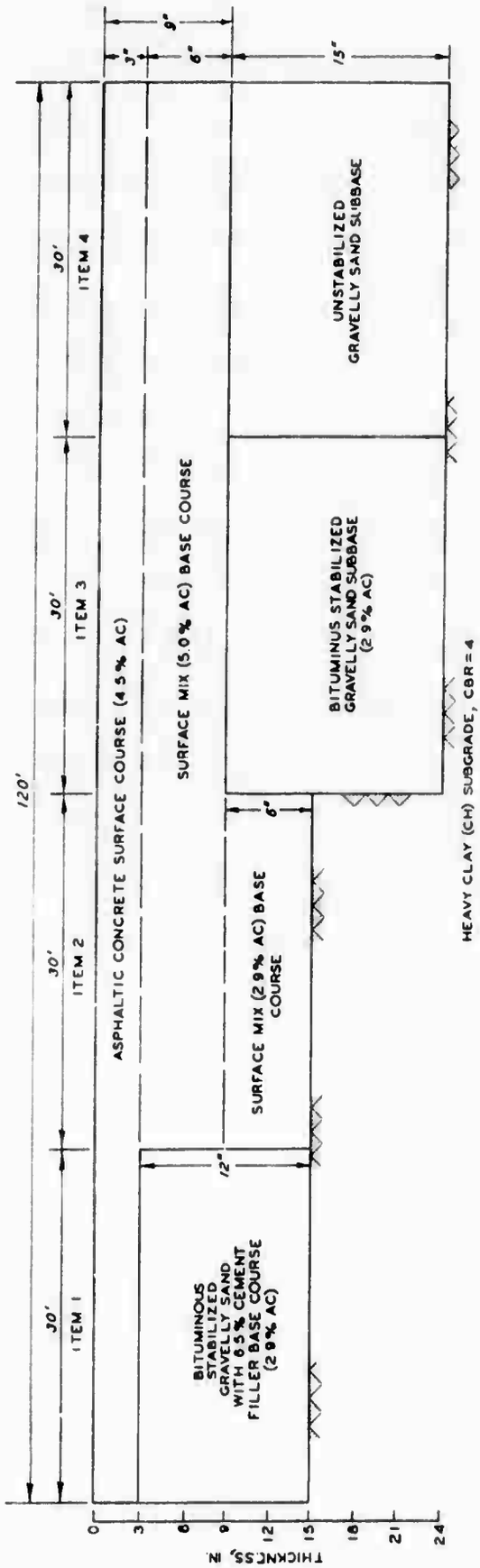

Figure 4. Longitudinal section of bituminous-stabilized base course test section.

6.5 percent portland cement and 2.9 percent 85-100 penetration grade asphalt cement. Gradations of the aggregate portions of the wearing and base courses are shown in figure 5. Mix design properties for both materials are shown in figures 6 and 7. Properties of the surface, base, and subbase materials as constructed and after traffic as determined from field cores, are indicated in table III. Item 2 consisted of a full 15-in. thickness of asphaltic concrete designed to meet surface course specifications (reference 6). Field properties of this material are also indicated in table III. Item 3 consisted of 9 in. of asphaltic concrete over 15 in. of gravelly sand treated with 2.9 percent 85-100 penetration grade asphalt cement. Item 4 was the same as items 3 except that the gravelly sand was untreated. Design mix properties of the base course in item 3 are indicated in figure 8. The gravelly sand used in items 3 and 4 was similar to the subbase material used in the MWHGL test section. Properties of the field mix as determined from core samples in items 3 and 4 are shown in table III. Actual asphalt content of the various materials are indicated in figure 4. Field in-place CBR, water content, and dry density data for the subgrade material and for the base course in item 4 are shown in table IV.

b. Test Loads

Wheel and assembly loadings involved from the bituminous-stabilized base course test section that were considered in the study reported herein are given below:

Configuration	Assembly Load, kips	Tire Pressure, psi	Contact Area, in.^{2}
12-wheel (C-5A)	360	100	285
Single-wheel	30	100	285
Single-wheel	75	290	270

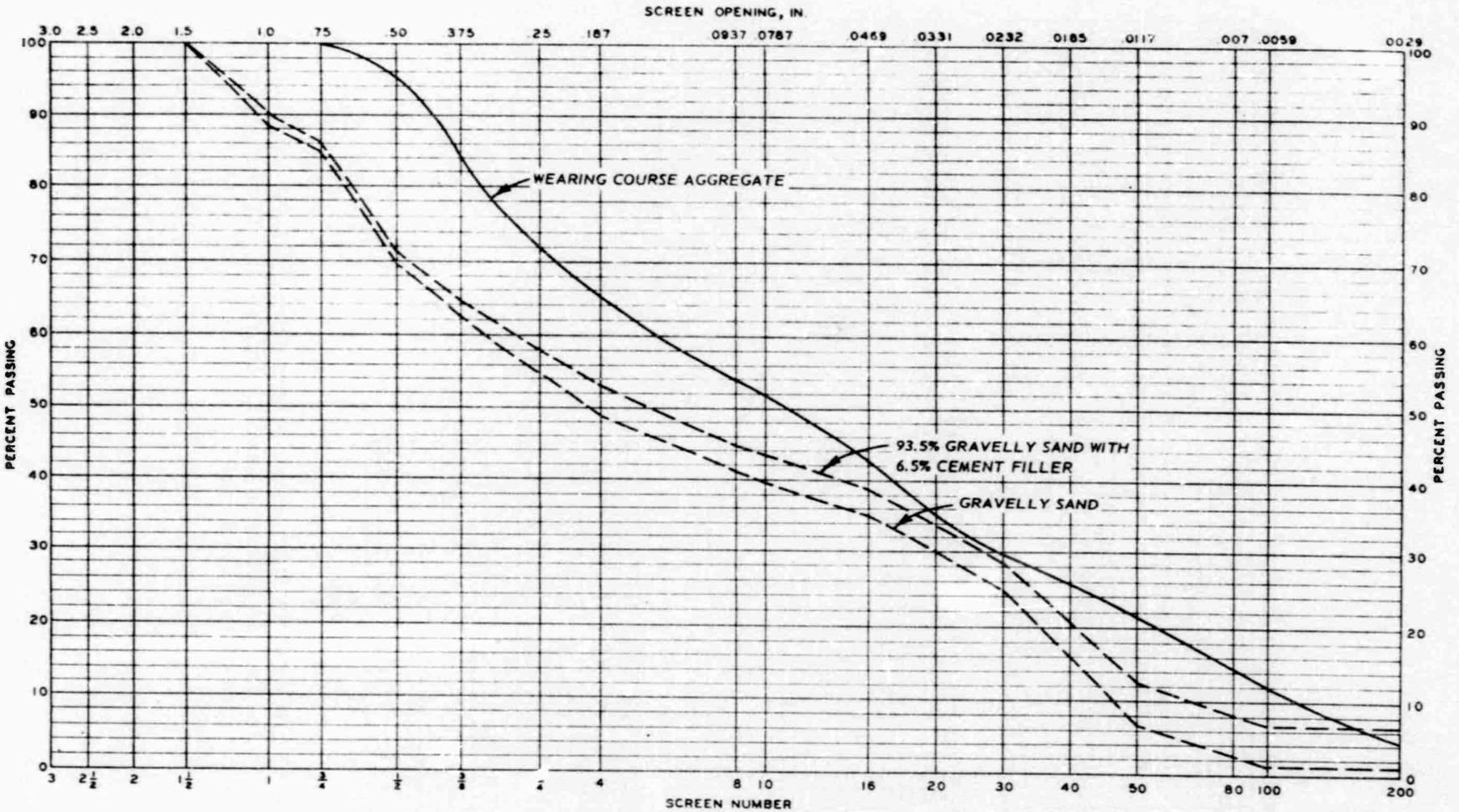

Figure 5. Gradations of aggregate portions of wearing and base courses of the bituminous base course test section.

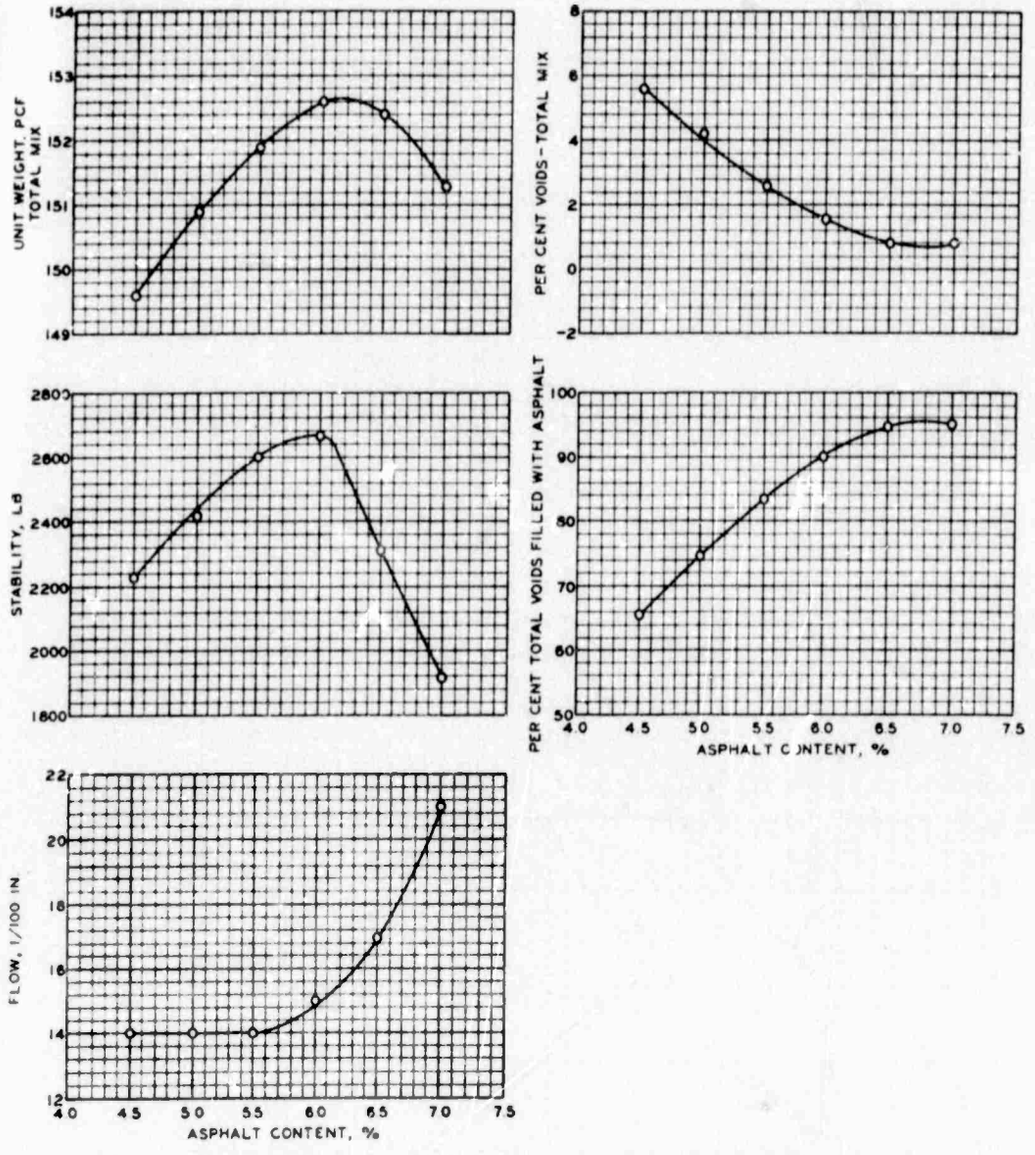

Figure 6. Laboratory mix design properties (75-blow compaction) of asphaltic concrete wearing course for bituminous base course test section.

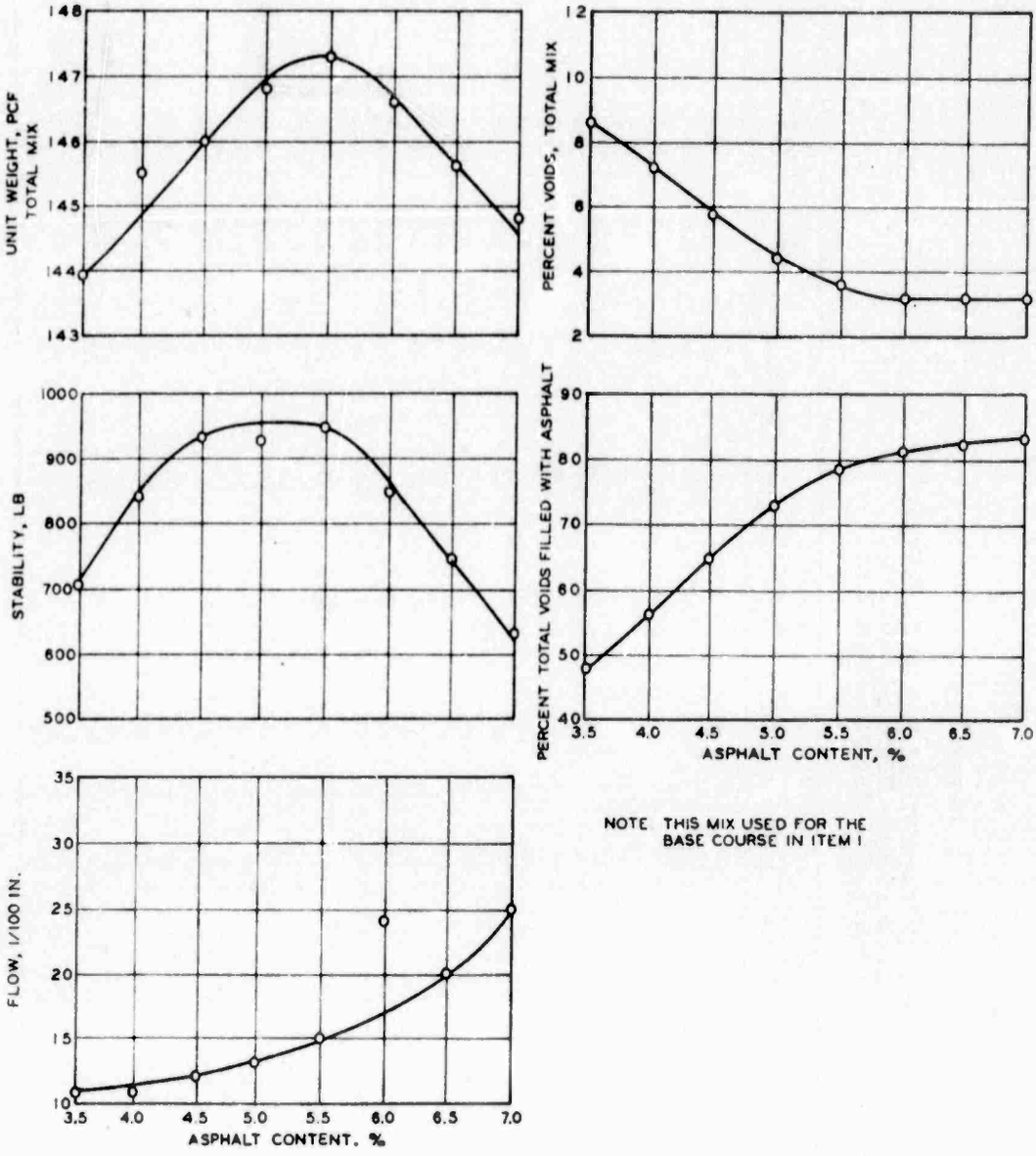

Figure 7. Laboratory mix design properties (50-blow compaction) of gravelly sand with 6.5 percent cement filler used as base course of item 1, bituminous base course test section.

Table III

Summary of Laboratory Test Data for Field Cores
Lane 1, 12-Wheel, 360,000-lb Gear Load,
Bituminous-Stabilized Base Course Study

Test Item	Coverages	Material	Depth in.	Asphalt Content %	Stability lb	Flow Units of 1/100 in.	Tensile Strength psi	Density lb/cu ft	Density % of Lab	Voids, % Total Mix	Voids, % Filled	Condition of Core
1	0	Surface course	0-3	4.5	2670	16	124	153.4	100	3.2	76.8	
		Stabilized base*	3-7	2.9	1300	11	62	144.6	98	8.8	42.8	
	96	Surface course	0-3	4.5	1591	30	105	150.7	98	4.9	66.8	Surface cracked
		Stabilized base*	3-7	2.9	--	--	75	145.7	99	8.1	44.9	
2	0	Surface course	0-3	4.5	2755	16	108	153.7	100	3.0	78.2	
		Base course	3-9	5.0	2784	16	106	154.1	100	2.1	85.4	
			9-12	2.9	1584	13	102	149.2	--	8.2	48.0	
	425	Surface course	0-3	4.5	2688	26	82	154.4	101	2.5	81.0	Surface cracked
		Base course	3-9	5.0	2230	29	58	153.4	100	2.7	81.8	
	734	Surface course	0-3	4.5	1606	15	89	154.5	101	2.5	81.1	Surface cracked
		Base course	3-9	5.0	2748	30	101	152.9	99	2.8	81.1	
			9-12	2.9	2417	12	102	152.3	--	6.3	52.6	
3	0	Surface course	0-3	4.5	2722	24	97	154.2	101	2.7	80.2	
		Base course	3-9	5.0	2440	39	57	154.0	100	2.1	85.2	
	434	Surface course	0-3	4.5	--	--	103	154.4	101	2.6	81.0	
		Base course	3-9	5.0	2722	24	65	153.2	100	2.7	81.8	
	2198	Surface course	0-3	4.5	2825	19	97	154.8	101	2.4	82.0	Surface cracked
		Base course	3-9	5.0	2300	30	57	154.1	100	2.1	85.1	
		Stabilized subbase*	9-12	2.9	1175	11	89	146.1	105	6.9	46.9	
			12-15	2.9	520	10	70	144.5	104	7.9	45.5	
4	0	Surface course	0-3	4.5	2132	17	119	150.1	98	5.2	66.8	
		Base course	3-9	5.0	4233	16	106	154.4	100	1.9	86.6	
	442	Surface course	0-3	4.5	2398	20	77	153.9	101	2.9	78.8	Surface cracked
		Base course	3-9	5.0	2245	27	60	153.8	100	2.2	84.6	
	1422	Surface course	0-3	4.5	3300	20	--	155.2	102	2.2	83.5	Surface cracked
		Base course	3-9	5.0	3000	23	--	153.7	100	2.3	84.0	

* 50-blow Marshall compaction.

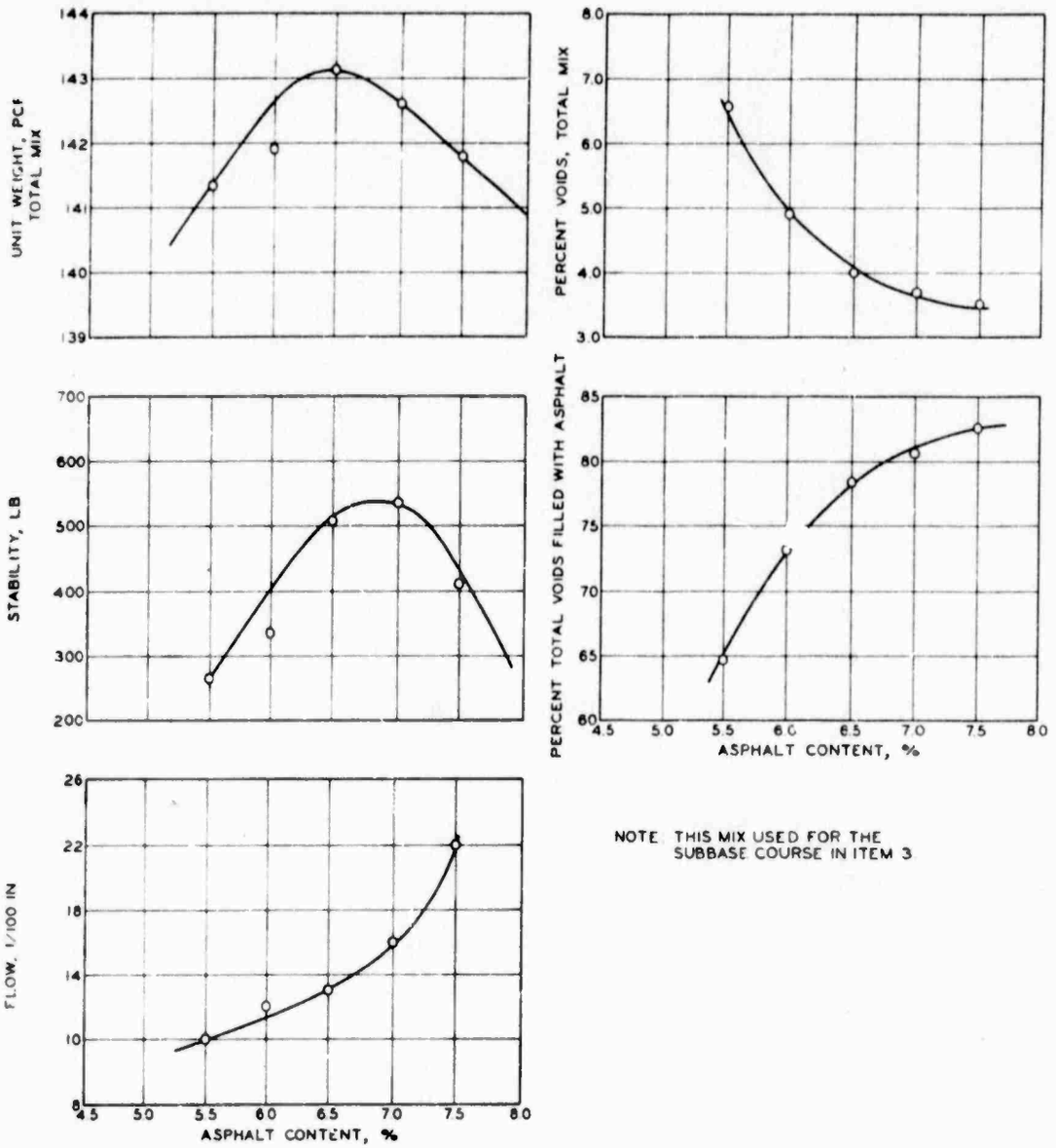

Figure 8. Laboratory mix design properties (50-blow compaction) of gravelly sand used as base course of item 3, bituminous base course test section.

Table IV

Summary of As-Constructed Thickness, CBR, Water Content, and Density Data
Bituminous-Stabilized Base Course Study

Test Item	Station*	Material**	Elevation ft	Layer Thickness ft	Layer Thickness in.	Total Thickness in. Design	Total Thickness in. Actual	CBR	Water Content %	Dry Density, pcf In Place (A)	Dry Density, pcf CE 55 (B)***	Percent CE 55 Density A/B
1	3+45	Surface course	193.94	0.22	2.64	15	14.64	-	-	-	-	-
		Stabilized base cour	193.72	1.00	12.00			-	-	-	-	-
		Subgrade (CH)	192.72					2.9	31.0	87.0	90	97
2	3+15	Surface course	193.83	0.26	3.12	15	14.88	-	-	-	-	-
		Surface-mix base course	193.57	0.98	11.76			-	-	-	-	-
		Subgrade (CH)	192.59					2.5	30.6	86.8	90	97
		(CH)	192.09					3.1	30.6	86.6	90	96
		(CH)	191.59					5.7	32.6	85.4	87	98
3	2+85	Surface course	193.69	0.25	3.00	24	23.83	-	-	-	-	-
		Surface-mix base course	193.44	0.60	7.20			-	-	-	-	-
		Stabilized subbase	192.84	1.14	13.68			-	-	-	-	-
		Subgrade (CH)	191.70					5.2	29.1	89.8	91	99
		(CH)	191.20					2.3	30.2	87.5	90	97
		(CH)	190.70					5.8	31.4	86.4	89	97
4	2+55	Surface course	193.46	0.23	2.76	24	23.64	-	-	-	-	-
		Surface-mix base course	193.23	0.49	5.88			-	-	-	-	-
		Unstabilized subbase	192.74	1.25	15.00			14.0	4.8	-	-	-
		Subgrade (CH)	191.49					3.0	31.0	89.2	90	99
		(CH)	190.99					3.8	34.4	-	88	-

* All measurements made in center of item.
** See plate 1 for complete description of layers.
*** CE 55 dry density at field in-place water content.

4. STRUCTURAL LAYERS IN FLEXIBLE PAVEMENTS

a. Pavements

This test involved four types of pavements, each 24 in. thick and constructed on a heavy clay subgrade. A longitudinal section of these pavements is shown in figure 9. All items had a 3-in.-thick asphaltic concrete wearing course designed to meet the specifications given in reference 6. Mix design properties of this material are shown in figure 10. Properties of in-place asphaltic concrete as determined from core samples are indicated in table V. Items 1 and 2 each had a 6-in.-thick base course of crushed limestone graded to conform to specification requirements given in reference 7. Under the base course in item 1, there was a 15-in.-thick layer of compacted lean clay treated with slaked lime at a rate of 3.5 percent by dry soil weight. This layer essentially served as a subbase course. Item 2 included a layer of compacted lean clay that was treated with portland cement at a rate of 10 percent by dry soil weight. Item 3 consisted of the 3-in.-thick wearing course over 21 in. of crushed limestone similar to the base course in items 1 and 2. Item 4 consisted of 3 in. of asphaltic concrete over 21 in. of clayey gravelly sand stabilized with portland cement applied at a rate of 6.0 percent by dry soil weight. Gradation and classification data for the crushed limestone, clayey gravelly sand, aggregate portion of the asphaltic concrete, and the lean clay, are shown in figure 11. A summary of field in-place CBR, dry density, and moisture content data for the various soils after construction is shown in table VI.

b. Test Loads

Wheel and assembly loadings from the structural layer tests that were considered in this study are given below:

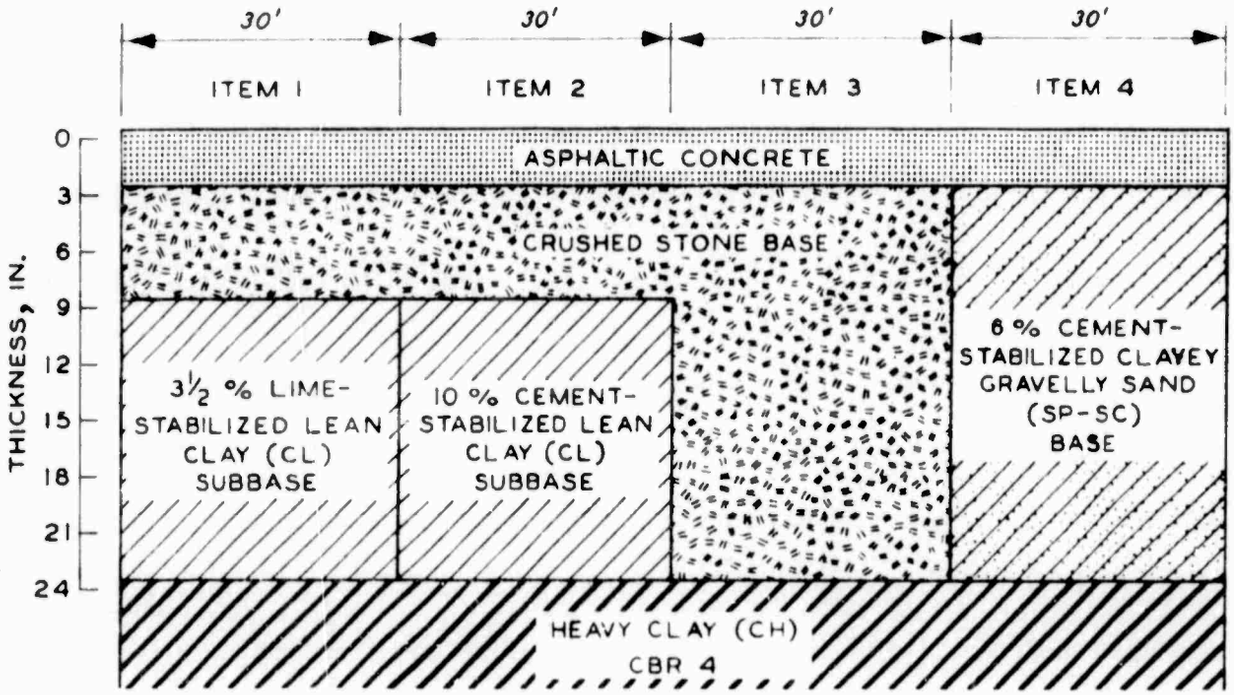

Figure 9. Longitudinal section of test section for the evaluation of structural layers in flexible pavement

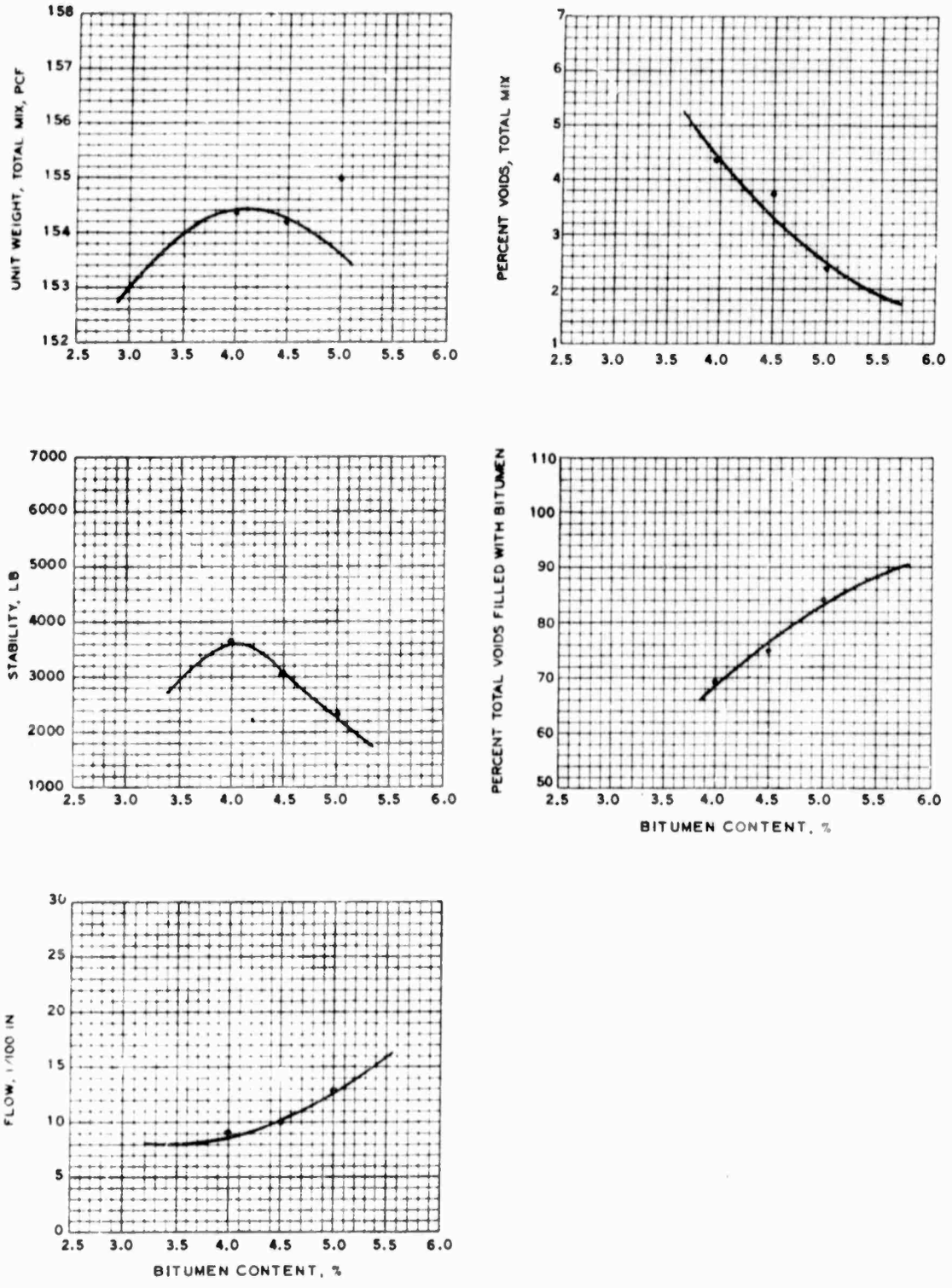

Figure 10. Laboratory mix design properties (75-blow compaction) of the asphaltic concrete wearing course for the structural layers test section.

Table V

Physical Properties of Asphaltic Concrete Wearing Course for Structural Layers Test Section

Test Item	Coverages	Asphalt Content % Total Wt	Stability lb	Flow 1/100 in.	Percent Voids Total Mix	Percent Voids Filled/AC	Unit Wt Total Mix pcf	Percent Plant Laboratory Density
			Plant-Mixed, Laboratory-Compacted Samples					
--	--	4.0	3673	9	4.3	69.1	154.4	100.0
			Field Cores - Prior to Traffic					
1	0	4.0	1274	18	6.3	59.9	151.3	98.0
2	0	4.0	1108	15	7.5	55.6	149.3	96.7
3	0	4.0	1253	18	6.0	61.4	151.8	98.3
4	0	4.0	1099	18	7.0	57.5	150.1	97.2
			Field Cores - After Traffic					
1	198	4.0	780	28	8.6	51.6	147.4	95.5
	0	4.0	966	19	6.9	57.6	150.2	97.3
2	1,342	4.0	912	24	6.1	60.9	151.6	98.2
	0	4.0	854	22	6.4	59.6	151.1	97.9
3	5,037	4.0	1108	26	5.1	65.2	153.2	99.2
	0	4.0	1182	22	5.8	62.1	151.9	98.4
4	10,406	4.0	1184	22	6.1	60.9	151.5	98.1
	0	4.0	1267	21	6.0	61.2	151.7	98.3

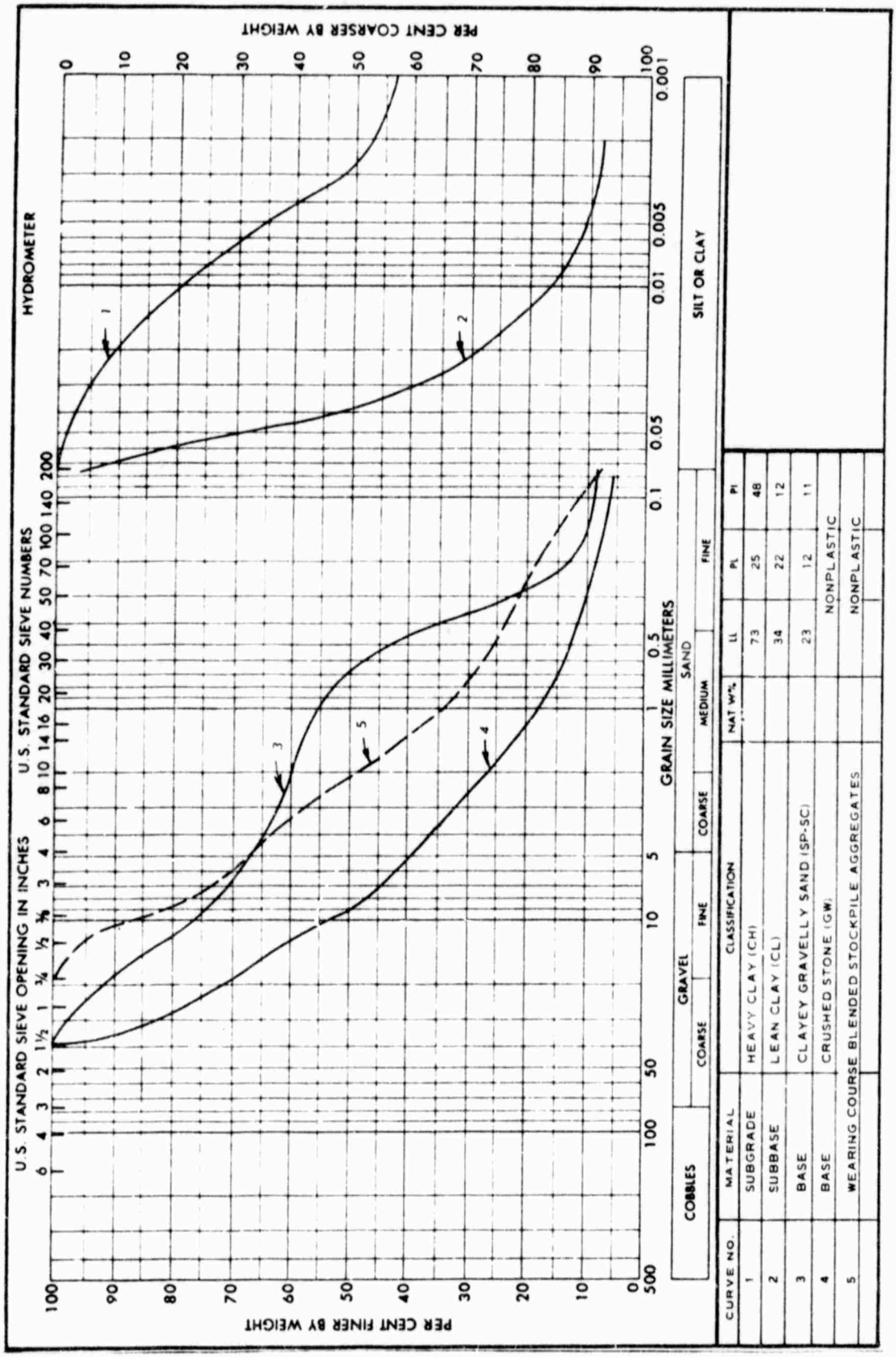

CURVE NO.	MATERIAL	CLASSIFICATION	NAT W%	LL	PL	PI
1	SUBGRADE	HEAVY CLAY (CH)		73	25	48
2	SUBBASE	LEAN CLAY (CL)		34	22	12
3	BASE	CLAYEY GRAVELLY SAND (SP-SC)		23	12	11
4	BASE	CRUSHED STONE (GW)			NONPLASTIC	
5	WEARING COURSE	BLENDED STOCKPILE AGGREGATES			NONPLASTIC	

Figure 11. Gradation and classification data for base, subbase, and subgrade materials and for the aggregate component of the asphaltic concrete of the structural layers test section.

Table VI

EVALUATION OF STRUCTURAL LAYERS IN FLEXIBLE PAVEMENT

Summary of Thicknesses, CBR, Water-Content, and Density Data

Test Item	Assembly	Station	Location	Material	Elev.	Layer Thickness, ft in.	Total Thickness, in. Design	Total Thickness, in. Actual	Traffic Coverages	Water Content Prior to Compaction, %	CBR	Water Content, %	Dry Density pcf, In-Place A	Dry Density pcf, Laboratory B	Percent Laboratory Density, A/B	Saturation %	Data Tested*
								As-Constructed Data									
1	-	3+45	℄ item	Asphaltic concrete	193.88	0.19 2.28	24.00	22.44	0		-	-	-	-	-	--	--
				Crushed stone base	193.69	0.40 4.80					200	4.9	140.1	140*	100	62	November 6, 1970
				Lime-stabilized subbase (CL)	193.29	1.22 15.36					38	17.6	104.5	103.4**	101	78	November 6, 1970
				Subgrade (CH)	192.01					18.7	4.2	31.3	87.5	91.5*	96	91	--
				(CH)	191.51						3.3	32.2	86.4	95.0*	90	92	--
				(CH)	191.01						6.0	32.7	86.3	88.5*	100	90	--
				(CH)	190.01						4.6	34.0	83.8	86.0*	97		--
2	-	4+17	℄ item	Asphaltic concrete	193.61	0.21 2.52	24.00	22.96	0		-	-	-	-	-	57	November 4, 1970
				Crushed stone base	193.40	0.31 3.72					150	6.0	132.5	140*	95	73	November 4, 1970
				Cement-stabilized subbase (CL)	193.19	1.31 15.72				18.3	80	15.7	104.9	105.5**	101	90	--
				Subgrade (CH)	191.88						2.7	32.7	85.3	87.5*	97	89	--
				(CH)	191.38						2.7	33.1	84.5	86.5*	98	92	--
				(CH)	190.88						4.1	31.8	87.1	88.0*	99	90	--
				(CH)	189.38						5.7	31.3	87.3	90.0*	97		--
	-	2+85	℄ item	Asphaltic concrete	193.66	0.23 2.76	24.00	23.64	0		-	-	-	-	-	58	November 6, 1970
				Crushed stone base	193.39	1.74 20.88					132	4.4	141.4	140*	101	22	November 4, 1970
				Crushed stone base	191.65						35	1.7	140.4	140*	100	91	--
				Subgrade (CH)	191.15						3.4	31.3	87.5	90.5*	97	91	--
				(CH)	190.65						3.0	32.7	85.8	86.5*	99	91	--
				(CH)	190.15						4.3	31.9	86.8	88.0*	99	88	--
				(CH)	189.65						4.9	33.1	84.3	89.0*	95		--
4	-	2+55	℄ item	Asphaltic concrete	193.52	0.23 2.76	24.00	24.60	0		-	-	-	-	-	36	November 6, 1970
				Cement-stabilized base	193.29	1.82 21.84				6.2	209	2.7	139.8	-	-	47	November 4, 1970
				Cement-stabilized base	191.79					7.0	285	4.5	133.7	-	-	91	--
				Subgrade (CH)	191.47						3.7	32.5	85.3	88.5*	96	91	--
				(CH)	190.97						3.3	32.2	85.8	88.0*	98	93	--
				(CH)	190.47						5.5	32.3	87.3	90.5*	101	89	--
				(CH)	189.47						6.3	31.8	86.2	88.5*	97		--
								After-Traffic Data									
1	300 kip 12 wheel	4+50	℄ traffic lane	Asphaltic concrete	194.74	0.25 3.00	24.00	23.02	1.38		-	-	-	-	-	97	December 23, 1970
				Crushed stone base	194.51	0.41 4.92					44	5.7	142.8	140*	105	80	December 23, 1970
				Lime-stabilized subbase (CL)	194.10	1.[illegible]					34	13.4	103.1	104.2**	100	87	--
				Subgrade (CH)	[illegible]						4.2	29.2	[illegible].7	[illegible]*	[illegible]	85	--
				[illegible]	[illegible]						[illegible]	28.[illegible]	[illegible].1	[illegible]	4	84	--
				(CH)	+190.74						[illegible]	[illegible].2	[illegible]	[illegible]	[illegible]	[illegible]	--
1	300 kip 12 wheel	4+50	[illegible] lane	Asphaltic concrete	[illegible]	0.25 3.00	24.00	22.57	0		-	-	-	-	-	44	December 23, 1970
				Crushed stone base	[illegible]	0.39 4.68					55	2.[illegible]	1[illegible].0	140*	107	80	December 23, 1970
				Lime-stabilized subbase (CL)	194.02	1.24 14.[illegible]					72	19.[illegible]	103.0	104.[illegible]**	100	85	--
				Subgrade (CH)	191.79						[illegible].7	28.[illegible]	[illegible].[illegible]	[illegible].0*	[illegible]	87	--
				(CH)	191.29						[illegible].0	29.7	[illegible].2	[illegible].[illegible]*	[illegible]	--	--
				(CH)	190.[illegible]						[illegible].5	-	-	-	-		

[illegible] compaction effort.

** CL 12 compaction effort.

* All base and subbase as-constructed data were taken one day after compaction of the respective layers.

(Sheet 1 of 3)

Table VI (Continued)

Test Item	Assembly	Station	Location	Material	Elevation, ft	Layer Thickness, ft	Layer Thickness, in.	Total Thickness, in. Design	Total Thickness, in. Actual	Traffic Coverages	Water Content Prior to Compaction %	CBR	Water Content, %	Dry Density, pcf In-Place A	Dry Density, pcf Laboratory B	Percent Laboratory Density, A/B	Saturation %	Date Tested
3	360 kip 12 wheel	3+20	℄ traffic lane	Asphaltic concrete	193.63	0.32	3.84	24.00	23.80	1871		-	-	-	-	-	--	--
				Crushed stone base	193.31	0.33	3.96					72	1.4	149.5	140*	107	37	January 6, 1971
				Cement-stabilized subbase (CL)	189.98	1.33	16.00					122	20.	107.4	-	-	98	January 6, 1971
				Subgrade (CH)	191.65							3.7	34.5	95.1	94.0*	101	94	--
				(CH)	191.15							5.5	32.2	87.2	87.5*	100	93	--
				(CH)	190.65							7	32.6	87.4	86.9*	101	95	--
			outside traffic lane	Asphaltic concrete	193.68	0.37	4.44	24.00	24.96	0		-	-	-	-	-	--	--
				Crushed stone base	193.31	0.33	3.96					56	3.2	137.0	140*	112	106	January 6, 1971
				Cement-stabilized subbase (CL)	190.98	1.38	16.53					121	20.9	106.3	-	-	97	January 6, 1971
				Subgrade (CH)	191.50							2.3	34.2	84.1*	84.1*	101	93	--
				(CH)	191.10								30.1	91.0	90.8*	100	95	--
				(CH)	190.60							7	33.6	88.7	89.0*	102	95	--
1	360 kip 12 wheel	2+80	℄ traffic lane	Asphaltic concrete	193.36	0.22	2.64	24.00	22.80	5047		-	-	-	-	-	--	--
				Crushed stone base	193.12	1.68	20.16					2	1.9	144.4	140*	103	29	January 12, 1971
				Subgrade (CH)	191.14							1.2	32.5	86.7	86.4*	100	92	--
				(CH)	190.64								29.9	87.7	91.4*	96	87	--
				(CH)	190.44							3	32.1	85.1	95.4*	90	89	--
			outside traffic lane	Asphaltic concrete	193.35	0.29	3.48	24.00	23.16	0		-	-	-	-	-	--	--
				Crushed stone base	193.10	1.64	19.68					87	1.6	147.4	140*	104	28	January 12, 1971
				Subgrade (CH)	191.46							1.0	33.4	84.5	89.7*	94	90	--
				(CH)	190.96							5	29.5	91.2	92.1*	99	94	--
				(CH)	190.46							7	31.0	88.8	89.9*	99	93	--
4	160 kip Twin tandem	3+50	℄ traffic lane	Asphaltic concrete	193.91	0.29	3.48	24.00	22.68	140		-	-	-	-	-	--	--
				Crushed stone base	193.70	0.44	5.28					55	2.8	147.4	140*	105	49	March 30, 1971
				Lime-stabilized subbase (CL)	193.26	1.24	14.88					82	20.4	90.5	103.3**	88	78	March 30, 1971
				Subgrade (CH)	192.02							4.1	32.0	86.3	86.1*	100	93	--
				(CH)	191.52								31.4	87.0	92.0*	95	91	--
				(CH)	191.02								32.4	85.7	94.4*	100	91	--
			outside traffic lane	Asphaltic concrete	194.00	0.24	2.88	24.00	23.16	0		-	-	-	-	-	--	--
				Crushed stone base	193.76	0.42	5.04					-	2.5	145.7	140*	104	50	March 30, 1971
				Lime-stabilized subbase (CL)	193.34	1.27	15.24					111	19.4	102.4	103.3**	99	81	March 30, 1971
				Subgrade (CH)	192.07							4.2	32.7	86.1	90.8*	100	92	--
				(CH)	191.57								30.9	87.2	92*	95	94	--
				(CH)	191.07							7	31.8	87.1	96.1*	91	91	--
2	160 kip Twin tandem	3+20	℄ traffic lane	Asphaltic concrete	194.42	0.26	3.12	24.00	22.24	1000		-	-	-	-	-	--	--
				Crushed stone base	193.46	0.55	6.56					77	1.6	149.6	140*	106	--	--
				Cement-stabilized subbase (CL)	193.08	1.38	16.56					124	19.9	107.0	-	-	28	April 6, 1971
				Subgrade (CH)	191.70							3.4	35.0	84.7	83.5*	101	93	April 6, 1971
				(CH)	191.20							5.4	32.4	87.8	90.8*	100	94	--
				(CH)	190.70							7	32.7	86.5	93.9	92	93	--
			outside traffic lane	Asphaltic concrete	194.04	0.24	2.88	24.00	23.04	0		-	-	-	-	-	--	--
				Crushed stone base	193.80	0.47	5.64					77	1.4	149.6	140*	107	43	April 6, 1971
				Cement-stabilized subbase (CL)	193.16	1.25	15.00					124	19.0	107.4	-	-	90	April 6, 1971
				Subgrade (CH)	191.90							2.7	33.9	84.6	84.6*	100	91	--
				(CH)	191.40							4.7	32.5	87.1	90.8*	96	91	--
				(CH)	190.90								33.0	87.1	95.6*	91	91	--

(Sheet 2 of 3)

Table VI (Concluded)

Test Item	Assembly	Station	Location	Material	Elevation, ft	Layer Thickness, ft	Layer Thickness, in.	Total Thickness, in. Design	Total Thickness, in. Actual	Traffic Coverages	Water Content Prior to Compaction, %	CBR	Water Content %	Dry Density, pcf In-Place A	Dry Density, pcf Laboratory B	Percent Laboratory Density A/B	Saturation %	Date Tested
3	200 kip Twin tandem	2+90	℄ traffic lane	Asphaltic concrete	193.40	0.23	2.7[illegible]	24.00	21.[illegible]	5[illegible]		-	-	-	-	-	--	--
				Crushed stone base	193.17	1.57	[illegible].84					63	1.3	143.2	140*	10[illegible]	19	April 8, 1971
				Subgrade (CH)	191.60							2.1	30.8	88.2	90.0*	98	91	--
				(CH)	191.10							4.0	31.2	88.2	89.4*	99	92	--
				(CH)	190.60							4.0	31.7	87.8	88.1*	100	92	--
			outside traffic lane	Asphaltic concrete	193.77	0.19	2.28	24.00	[illegible].84	0		-	-	-	-	-	--	--
				Crushed stone base	193.58	1.88	22.56					67	0.6	138.4	140*	99	7	April 8, 1971
				Subgrade (CH)	191.70							2.3	32.2	86.0	87.5*	98	90	--
				(CH)	191.20							3.[illegible]	30.3	88.7	90.6*	98	91	--
				(CH)	190.70							[illegible]	32.2	87.3	87.5*	100	93	--
1	50 kip Single wheel	3+50	℄ traffic lane	Asphaltic concrete	193.44	0.1[illegible]	2.28	24.00	[illegible].96	4[illegible]		-	-	-	-	-	--	--
				Crushed stone base	193.[illegible]	0.47	5.64					93	3.9	151.8	140*	108	87	March 30, 1971
				Lime-stabilized subbase (CL)	193.28	1.12	13.44					51	18.8	103.3	103.3**	100	79	March 30, 1971
				Subgrade (CH)	192.1[illegible]							2.9	33.0	86.1	86.1*	100	92	--
				(CH)	191.6[illegible]							4.7	31.7	87.5	86.1*	99	92	--
				(CH)	190.1[illegible]							[illegible]	32.7	[illegible]	86.8*	101	94	--
2	50 kip Single wheel	3+20	℄ traffic lane	Asphaltic concrete	193.7[illegible]	0.21	2.52	24.00	23.2	120		-	-	-	-	-	--	--
				Crushed stone base	193.57	0.52	[illegible].2[illegible]					42	25	146.9	140*	105	63	--
				Cement-stabilized subbase (CL)	193.05	1.21	14.52					109	19.[illegible]	109.2	-	-	92	April 6, 1971
				Subgrade (CH)	191.84							1.7	35.[illegible]	93.2	92.0*	101	93	April 6, 1971
				(CH)	191.34							2.[illegible]	32.3	87.1	87.5*	100	93	--
				(CH)	190.84							3.9	34.[illegible]	83.9	83.2*	101	92	--
3	75 kip Single wheel	2+90	℄ traffic lane	Asphaltic concrete	193.[illegible]1	0.23	2.7[illegible]	24.00	22.68	50		-	-	-	-	-	--	--
				Crushed stone base	193.38	1.66	19.92					[illegible]	1.3	[illegible].1	140*	104	21	April 6, 1971
				Subgrade (CH)	191.72							[illegible].0	30.[illegible]	88.7	87.[illegible]*	101	92	--
				CH)	191.22							[illegible].[illegible]	29.[illegible]	[illegible].9	[illegible].4*	[illegible]	92	April 16, 1971
				CH)	190.72							[illegible]	31.[illegible]	87.[illegible]	88.0*	100	93	--
4	75 kip Single wheel	2+30	℄ traffic lane	Asphaltic concrete	-	-	-	24.00	[illegible]	200+		-	-	-	-	-	--	--
				Cement-stabilized base	-[illegible]	-	-					159	[illegible].2	141.1	-	-	86	April 16, 1971
			outside traffic lane	Asphaltic concrete	-	-	-	24.00	-	0		-	-	-	-	-	--	--
				Cement-stabilized base	-	-	-					261	.7	137.7	-	-	82	--

[illegible] In addition to [illegible] assembly

(sheet 3 of 3)

Configuration	Assembly Load, kips	Tire Pressure, psi	Contact Area, in.^{2}
12-wheel*	360	100	285
Single-wheel	30	100	285
Single-wheel	50	170	280

*Initial analytical studies showed that practically identical results were obtained when using either the 12-wheel load or the 6-wheel load. Therefore, to conserve computer time, the 6-wheel load was used.

c. Instrumentation

(1) Description. Both stress and strain sensors were placed in each item of the test section during construction. The strain gage system consisted of paired strain sensors with an external instrument package, all manufactured by the Bison Instrument Co. The strain sensors used in this test were 4-in.-diam disk-shaped coils (see figure 12) installed as shown in figure 13. The strain sensors were imbedded in the soil in face-to-face vertical and horizontal alinement; the distance between any two sensors was then related by electromagnetic coupling. By means of an inductance bridge, output voltages were used to determine gage separation, or strain, since a change in the initial spacing caused a corresponding bridge unbalance. The pressure cells were 6 in. in diameter and were fabricated at the WES from stainless steel. Each cell consists of a mercury-filled chamber with a diaphragm and a full wheatstone bridge circuit utilizing four SR-4 strain gages hermetically sealed within the cell, as shown in figure 14. Pressure applied to the faceplate of the cell is transmitted through the mercury in the fluid chamber to an internal flexible diaphragm to produce deflection of the diaphragm proportional to the load. The four SR-4 strain gages are mounted on the diaphragm and are actuated by its deflection.

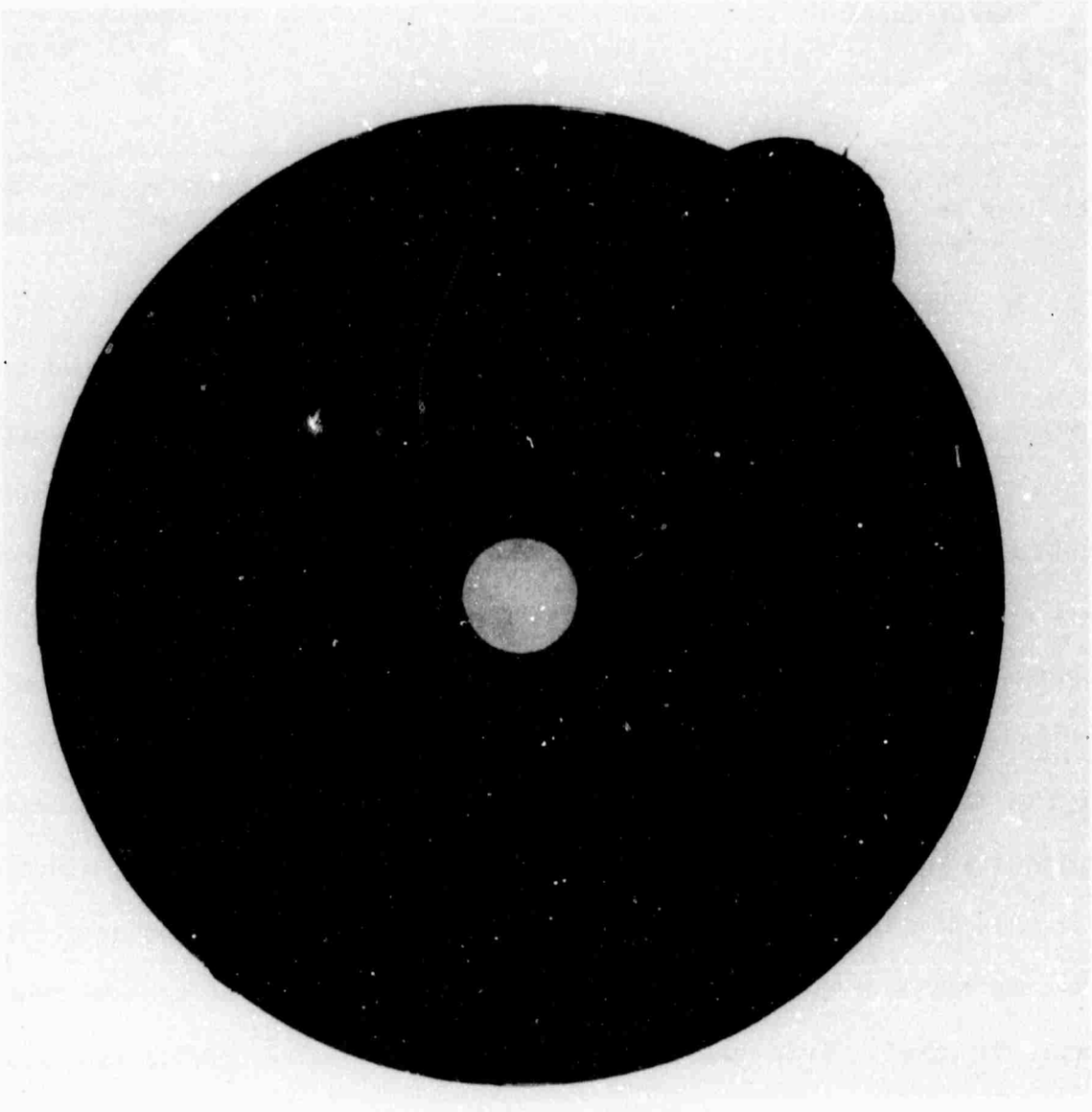

Figure 12. Four-in.-diam strain sensor used in instrumentation of the structural layer test section.

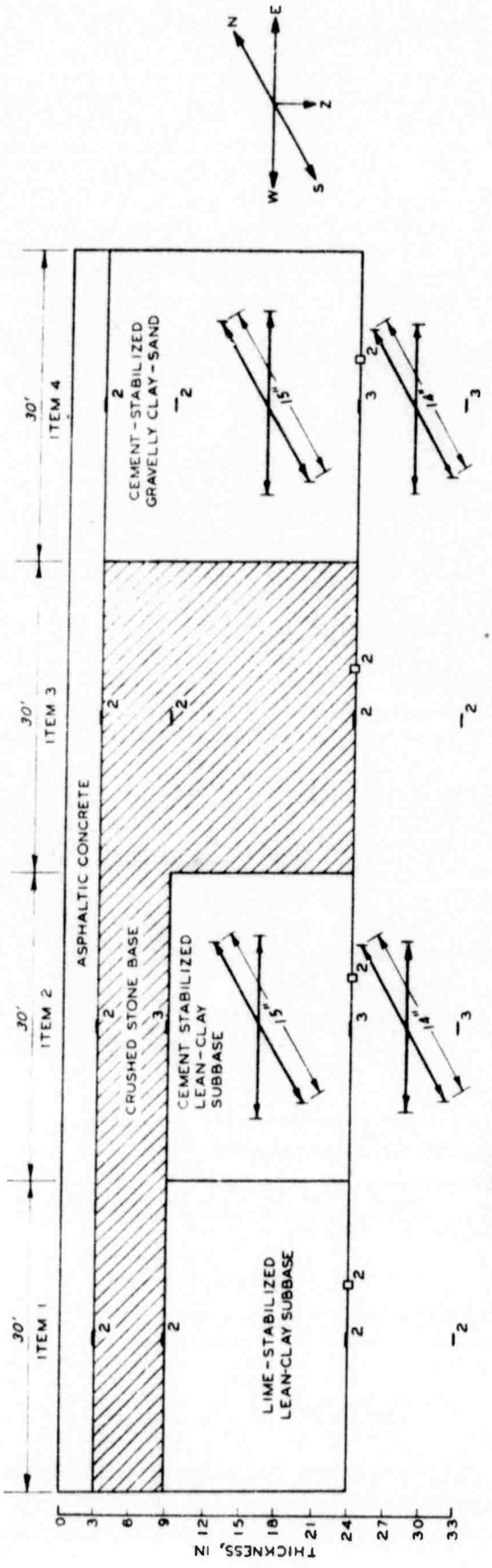

Figure 13. Location of instrumentation in the structural layers test section.

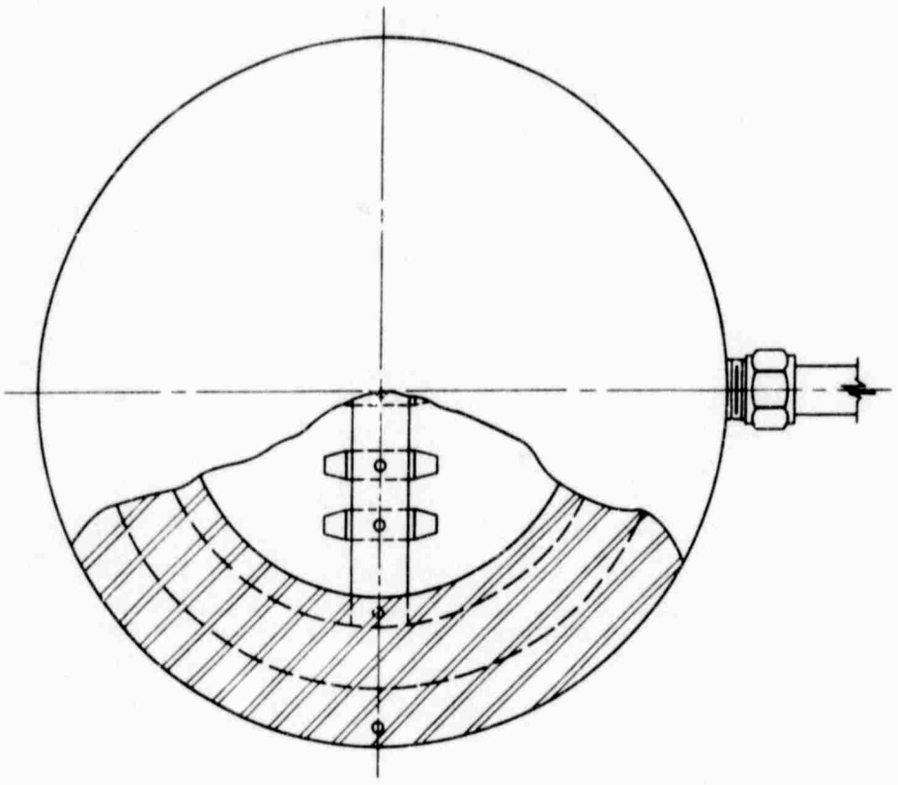

PLAN

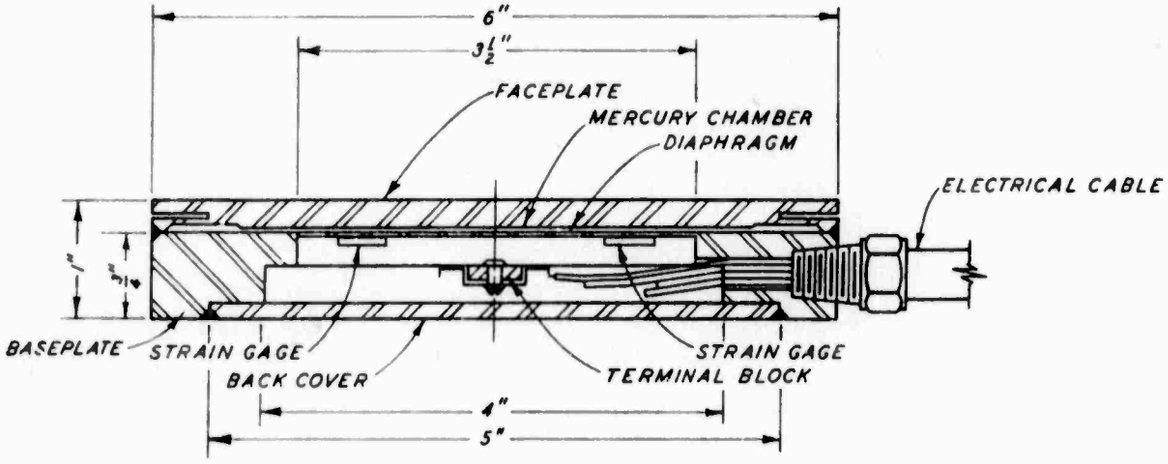

SECTION

Figure 14. WES-designed soil pressure cell used in instrumentation of the structural layers test section.

(2) Location. Locations of the sensors are shown in figure 13. In each item, strain gages were positioned in vertical columns at depths of 3, 9, 24, and 33 in. below the pavement surface. In items 1 and 2, the 3-, 9-, and 24-in. depths corresponded to layer interfaces, e.g., the interface between the wearing and base courses at the 3-in. depth, and so on. In items 3 and 4, only the 3- and 24-in. depths corresponded to layer interfaces, while the gage at the 9-in. depth was imbedded within the second layer. In all items the gage at the 33-in. depth was positioned within the subgrade. Two vertical columns of strain gages were located in each item and the columns were spaced 53 in. apart. In items 2 and 4, pairs of strain gages were also positioned to obtain horizontal strain readings in the longitudinal and transverse directions with respect to the test section. Two pairs of gages were positioned at the 16.5-in. depth and two additional pairs were set at the 28.5-in. depth. In addition to strain gages, two WES pressure cells were included in each item. These cells were all located at the interface of the subgrade and the next overlying layer.

(3) Data acquisition. Stress and strain data were obtained with various wheel loads and gear configurations. The data included in this report were obtained with the loads in a static position. These data are presented in Appendix I. The coordinate systems to which the various stress and strain readings are referenced are oriented with respect to the loading assembly configuration (figure 15). For the single-wheel load, a cylindrical coordinate system is used with the origin coincident with the center of the contact area. For the 12-wheel assembly, a Cartesian coordinate system was selected that was oriented with respect to the 12-wheel assembly as shown in figure 15.

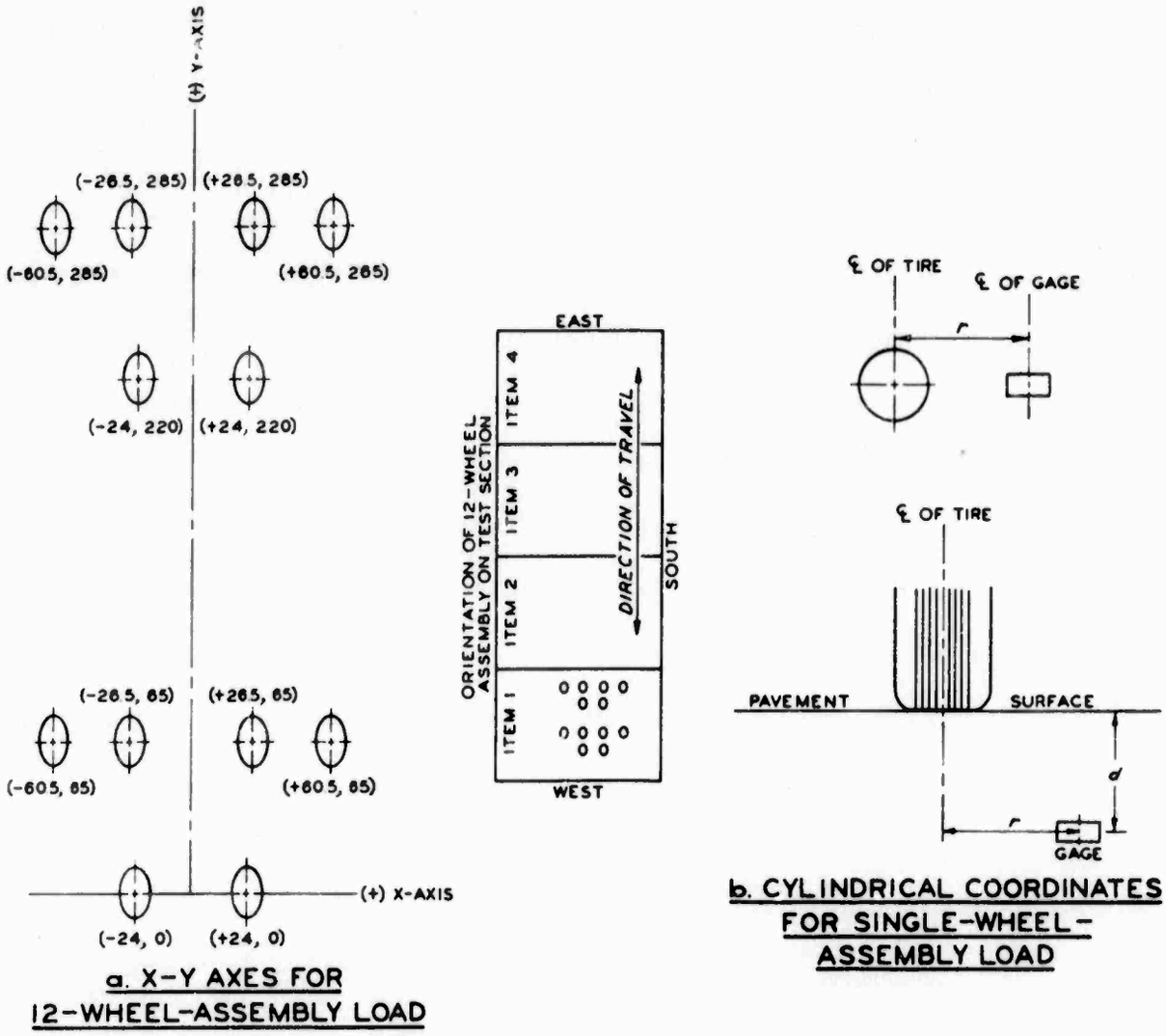

a. X-Y AXES FOR 12-WHEEL-ASSEMBLY LOAD

b. CYLINDRICAL COORDINATES FOR SINGLE-WHEEL-ASSEMBLY LOAD

Figure 15. Coordinate systems for 12-wheel and single-wheel assemblies.

SECTION III

METHODS OF ANALYSIS AND BEHAVIORAL CHARACTERIZATION OF MATERIALS

1. METHODS OF ANALYSIS

a. Approach

For the analysis of pavement systems, the most commonly used techniques are the Westergaard method, multilayer theory, and the finite difference and finite element approaches. To date the Westergaard and finite difference methods have been used primarily for the analysis of rigid pavements; while multilayer theory has been used for the analysis of flexible pavements. Most recently, the finite element procedure has gained acceptance in the analysis of both rigid and flexible pavements.

When the pavement is considered to be linearly elastic, many investigators have felt that the multilayer theory yields results comparable to those obtained by the finite element solution. In general, the programs utilizing the multilayer theory are simpler, easier to use, and more economical than finite element programs. This is particularly true when multiple-wheel loadings are encountered, such as is the case of the loading by the C-5A landing gear.

For these reasons, in conjunction with the fact that laboratory response data were not available for a nonlinear analysis, the elastic theory was chosen as the primary analysis tool. It was recognized that pavement materials are not truly linearly elastic and that the computed response values would not necessarily be true values; however, an investigation was made of the prospect that some computed pavement response parameter could be correlated with pavement performance to yield a basis for a pavement design procedure. The development of such a basis could be expanded through further

investigation and extensive laboratory tests for a nonlinear analysis of pavements similar to the types of pavements involved in this study. For comparison with the layer theory analysis, a limited analysis was also conducted utilizing linear and nonlinear finite element programs.

b. Computer Programs

Three basic computer programs were used in the analysis phase of this investigation: the CHEVRON, FEPAVE II, and AFPAV programs. In each program input is provided in terms of static loading conditions, pavement geometry, and material structural characteristics, i.e., elastic modulus and Poisson's ratio. Material response is given in terms of stress, strain, and/or deflection. The coordinate systems used in the computations are shown in figure 15. The three programs are described below:

(1) CHEVRON. Linearly elastic layer theory analysis of the various pavements was performed utilizing a basic computer program developed by the Chevron Research Company (reference 2). The program produces the coordinate stresses, strains, and deformations at selected points in a pavement system subjected to a single load uniformly distributed on a circular area. The pavement system may have any number of layers with the interface between layers being considered rough. The program was modified to run on a GE 600 computer, to handle multiple-wheel loading, and to compute principal stresses and strains.

(2) FEPAVE II. The finite element program used in the analysis was obtained from the University of California at Berkeley through Professor Carl Monismith. The program is an axisymmetric program (based on a program developed by Professor E. L. Wilson and reported in reference 9) which utilizes a single forward step incremental loading employing the tangent modulus with accumulation of stresses and strains.

The program had been specially adapted for pavement analysis such that data could be input with a minimum of effort and material characterization where those typically used in pavement analysis. The mesh is automatically generated in a layered system and materials divided by layers.

(3) AFPAV. The AFPAV code is a linearly elastic finite element code utilizing prismatic elements and a Fourier series representation of the loads (reference 10). The code was developed by the Naval Civil Engineering Laboratory for the Air Force Weapons Laboratory (AFWL) as a special program for analyzing three-dimensional loadings of pavement systems. Extensive work with the AFPAV code has been accomplished by Pichumani as reported in reference 10.

2. CHARACTERIZATION OF MATERIALS

a. General

In all the methods of analysis used in this investigation, the structural characteristics of the materials comprising any layer of the pavement under consideration were defined in terms of modulus of elasticity and Poisson's ratio. In the CHEVRON program, materials within any given layer are considered to be linearly elastic and, therefore, the elastic modulus and Poisson's ratio are constant. The AFPAV program also utilizes the linear elasticity approach; therefore, the material structural characteristics within each prismatic element are similarly constant. Structural characterization of materials for the FEPAVE II program can involve either a linear or a nonlinear approach. For the latter, suitable expressions must be assumed for the elastic modulus. However, Poisson's ratio must be assumed to be constant. In this investigation, four different basic material types were considered. These were:

(1) Asphalt-treated granular materials, such as the asphaltic concrete wearing course and the asphalt-bound materials used in the bituminous base test section.

(2) Unbound granular materials, such as the crushed limestone and the gravelly sand materials.

(3) Stabilized or cemented materials that depend to some degree on pozzalanic action for stability, such as the cement-treated lean clay and clayey gravelly sand and the lime-treated lean clay.

(4) The heavy clay subgrade.

Characterizations of each material type are discussed below.

b. Asphalt-Stabilized Materials

The response of asphaltic concrete to load is greatly dependent on the temperature of the material. Within the range of temperatures that exist in a pavement surface, the E-modulus has been shown to vary by more than an order of magnitude. The relationship between temperature and E-modulus for a moving load shown in figure 16 was published by the Shell International Petroleum Company (reference 11). A comparison of these moduli with values determined by the Asphalt Institute for beam samples taken from the WES bituminous base course test section can be seen in table VII.* The Asphalt Institute data indicate a variation of stiffness moduli of from 53,000 to 1,460,000 psi. These tests were conducted at various stress levels and at a constant temperature of approximately 80° F.

Surface temperatures in asphaltic concrete versus volume of test traffic applied as determined during the MWHGL tests at the WES are shown in figure 17. These tests were conducted during the period June-August 1970. As can be seen, surface temperature ranges varied from 60 to 70° F in lane 2A, and from 90 to 135° F in lane 1, during the period test traffic was applied

*Information transmitted to WES in a letter from the Asphalt Institute Laboratory, College Park, Maryland, dated 5 April 1971.

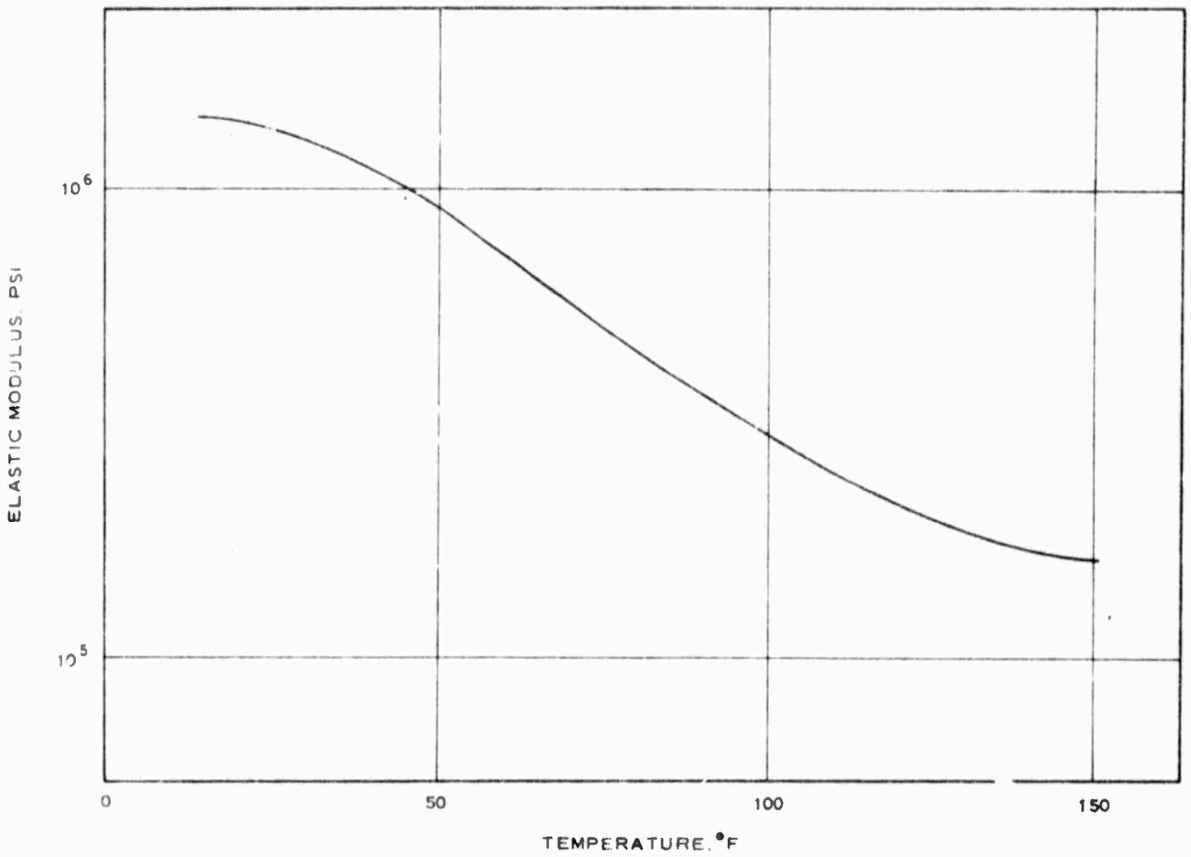

Figure 16. Variation of elastic modulus of asphaltic concrete with temperature (from reference 11).

Table VII

Flexural-Fatigue of Asphaltic Concrete and Hot-Mix Gravelly Sand Beam Samples from Bituminous Base Course Test Section*

Item No.	Material Tested	Depth from Surface, in.	Beam No.	Unit Wt Total Mix pcf	Fatigue Life N_f**	Stress psi	Strain*** 10^{-6} in./in.	Stiffness Modulus 10^5 psi
1	Hot-mix gravelly sand base course	6	33	--	128	119.3	1731	0.69
2	Asphaltic concrete surface course	0-4	1	152.9	176	196.6	2331	0.84
			7	153.5	1,815	141.4	1625	0.87
			5	153.4	4,540	124.5	1183	1.05
			3	153.6	25,350	99.0	698	1.42
			9	153.7	121,080	77.4	530	1.46
		4-8	8	154.4	920	147.4	2780	0.53
			6	154.0	1,875	126.8	2119	0.60
			10	154.1	8,420	98.1	1123	0.87
			4	154.3	57,850	76.6	742	1.03
			2	154.3	321,000	51.1	399	1.28

* Samples obtained 1 to 3 ft south of north edge of test section, outside traffic lane.

** All fatigue tests conducted at 80°F, constant stress mode. N_f = Number of stress repetitions to cause failure.

*** Strain values are initial bending strain based on center point deflection of beam, and stiffness modulus values are calculated from initial bending strains.

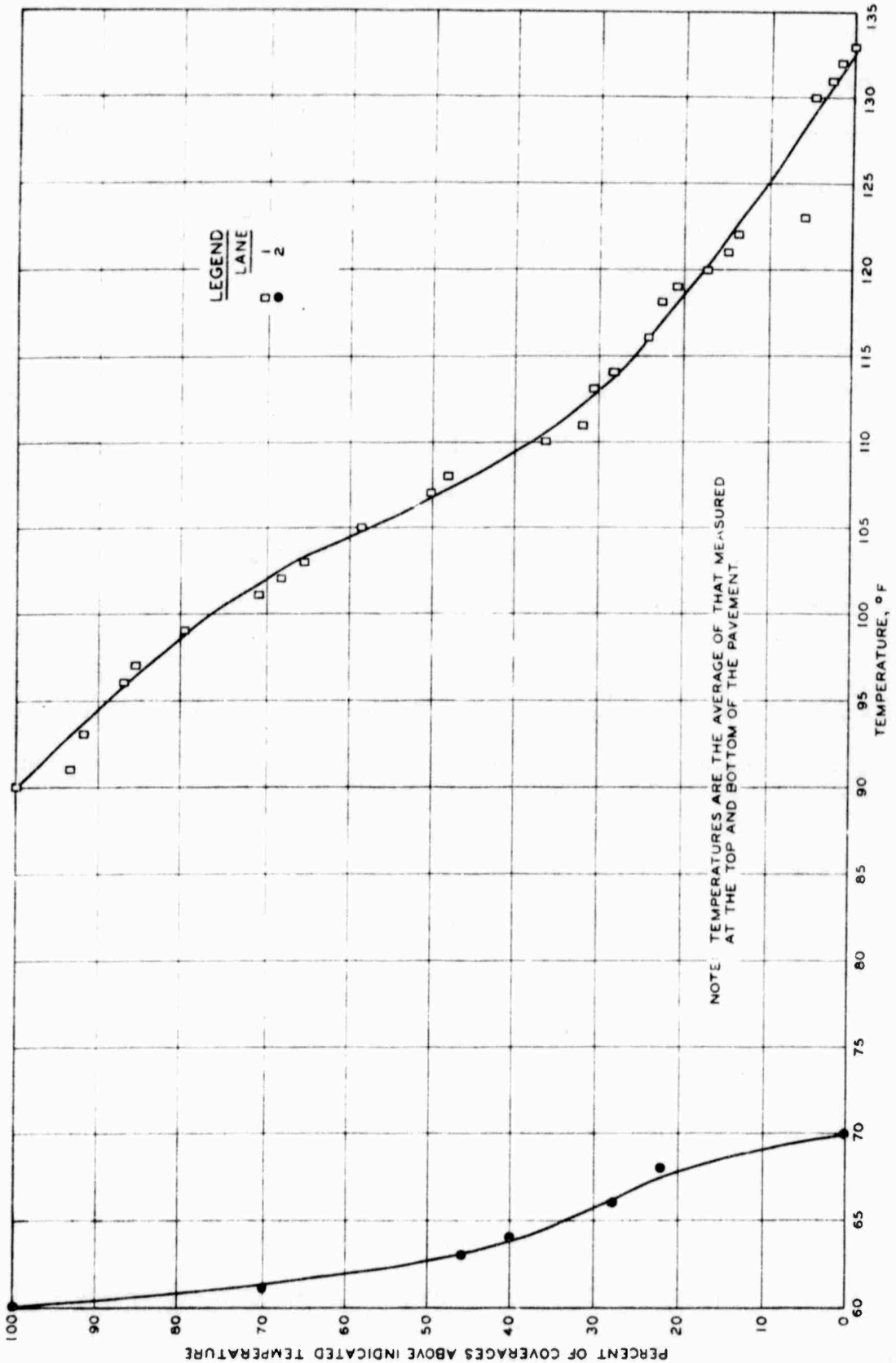

Figure 17. Traffic and pavement temperature distribution measured in the wearing course of the MWHGL test section.

in each. Therefore, it was determined that modulus values for asphaltic concrete should be based on both a low-temperature and a high-temperature condition.

Based on the foregoing data, it was determined that typical low and high temperature modulus values of 300,000 and 50,000 psi, respectively, should be used. Data from the literature indicate a typical value of 0.5 would be suitable for Poisson's ratio.

c. Unbound Granular Materials

In the analysis of layered systems by the Shell International Petroleum Company (references 11, 12), the quasi E-modulus for granular materials was selected based on the thickness of the granular layer and on the E-modulus of the underlying layer. It was found that the modulus of the granular material was between two to five times the modulus of the underlying layer. Figure 18 gives the comparison of the E-modulus of the granular materials and the E-modulus of the lower layer. Figure 19 presents the relationship between layer thickness and the ratio E_2/E_3 where E_2 is the modulus of granular material and E_3 is the modulus of the layer below the granular materials.

Other researchers (references 13-17) have used a direct relationship between the modulus and the state of stress existing in the material. The three principal relationships that have been proposed are:

$$M_R = K_1 \sigma_3^{K_2} \quad (1)$$

$$M_R = K_1' \theta^{K_2'} \quad (2)$$

$$M = K_2'' + 2K_3'' \sigma_r \quad (3)$$

Values of K_1, K_2, K_1', K_3'', which have been proposed for different granular materials, are listed in table VIII. Equations 1 and 2 are from reference 14; equation 3 is from reference 16.

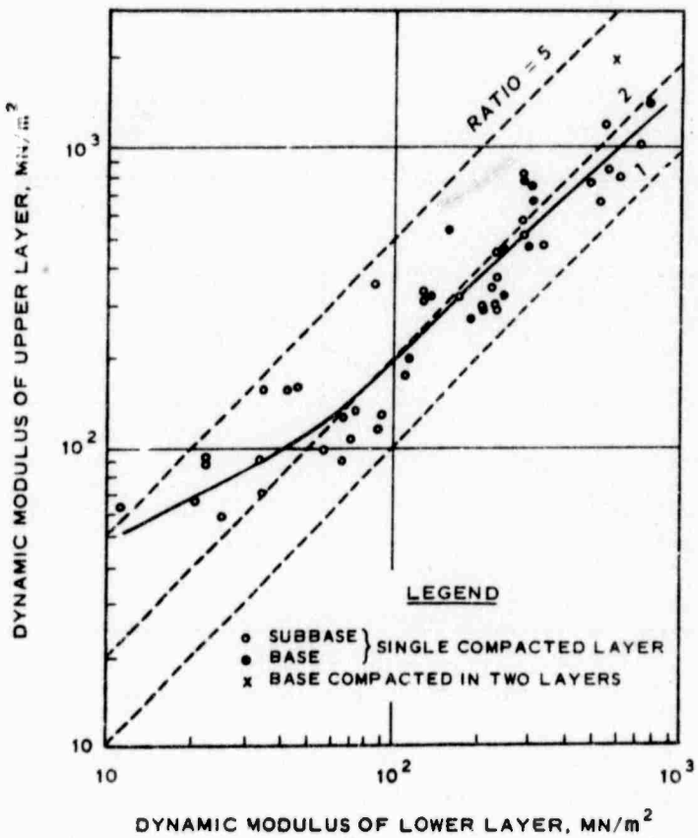

Note: $MN/m^2 \times 2.09 \times 10^4$ = approximate modulus in lb/ft^2

Figure 18. Dynamic moduli of unbound layers (from reference 12).

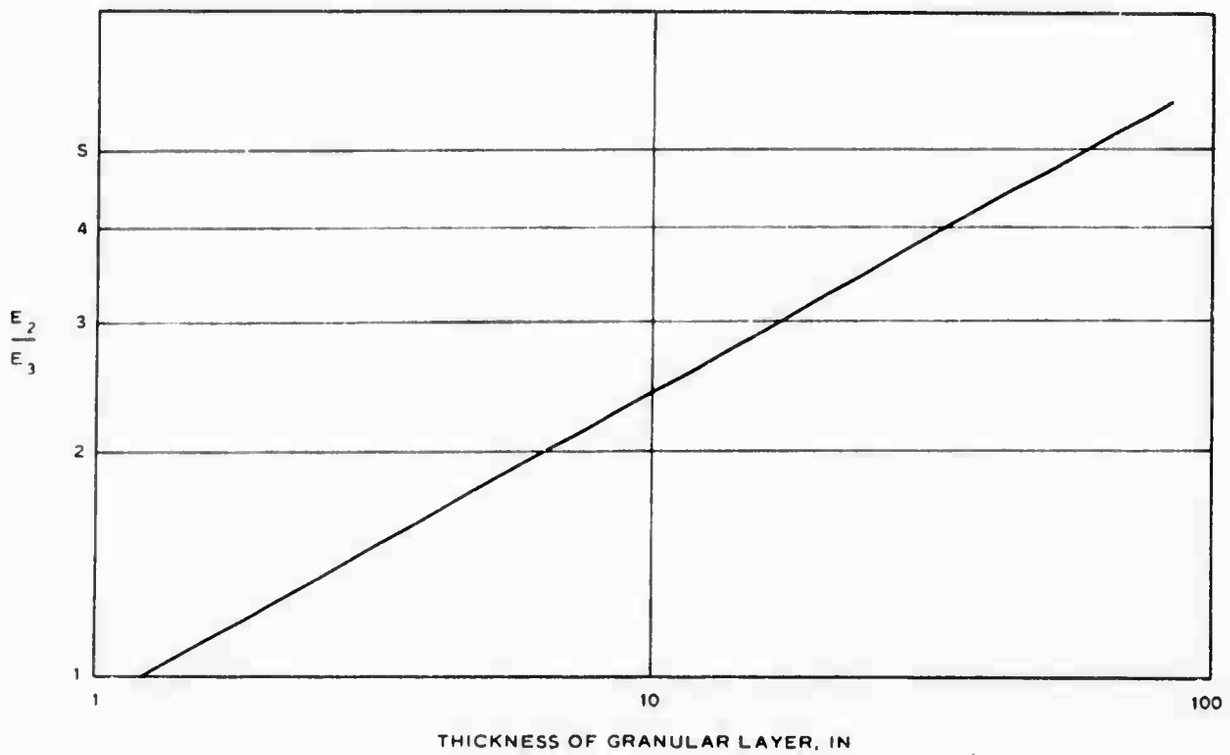

Figure 19. Relation of modular ratio to granular base thickness (from reference 11).

Table VIII

Material Constant Values Proposed for Various Granular Materials by Other Researchers

No.*	Description	Constants		Reference
	Expression: $M_R = K_1\sigma_3^{K_2}$ (reference 14)	K_1	K_2	
1	Dry, partially crushed gravel	10,094	0.580	14
2	Dry, crushed gravel	13,126	0.550	14
3	Partially saturated, partially crushed gravel	7,650	0.591	14
4	Partially saturated, crushed gravel	8,813	0.569	14
5	Saturated, partially crushed gravel	9,894	0.528	14
6	San Diego base	12,225	0.540	14
7	Gonzales Bypass base	15,000	0.480	17
8	Gonzales Bypass subbase	10,000	0.400	17
9	Morro Bay base	11,800	0.390	13
10	Morro Bay subbase	6,310	0.430	13
	Expression: $M_R = K_1\theta^{K_2'}$ (reference 14)	K_1'	K_2'	
11	San Diego base	3,933	0.61	14
12	Dry, crushed gravel	2,156	0.71	14
13	Partially saturated, crushed gravel	2,033	0.67	14
14	Morro Bay subbase	2,900	0.47	13,18
15	Morro Bay base	3,030	0.53	13,18
	Expression: $M = K_2'' + 2K_3''\sigma_r$ (reference 16)	K_2''	K_3''	
16	Crushed limestone	4,856	390	16
17	Crushed limestone after 36,000 repetitions	37,710	1082	16

* Some material numbers correspond to curve numbers shown in figure 20.

Of the relationships studied, the expression $M_R = K_1\sigma_3^{K_2}$ appeared to be most adatable for use in this study, especially since it can be applied to both linear and nonlinear analysis. For comparison, several relationships between modulus and confining pressure were determined from equations 1 and 3 using various material constant values from references 14, 16, and 17. These relationships are presented in figure 20. The number shown for each curve in figure 20 indicates a corresponding set of material constants and the expression in which they are used as presented in table VIII. As can be seen, the relationships proposed by Hicks in reference 14 produce E-values that are between those obtained by the relationships proposed by Dunlap (reference 16). Therefore, Hicks' values of K_1 = 13,126 and K_2 = 0.55 for dry crushed gravel and K_1 = 7,650 and K_2 = 0.591 for partially saturated gravel would serve as reasonable estimates of the K_1 and K_2 values for the crushed limestone and gravelly sand subbase, respectively. Thus curve 2 of figure 20 would represent the modulus-stress relationship for the crushed limestone, and curve 3 would represent the modulus-stress relationship for the gravelly sand.

In work by various researchers, estimated values for Poisson's ratio ν varied from 0.25 to 0.4. Therefore, an estimated value of $\nu = 0.3$ was selected for this study.

d. Cement- and Lime-Stabilized Materials

Since the tensile strength of stabilized layers is considerably lower than the compressive strength, it was decided to investigate the properties of these materials from a tensile standpoint. Therefore, indirect tensile tests were conducted utilizing equipment identical to that described in reference 19 and the elastic constants evaluated by an approach described in reference 20, which was based upon an analysis from reference 21. For the indirect tensile

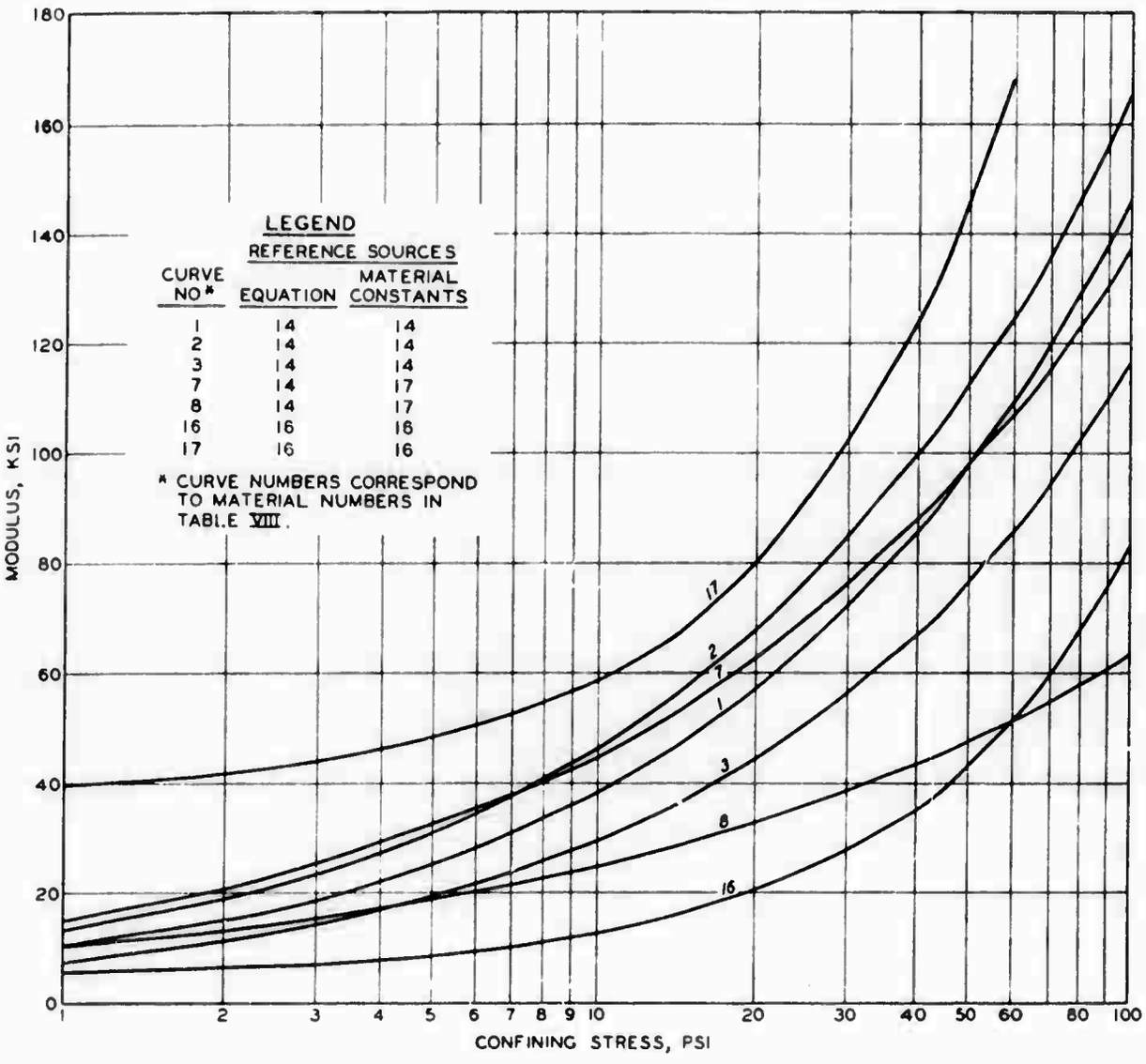

Figure 20. Elastic modulus versus confining pressure.

tests, the lean clay plus cement and the lean clay plus lime specimens were 4.0 in. in diameter by 2.5 in. in thickness. Because the clayey gravelly sand contained gravel exceeding the No. 4 sieve size, it was necessary to use a 6-in.-diam by 4.5-in.-high CBR mold. All specimens were impact-compacted in the laboratory to comparable densities and moisture conditions of the previously trafficked stabilized test sections at WES.

A major problem encountered in the tensile tests was the accurate measurement of the horizontal deformations, which were often in the order of magnitude of 0.0004 in. at failure. As a result of this difficulty, the Poisson's ratios calculated from the experimental data were often unacceptable; i.e., negative values were obtained. The problem was not quite so acute for the 6-in.-diam specimens as the deformations were larger; however, it is still felt that these measurements are probably inaccurate.

The modulus of elasticity and Poisson's ratio values as determined by indirect tensile tests are presented in table IX. In general, the values listed represent the average of results of three tests. In the table, elasticity values based upon the horizontal deformations E_h and vertical deformations E_v are given. Since the experimentally determined Poisson's ratios were unrealistic, an appropriate value for Poisson's ratio (0.25) was assumed and the E_h and E_v values were recalculated. These recalculated values are listed as modified E_h and E_v. It was determined that modified E_v values would be more appropriate for use in this study. The basis for this decision was twofold:

(1) In pavement systems, the primary loads are applied vertically.

(2) E_v values are relatively insensitive to Poisson's ratio; therefore, use of E_v would avoid the previously mentioned problem of experimentally determining Poisson's ratio. The test results for E_h and E_v indicated

Table IX

Tensile Strength and Modulus of Elasticity of Cement-Stabilized Materials

Material	Indirect Tensile Strength psi	Modulus of Elasticity, psi*			
		Determined by Test		Modified**	
		E_h	E_v	E_h	E_v
Lean clay - 3% cement	14.7	$0.85 \times 1\ 10^4$	0.85×10^4	0.99×10^4	0.84×10^4
10% cement	42.5	5.91×10^4	4.69×10^4	3.09×10^5	4.69×10^4
3.5% lime	7.3	1.35×10^4	1.31×10^4	9.385×10^4	1.35×10^4
Clayey gravelly sand					
3% cement	18.4	3.13×10^4	3.11×10^4	2.77×10^4	3.11×10^4
10% cement	141	2.19×10^5	2.23×10^5	6.23×10^5	2.23×10^5

* E_h = modulus of elasticity based on horizontal deformation

E_v = modulus of elasticity based on vertical deformation

** Moduli calculated using $\nu = 0.25$

in table IX indicate that the specimens behaved isotropically; i.e., E_h and E_v are approximately equal.

The E-values indicated above were used as constants in the linear analysis. For the nonlinear analysis, only the cement-stabilized lean clay was considered. In characterizing this material, the expression used was $E = K\left(K_2 - \log \sigma_d\right) I_1^{K_3}$, which was developed at the University of California (reference 21).

e. Heavy Clay Subgrade

Wang et al. (reference 22), in characterizing a highly plastic subgrade material, developed the expression for modulus of resilient deformation M_R as

$$M_R = K_1 + (K_2 - \sigma_d)\, K_3 \text{ for } \sigma_d < K_2 \tag{4}$$

$$M_R = K_1 + (\sigma_d - K_2)\, K_4 \text{ for } \sigma_d > K_2 \tag{5}$$

where K_1, K_2, K_3, and K_4 are material constants and σ_d is deviator stress. In earlier work by Heukelom and Foster (reference 23), a simpler relationship was found between dynamic E-modulus and CBR, which was given in the reference as

$$E(MN^2) = 110(CBR)$$

or as reported by Peattie (reference 24)

$$E(psi) = 1560(CBR)$$

Of the two means of determining a usable expression for subgrade modulus for pavement analysis, it appears that the more tractable expression of Heukelom and Foster would better suffice, at least in the initial phase of this study. The use of deviator or confining stress-dependent expressions did not appear feasible for this study. The linear expression of E = f(CBR) was also used in earlier works (reference 25), and it was decided that such an expression should be adopted for structural characterization of subgrade

material in this study. Selection of a suitable value for Poisson's ratio was based on the commonly accepted value of $\nu = 0.5$ for a saturated clay. Wang et al. (reference 22) used a value of $\nu = 0.48$ for a similar subgrade material.

For this, therefore, it was concluded that, for convenience, values for subgrade modulus would be estimated by the expression E(psi) = 1500(CBR) and that the value of Poisson's ratio should be taken as 0.5.

f. Remarks

It should be recognized that the values of modulus of elasticity and Poisson's ratio for the various materials indicated above are primarily base data used for comparison of analytical procedures. For this analysis, the effect on predicted response of varying the base value for modulus was also studied in several instances.

SECTION IV

RESULTS OF ANALYSIS

1. GENERAL

The programs utilized in this study basically compute stresses, strains, and deformation. It has been shown by other investigators that the three programs produce results that will compare very closely. Consider the comparison by Pichumani (reference 10) shown in figures 21 and 22, in which the results of the layer theory program are compared with results of a linearly elastic finite element program. Pichumani attributes the difference primarily to the fact that the finite element analysis has finite boundaries; whereas in the layered analysis, the boundaries extend infinitely in both the vertical and the horizontal directions. Thus the evidence is that for analogous problems, both programs will, within significant accuracy, give the same results. This evidence was born out in this analysis. Consider the following comparison of data from the structural layer study (360-kip 12-wheel assembly) with results from CHEVRON and AFPAV analyses.

Test Item	Maximum Surface Deflection, in.			Maximum Vertical Subgrade Stress, psi		
	CHEVRON	AFPAV	Measured	CHEVRON	AFPAV	Measured
1	0.225	0.178	0.24	17.7	19.5	20.4
2	0.159	0.143	0.25	11.7	15.8	18.4
4	0.128	0.101	0.19	6.5	12.3	10.0

As indicated above, the absolute difference between the layer theory (CHEVRON) results and those from AFPAV is not large and is attributable to the difference in the assumed boundaries.

This study was conducted almost entirely utilizing linearly elastic material characterization with the CHEVRON and AFPAV programs. Limited work was

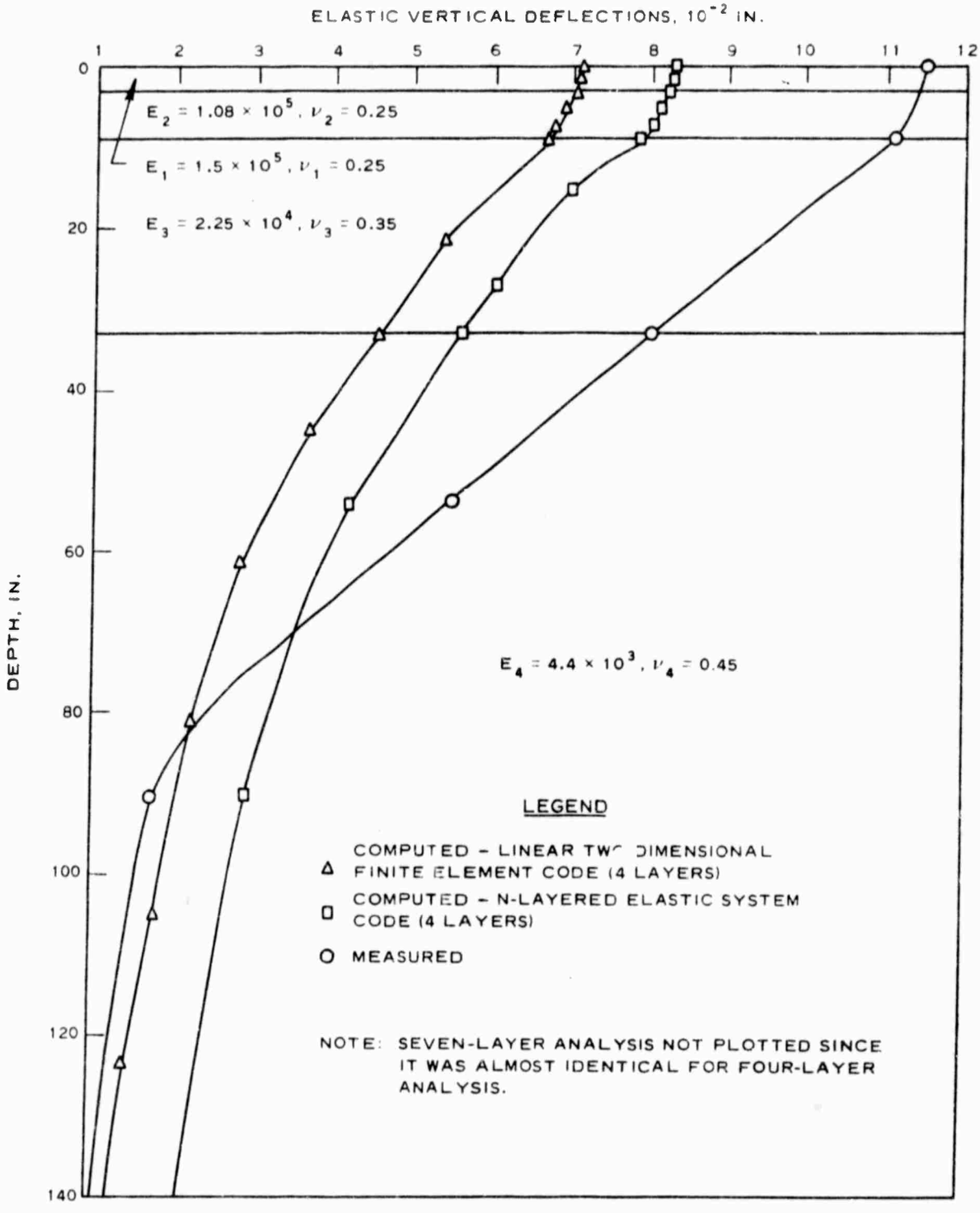

Figure 31. Measured and computed deflection due to a single-wheel load (C-5A 30 kips per wheel) versus depth for item 4, MWHGL test section (from reference 10)

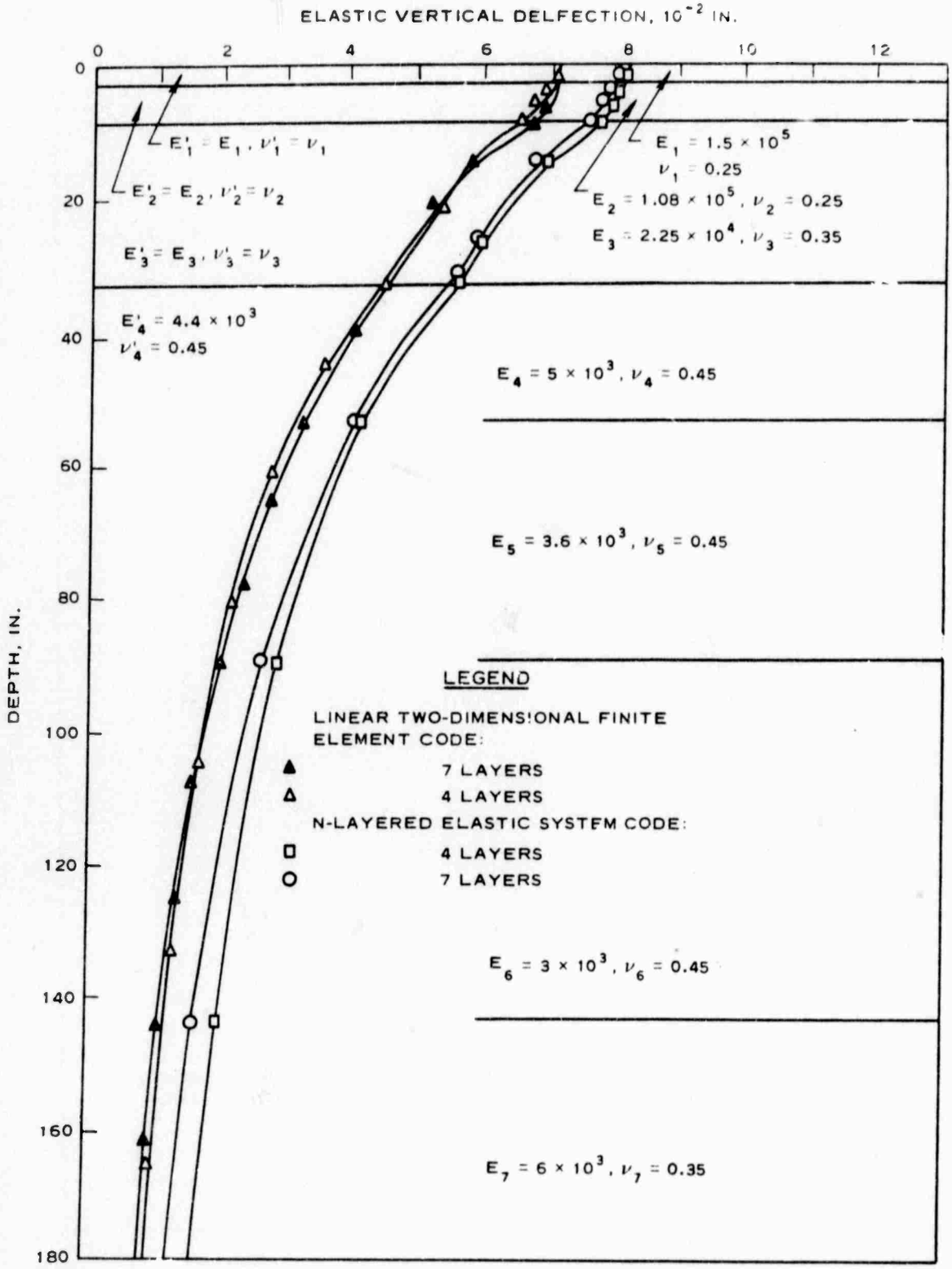

Figure 22. Deflections computed from four- and seven-layer analyses for a single-wheel load (C-5A 30 kips per wheel) versus depth for item 4, MWHGL test section (from reference 10).

conducted using the FEPAVE II program for nonlinear material properties, and the significance of this type of analysis will be discussed. Analysis of the pavement in each test section is indicated under the appropriate descriptive title for the test section.

2. MWHGL TESTS

The basis for analysis of the MWHGL data was the nonlinear characterization of the granular materials. In this analysis the response of the pavement systems to single-wheel loading was simulated by the use of the FEPAVE II finite element program. Since the finite element program was limited to single-wheel-load effects, no multiple-wheel-load data were considered for this analysis. The summary of the results is contained in table X.

Table X

Summary of Analysis of MWHGL Data
Using FEPAVE II Program

		Measured	Computed Response*			
Item	Load Kips	Deflection in.	Number of Load Increments**	Deflection in.	Stress σ psi	Strain ε in./in.
1	30	0.12	3	0.18	17.0	0.0022
	50	0.42	3	0.32	31.0	0.0034
	50	0.42	6	0.31	25.0	0.0030
2	30	0.11	3	0.19	12.5	0.0015
	50	0.23	3	0.36	18.5	0.0023
	50	0.23	6	0.29	14.0	0.0017
3	75	--	3	0.57	16.5	0.0020
	75	--	6	0.48	17.5	0.0020

* Deflection: surface deflection under center of tire.
Stress and strain: represents response at a point at top of subgrade under center of the tire.

** Number of load increments used in the finite element program.

Only comparison of computed and measured surface deflections were made for the MWHGL test section. Based on this limited analysis and previous

linear analyses conducted by others (references 3 and 10), it is possible to conclude that the nonlinear analysis gives results that compare more favorably with the measured results than does linear analysis. In the case of linear analysis, the deformation and stresses are underestimated; while it appears that in the nonlinear analysis, the deformation and stresses are overestimated.

In considering layered analysis versus nonlinear analysis, it might be interesting to look at the variation of the modulus values within a granular layer. Figure 23 shows the variation of the E-modulus after application of the first load increment (8.3 kips) of the 50-kip loading in the analysis of item 1. As can be seen, the variation in the horizontal direction is greater than the variation in the vertical direction. The variation in the horizontal direction illustrates the error made in use of layered theory. The nonlinear behavior of the pavement materials is probably the major factor in the inability for layered theory to accurately simulate pavement behavior.

3. BITUMINOUS BASE COURSE STUDY

The surface profiles were the only measured data used for verification of the CHEVRON analysis of the bituminous-stabilized base test section. When computed deflection is compared with measured deflection, it is seen that for each of the four items, the computed deflection is smaller than the measured deflection by an average factor of 4.2. Examples of this poor correlation with measured data are shown in figures 24 and 25. A summary of the results of the analysis of the bituminous base test section is given in table XI.

If the analysis is examined, it is seen that in most of the test items, the subgrade was overstressed and that yielding would have occurred. In addition the properties of asphalt paving materials are recognized as being highly temperature- and time-dependent. Thus the pavement temperature and the time required for taking the static deformation measurements would have had

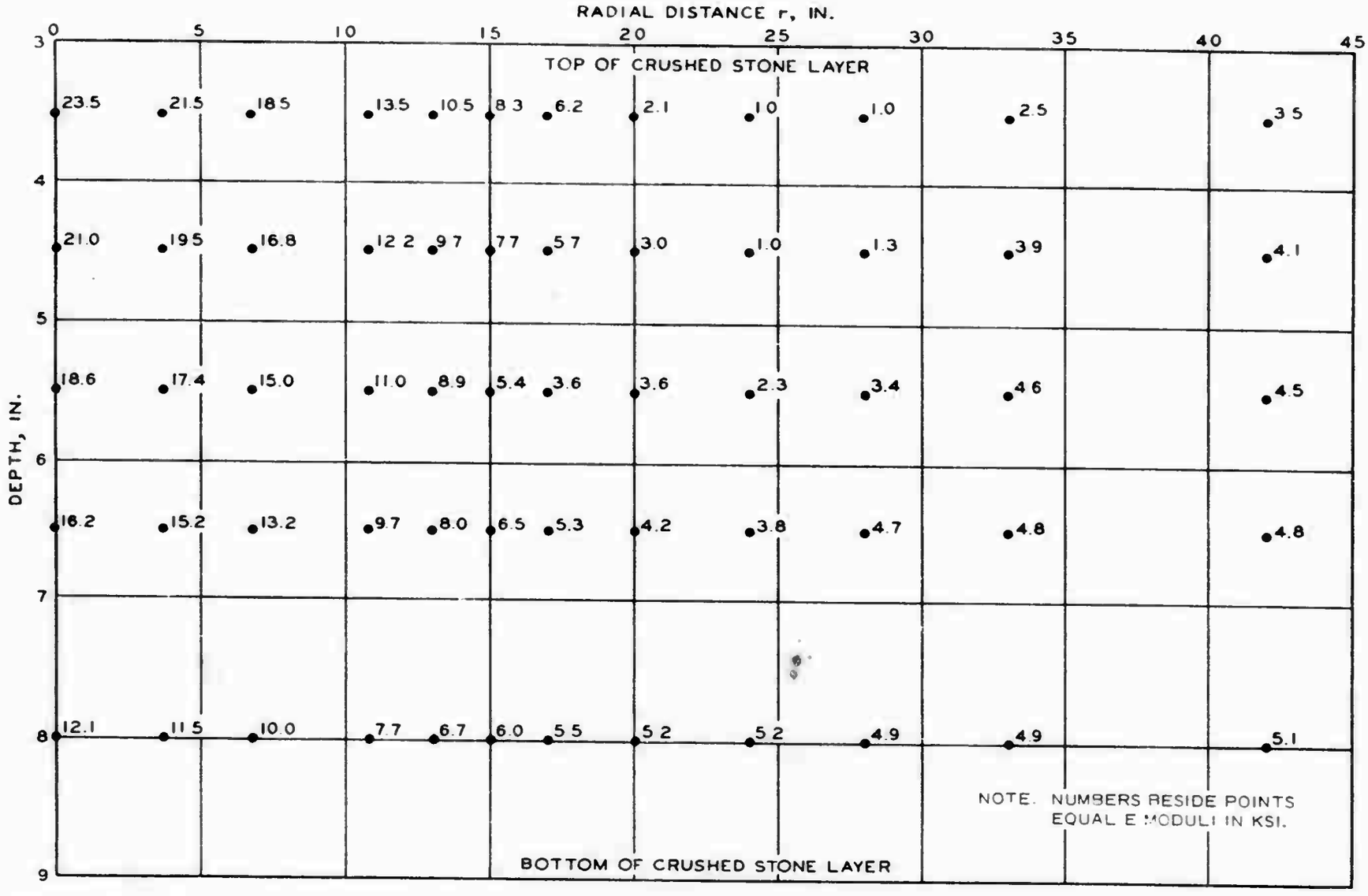

Figure 23. E-modulus values for crushed stone base course, item 1, MWHGL test section, after one load increment (8.3 kips) of 50-kip single-wheel load (FEPAVE II program).

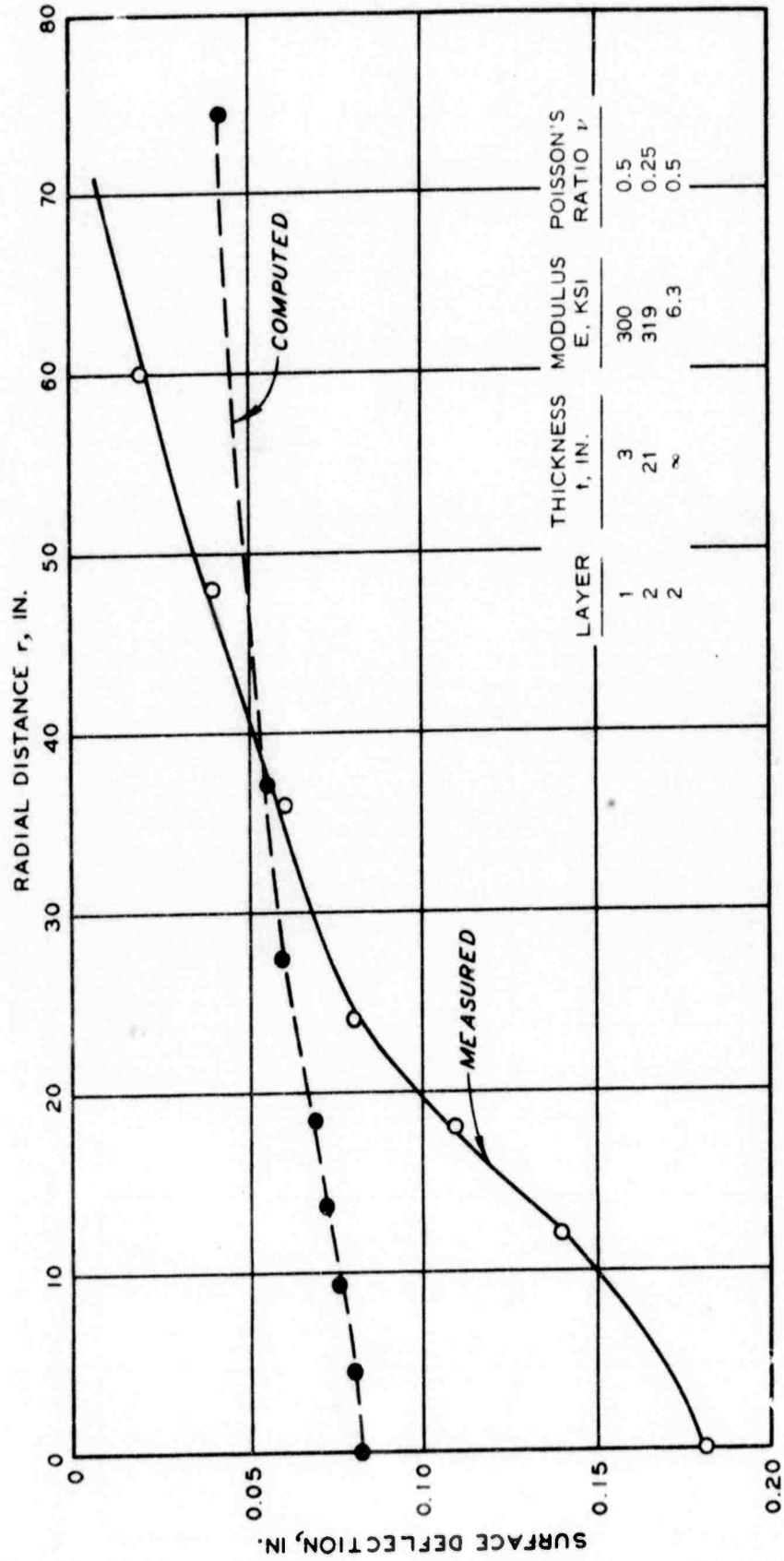

Figure 24. Measured and computed surface deflections, 75-kip single-wheel assembly on item 3, bituminous base course test section (CHEVRON program).

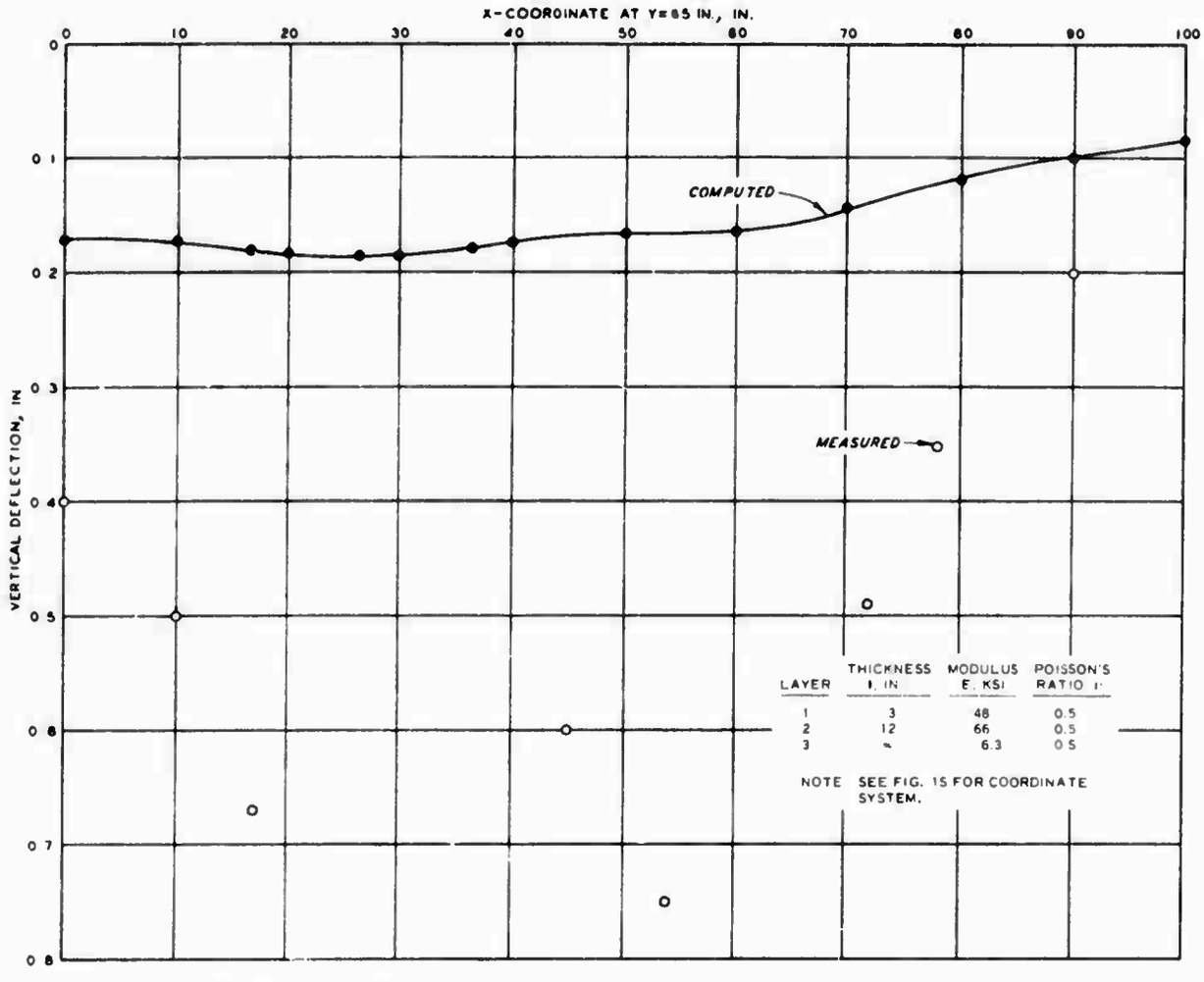

Figure 25. Measured and computed vertical deflection on X-coordinate at Y = 65 in. for 360-kip, 12-wheel assembly on item 2, bituminous base course test section (CHEVRON program).

Table XI

Summary of Analyses of Data from
Bituminous Base Course Study - CHEVRON Program

Item	Load Kips	Measured Deflection in.	Computed* Deflection in.	Vertical Stress σ_v psi	Vertical Strain ϵ_v in./in.	Horizontal Stress σ_H psi	Horizontal Strain ϵ_H in./in.
1	30	--	0.092	14.5	0.0018	-110	0.0009
	75	1.18	0.23	36	0.0046	-280	0.0023
	360	0.22	0.90	18	0.0018	-114	0.001
2	30	--	0.075	13.0	0.0014	-123	0.0007
	75	1.22	0.22	40	0.0045	-258	0.0023
	360	0.81	0.19	17	0.0013	-128	0.0008
3	30	--	0.061	8.4	0.0009	-38	0.0005
	75	0.61	0.12	18	0.0024	-126	0.00066
	360	0.58	0.15	13	0.0010	-43.7	0.0007
4	30	--	0.14	12.5	0.0016	-150	0.0612
	75	0.68	0.19	25	0.0043	-180	0.002
	360	0.42	0.21	16	0.0016	-138	0.0014

* Entries represent maximum values computed for the following locations:

Deflection	Surface
Vertical stress and strain	Top of subgrade
Horizontal stress and strain	Bottom of stabilized base

Negative values represent tensile stress.

considerable influence on the measurements. Certainly the deflection caused by the moving traffic loads would be much less than the deflection under the static load. Thus the computed pavement response probably more closely simulates the pavement response to a moving load than is indicated by the comparison with the static loading.

Two significant parameters in the performance of asphalt pavements are the tensile strength of the material and the tensile stress developed under loadings. Consider the comparison presented in the table XII.

Table XII

Comparison of Tensile Strength and Stress with Pavement Performance

Item	Layer	Tensile Strength* psi	Tensile Stress, psi		Strength/Stress		Coverages to Failure	
			75 kip	360 kip	75 kip	360 kip	75 kip	360 kip
1	Surface	-124	Compression	Compression	-	-	6	98
	Base	-	280	114	0.44	1.09		
2	Surface	-108	Compression	Compression	-	-	8	425
	Base	-106	258	128	0.41	0.78		
3	Surface	-97	Compression	-	-	-	100	2198
	Base	-57	Compression	6	-	-		
	Subbase	-89	126	44	0.71	2.00		
4	Surface	-119	Compression	Compression	-	-	100	734
	Base	-106	180	138	0.59	0.75		

*Tensile strength values were taken from reference 4.

4. STRUCTURAL LAYERS STUDY

a. Item 1

Analysis of item 1 was conducted utilizing linear elastic theory for 30-kip and 50-kip single-wheel loadings and 360-kip 12-wheel loadings. Instrumentation data were available for the 30-kip single-wheel loading and 360-kip

12-wheel loading. A nonlinear analysis was conducted for the 50-kip single-wheel loading. A summary of certain computed parameters are given in table XIII.

For the 30-kip single-wheel load, comparisons between computed and measured parameters are provided in figures 26 and 27. These figures indicate that closer agreement is obtained when a lower modulus is used for the asphalt surfacing. The shapes of the curves also indicate that smaller modulus values exist in the upper pavement layers than were used in the analysis.

Figure 28 shows the surface deflection contours resulting from loading by the 360-kip 12-wheel assembly. As shown, the maximum deflection occurred under the tire located at coordinates x = 26.5 in.; y = 65 in. The contours of the vertical stress at the top of the subgrade are shown in figure 29. The maximum stress occurred under the same tire as the maximum deflection.

For a comparison of computed versus measured surface deflections for the 360-kip 12-wheel load, profiles of the surface deflection along the section of x = 0 in. and along the section of y = 65 in. were plotted. These profiles, shown in figure 30, indicate good agreement between computed and measured deflections. The difference in the computed and measured deflections appears to be caused more by errors in the assumed subgrade modulus than by errors in the moduli for the upper material layers (as was the case of the single-wheel loading).

Figure 31 provides a comparison between the vertical stress distribution with depth for a single-wheel loading and for a 12-wheel loading. The measured vertical stress at top of the subgrade was plotted as an additional comparison. The difference between the vertical stress distribution is as would be expected; i.e., the difference between the vertical stress caused by the single-wheel and the 12-wheel assembly increased with depth.

Table XIII

Summary of Analyses of Structural Layers Test Section Item 1 Data

Assembly	Load kips	Method of Determination	Deflection in.	Subgrade		Stabilized Material	
				Vertical Stress σ_v psi	Vertical Strain ϵ_v in./in.	Horizontal Stress σ_H psi	Horizontal Strain σ_H in./in.
Single-wheel	30	CHEVRON (linear elastic)	0.112	12.4	0.0015	-9.5	-0.00075
		Measured at 0 coverages	0.09	18.1	0.0063	-	-
	50	CHEVRON (linear elastic)	0.175	19.8	0.0024	-15.4	-0.0012
		FEPAVE II (nonlinear base)	0.207	25.0	0.0031	-10.5	-0.001
		Measured at 0 coverages	0.13	-	-	-	-
Twelve-wheel	360	CHEVRON (linear elastic)	0.206	15.9	0.0015	-11.3	-0.001
		Measured at 0 coverages	0.24	20.4	0.0065	-	-

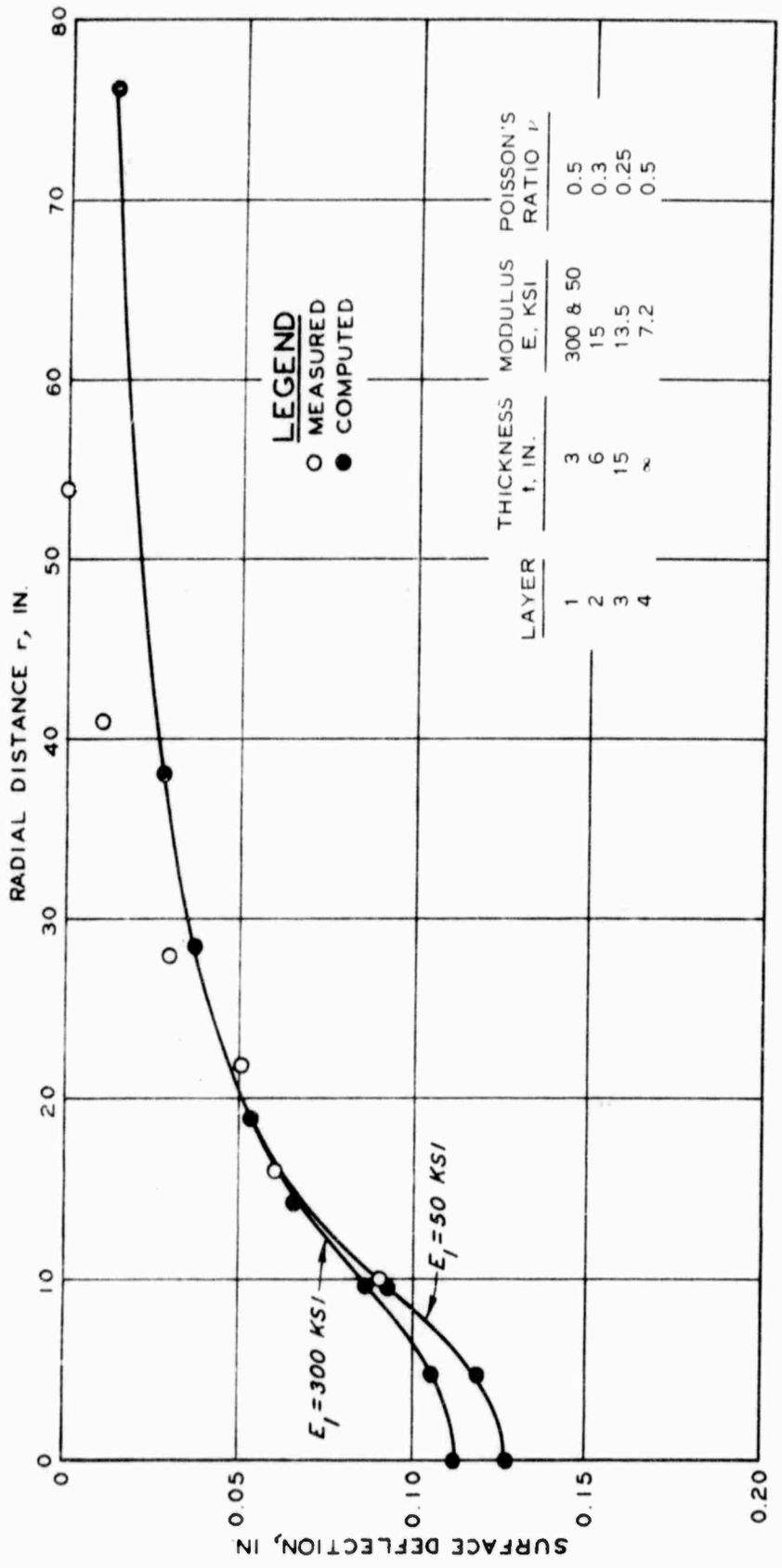

Figure 26. Measured and computed surface deflections for 30-kip single-wheel load on item 1, structural layer test section (CHEVRON program with E_1 = 300 and 50 ksi).

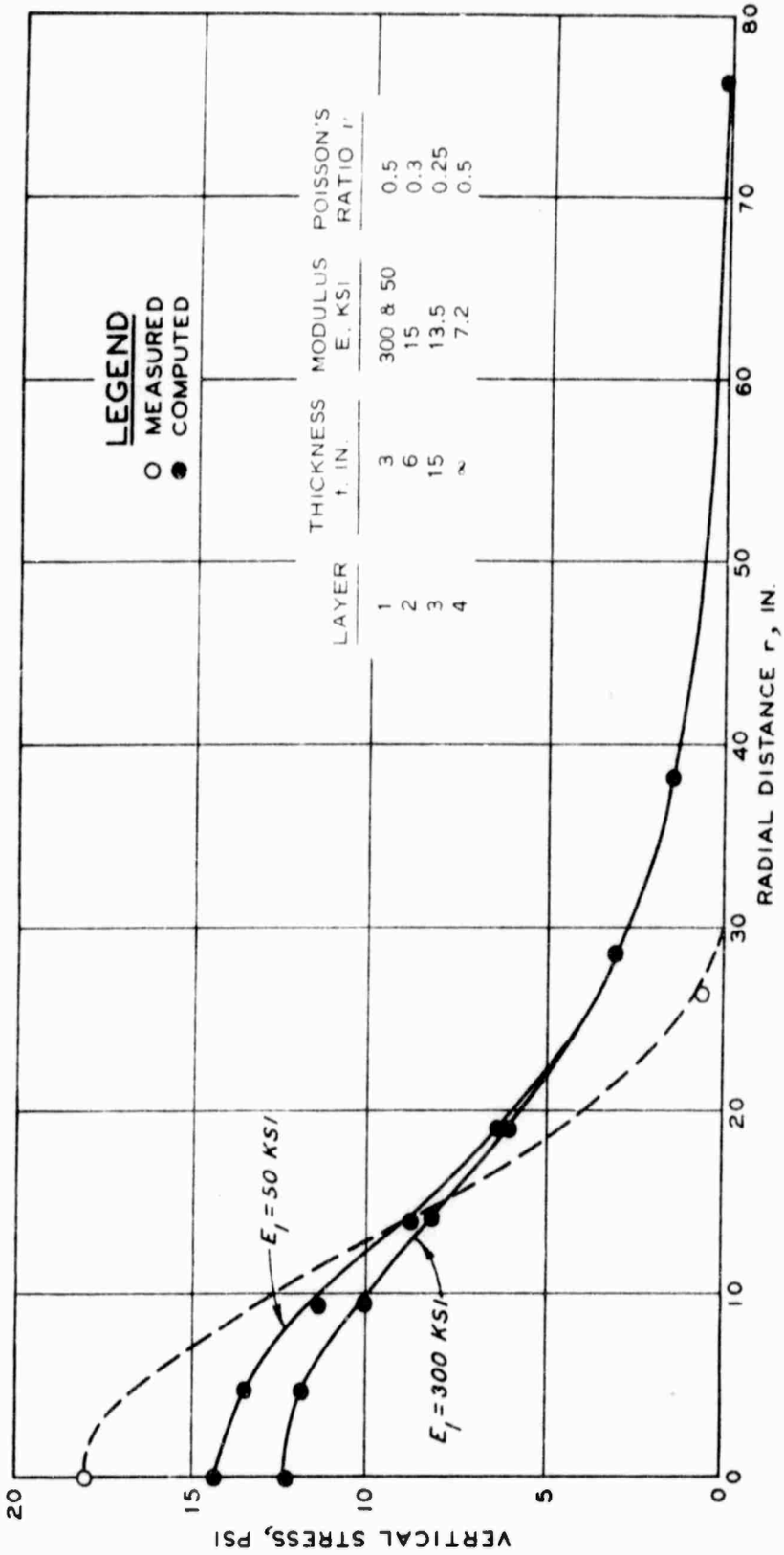

Figure 27. Measured and computed vertical stress at the top of the subgrade for 30-kip single-wheel assembly on item 1, structural layer test section (CHEVRON program with E_1 = 300 and 50 ksi).

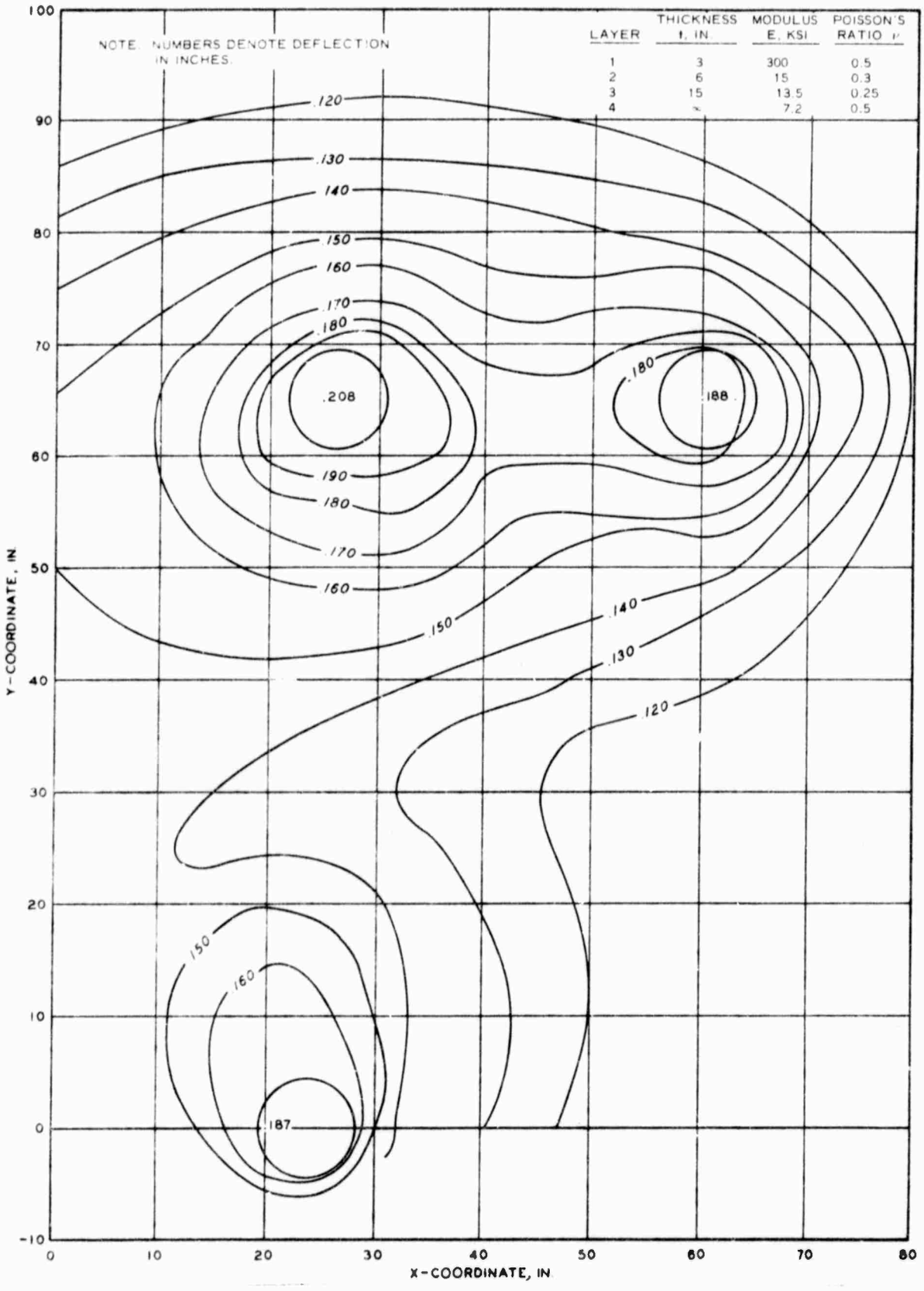

Figure 28. Computed surface deflection contours for 360-kip 12-wheel assembly on item 1, structural layer test section (CHEVRON program).

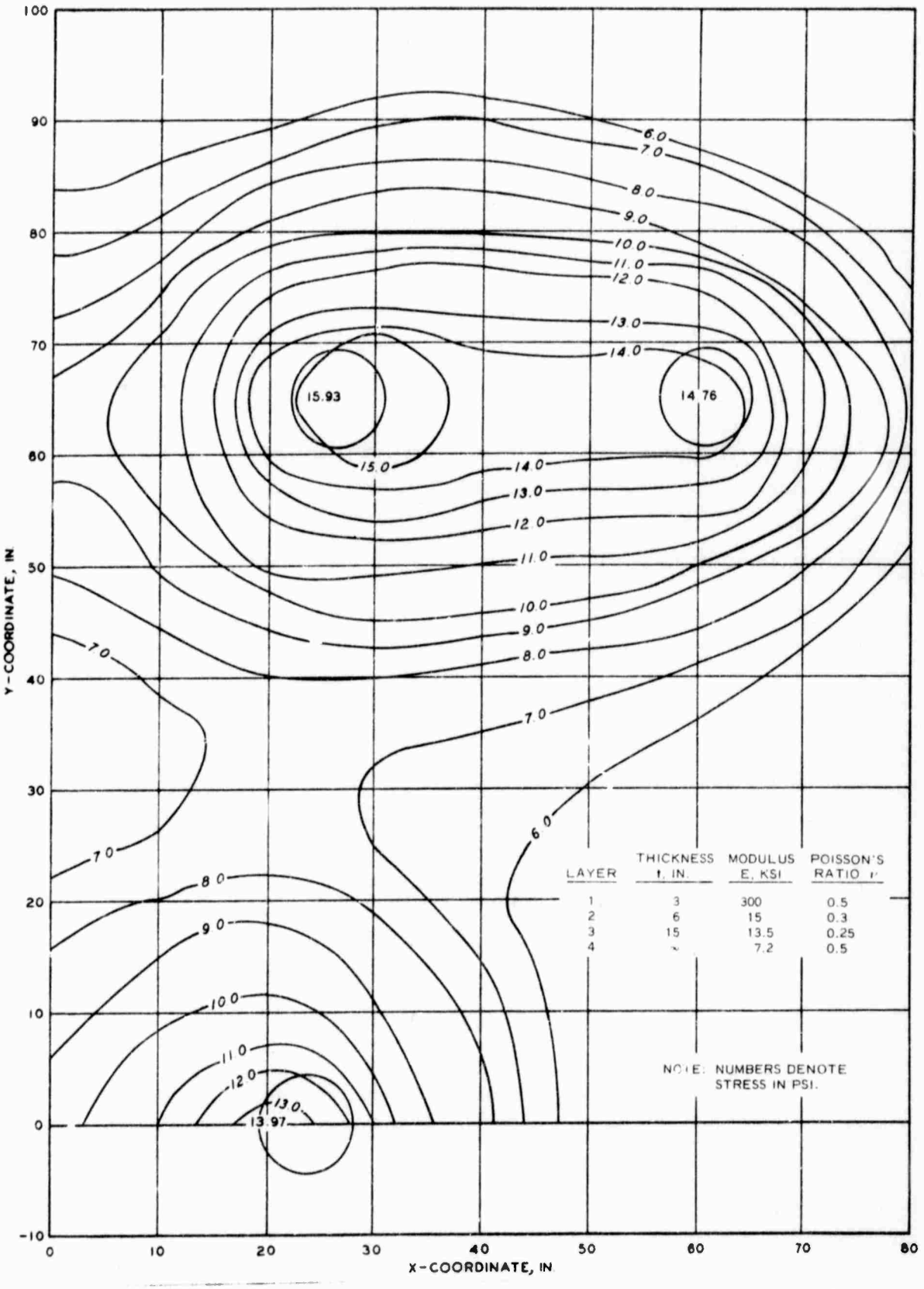

Figure 29. Computed stress contours at the top of the subgrade for 360-kip 12-wheel assembly on item 1, structural layer test section (CHEVRON program).

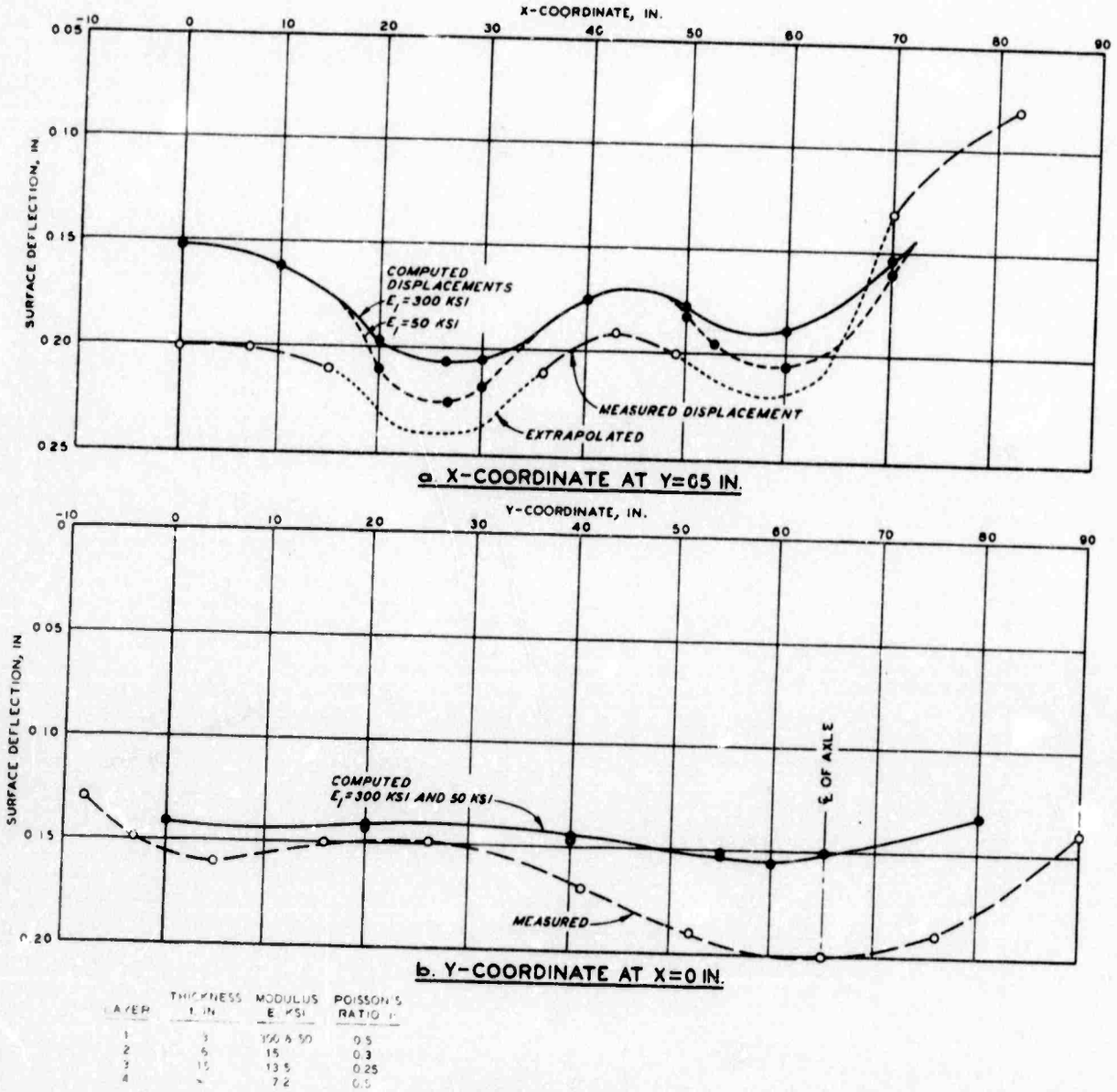

LAYER	THICKNESS t, IN	MODULUS E, KSI	POISSON'S RATIO μ
1	3	300 & 50	0.5
2	6	15	0.3
3	15	13.5	0.25
4	∞	7.2	0.5

Figure 30. Measured and computed surface deflections for section x = 0 in. and y = 65 in. for 360-kip 12-wheel assembly on item 1, structural layer test section (CHEVRON program E_1 = 300 and 50 ksi).

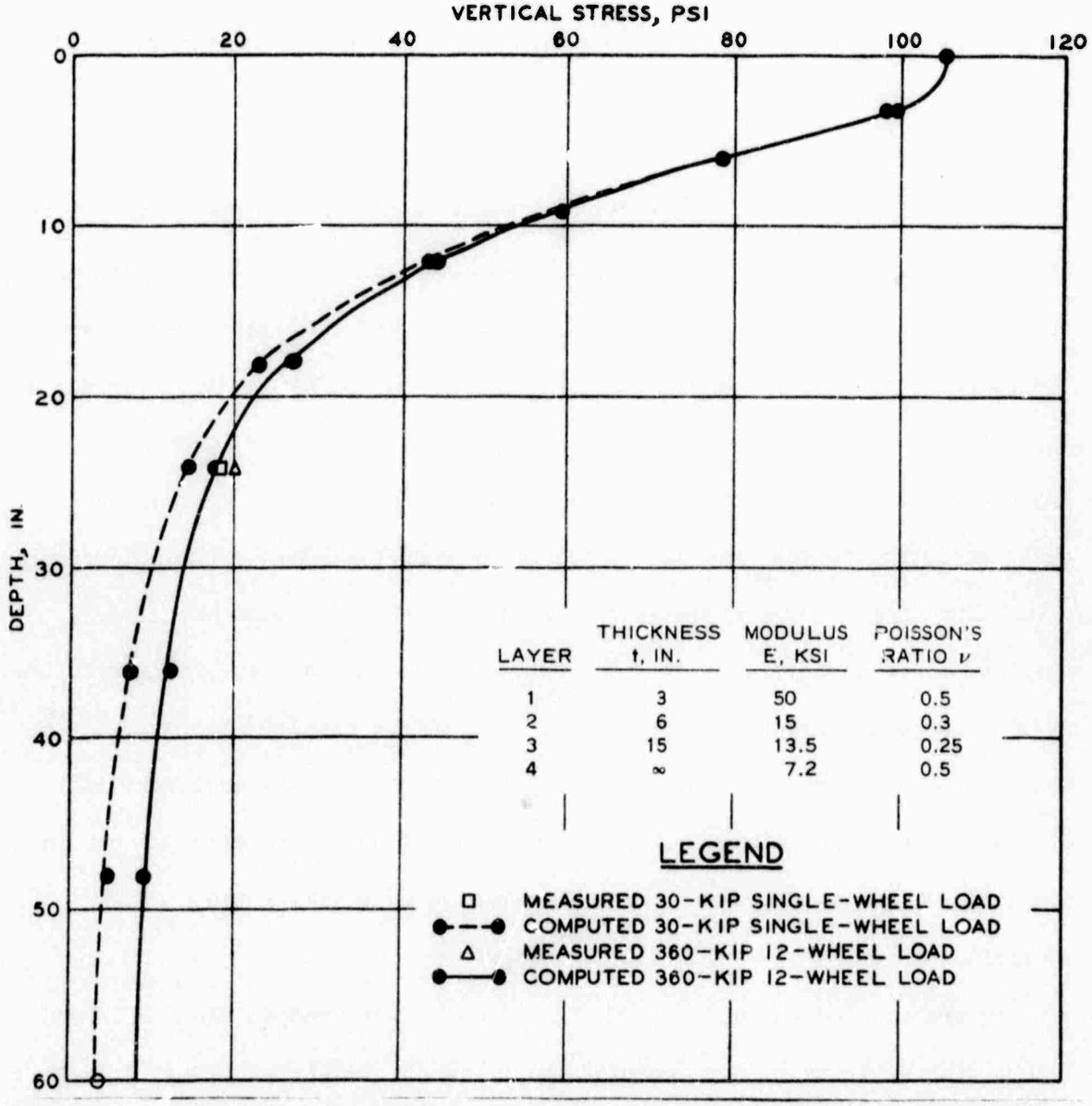

Figure 31. Measured and computed vertical stress distribution versus depth for single- and 12-wheel loadings at coordinate x = 26.5 in. and y = 65 in. on item 1, structural layer test section (CHEVRON program).

The magnitude and direction of the maximum tensile stresses at the bottom of the stabilized layer for the 360-kip 12-wheel load are indicated in figure 32. Unlike the maximum deflection, the maximum tensile stress did not occur under the center of a tire but at the periphery. When the maximum computed tensile stress (16.3 psi) is compared with the tensile strength (7.3 psi), the implication is that cracking of the stabilized layer would occur under initial loading.

A comparison of measured vertical strains with computed vertical strains is provided by figure 33. The comparison of strains in the base layer indicated good correlation, but the strains computed for the stabilized layer and the subgrade are not in agreement with the measured strains. The poor agreement of the subgrade strains is not unreasonable, considering the assumed subgrade material properties. The correlations between CBR and E-moduli were based on small strains; whereas in the upper part of the subgrade, the strains were quite large. If a stress-strain curve of saturated buckshot clay is examined (reference 26), it is seen that the E-moduli vary inversely with the strain. A rough comparison of the E-modulus may be obtained by computing a modulus value from the measured vertical stress and the measured vertical strain. Using this procedure, a modulus value of approximately 3000 psi is computed, which is less than one-half of the value used for the section analysis.

No explanation can be offered for extension measured in the stabilized layer. The validity of the measured values is substantiated by the fact that the same type of behavior was observed in the other two stabilized layers. To the authors' knowledge, no similar response has been reported by other investigators. The significance of this response is unknown, but certainly this behavior deserves further investigation.

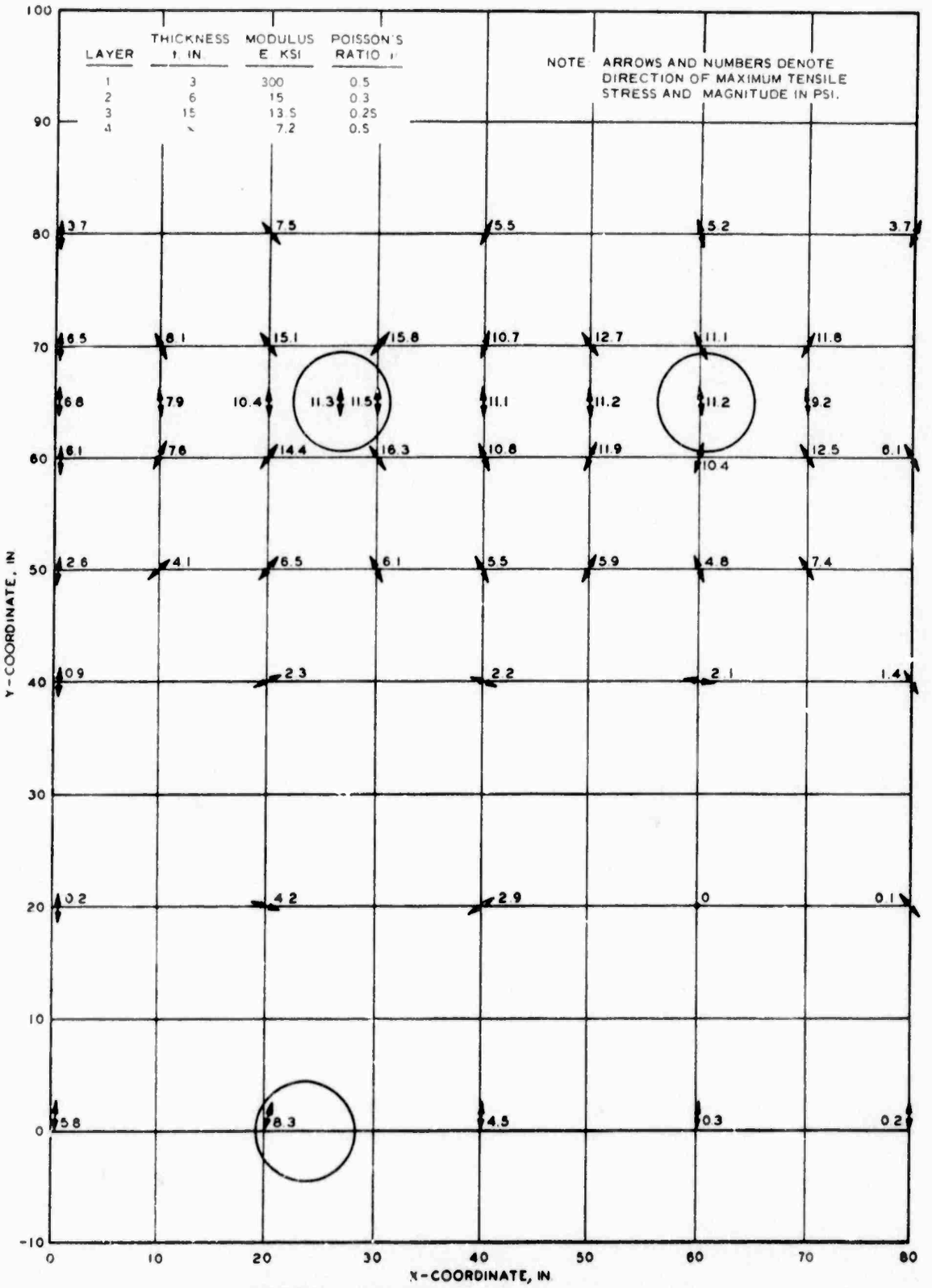

Figure 32. Computed maximum tensile stresses at bottom of stabilized layer for 360-kip 12-wheel assembly on item 1, structural layer test section (CHEVRON program).

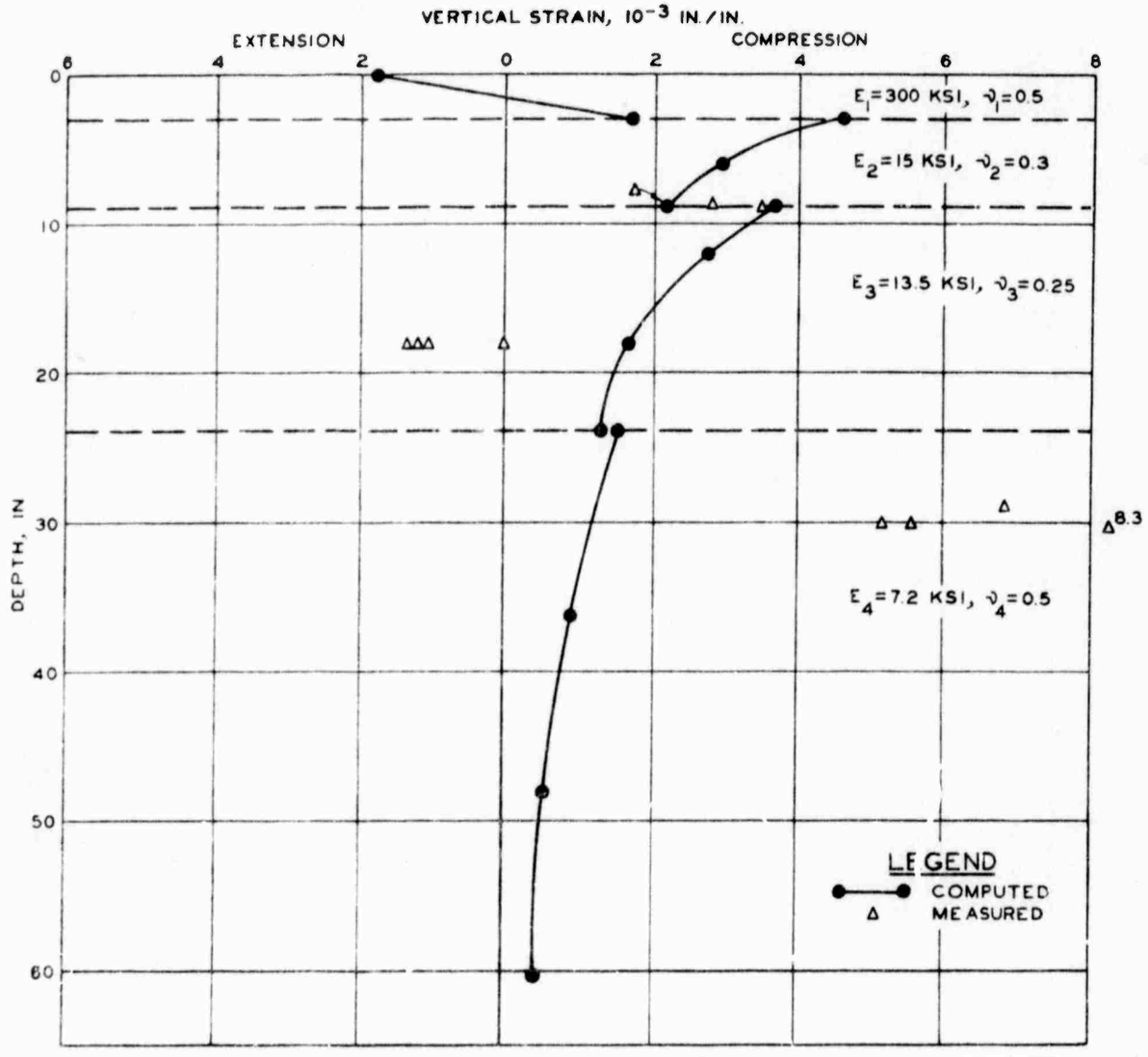

Figure 33. Measured and computed vertical strain versus depth for 30-kip single-wheel loading, item 1, stabilized layer test section (CHEVRON program).

b. Item 2

The analysis of item 2 was much the same as the analysis of item 1 and the same trends were indicated as were indicated in the analysis of item 1. An additional analysis of item 2 was performed utilizing nonlinear material characterization for the stabilized layer. The nonlinear characterization for the cement-stabilized clay was obtained from work by the University of California (reference 22). This nonlinear analysis provided an interesting comparison with the layered analysis and also provided some insight into why the layered theory did not correlate well with measured response. A summary of certain parameters for item 2 is given in table XIV.

Contours of surface deflection and vertical stress at the surface of the subgrade under the 360-kip 12-wheel load are shown in figures 34 and 35, respectively. Here, as was the case for item 1, the maximum values occurred under the interior tire. Figures 36 and 37 provide comparisons between computed and measured surface deflection and subgrade stresses for the same loading. The deflections computed by both the CHEVRON and the AFPAV programs are less than the measured values. Also the figures indicate that curvature of the measured profile is greater than the curvature of the computed profiles. Such discrepancies could be caused by the modulus values used in the computation of the upper part of the pavement structures being too high. This overestimation of modulus values could very well apply to the upper part of the subgrade as was suggested for item 1.

Figure 38 provides a presentation of the maximum tensile stress at the bottom of the stabilized layer under the 360-kip 12-wheel load. Again as was the case for item 1, the maximum value occurs at the periphery of the interior tire. Also when this maximum value (49.2 psi) is compared with the tensile strength (42.5 psi) of the stabilized material, the conclusion is that cracking

Table XIV

Summary of Analyses of Structural Layers Test Section Item 2 Data

Assembly	Load kips	Method of Determination	Deflection in.	Subgrade Vertical Stress σ_v psi	Subgrade Vertical Strain ϵ_v in./in.	Stabilized Layers Horizontal Stress σ_H psi	Stabilized Layers Horizontal Strain ϵ_H in./in.
Single-wheel	30	CHEVRON (linear elastic)	0.063	7.6	0.00093	-26.3	-0.00046
		FEPAVE II (nonlinear base)	0.082	15.5	0.0012	-22.0	-0.0005
		Measured at 0 coverages	0.075	18.1	0.0063	-	-
	50	CHEVRON (linear elastic)	0.104	12.7	0.0015	-43.8	0.00077
		FEPAVE II (nonlinear base)	0.115	24.5	0.0025	-58.0	-0.0005
		Measured at 0 coverages	0.14	-	-	-	-
Twelve-wheel	360	CHEVRON (linear elastic)	0.159	11.7	0.00055	-34.2	-0.00067
		AFPAV (linear elastic)	0.178	19.5	0.0030	-	-
		Measured at 0 coverages	0.25	18.4	0.0039		-0.003

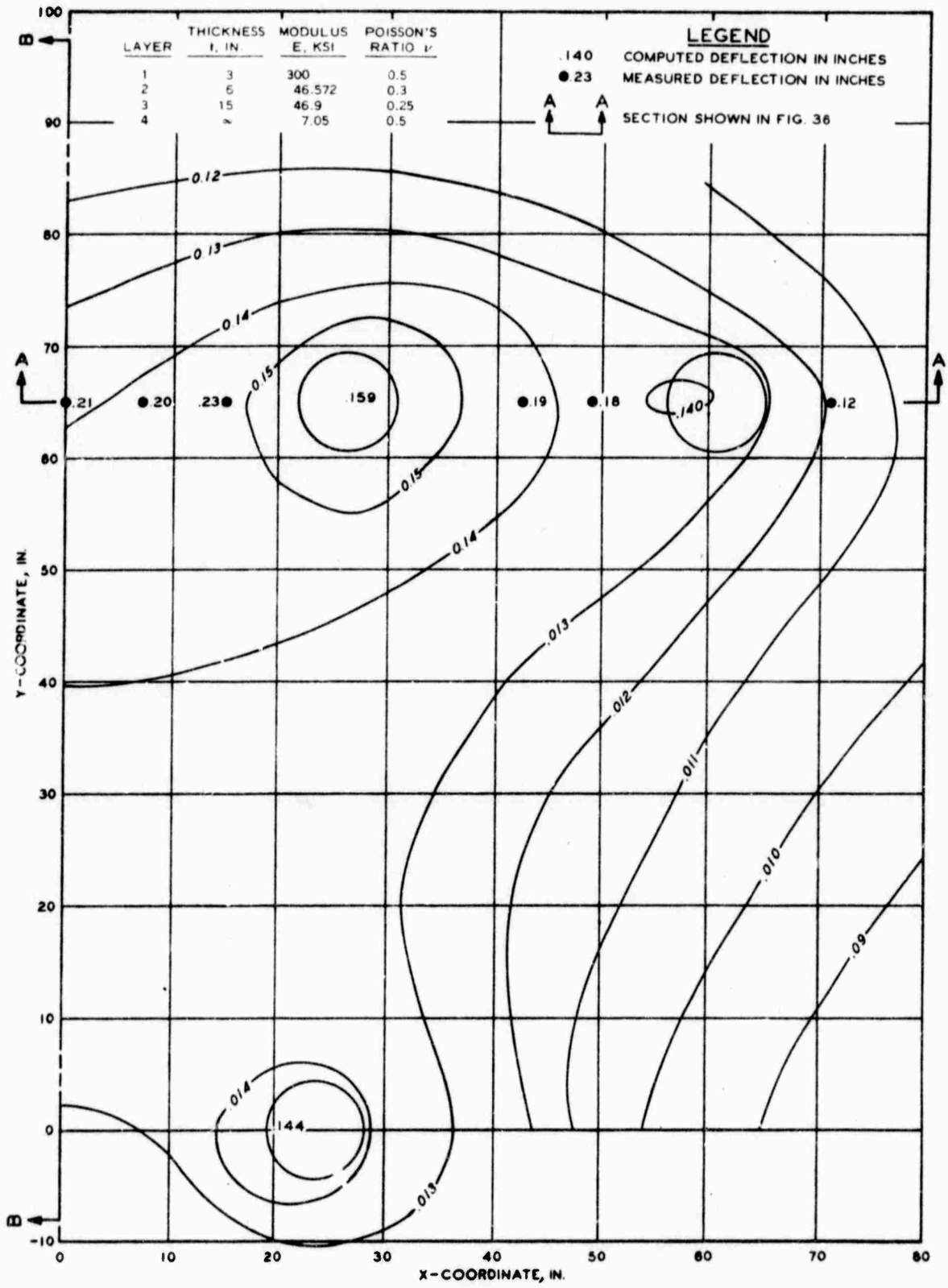

Figure 34. Measured and computed surface deflection contours for 360-kip 12-wheel assembly on item 2, structural layer test section (CHEVRON program).

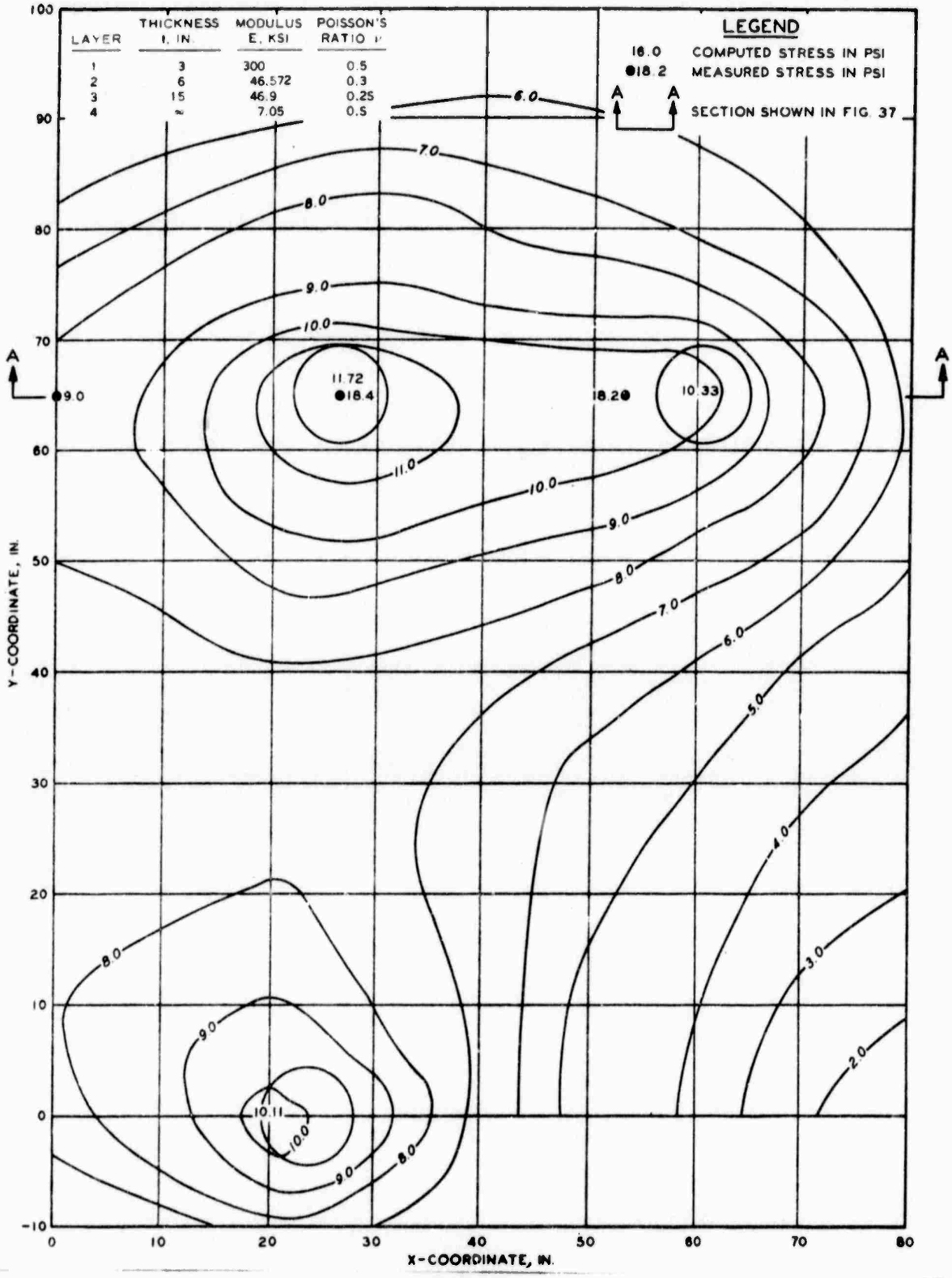

Figure 35. Measured and computed vertical stress contours at the top of the subgrade for 360-kip 12-wheel assembly on item 2, structural layer test section (CHEVRON program).

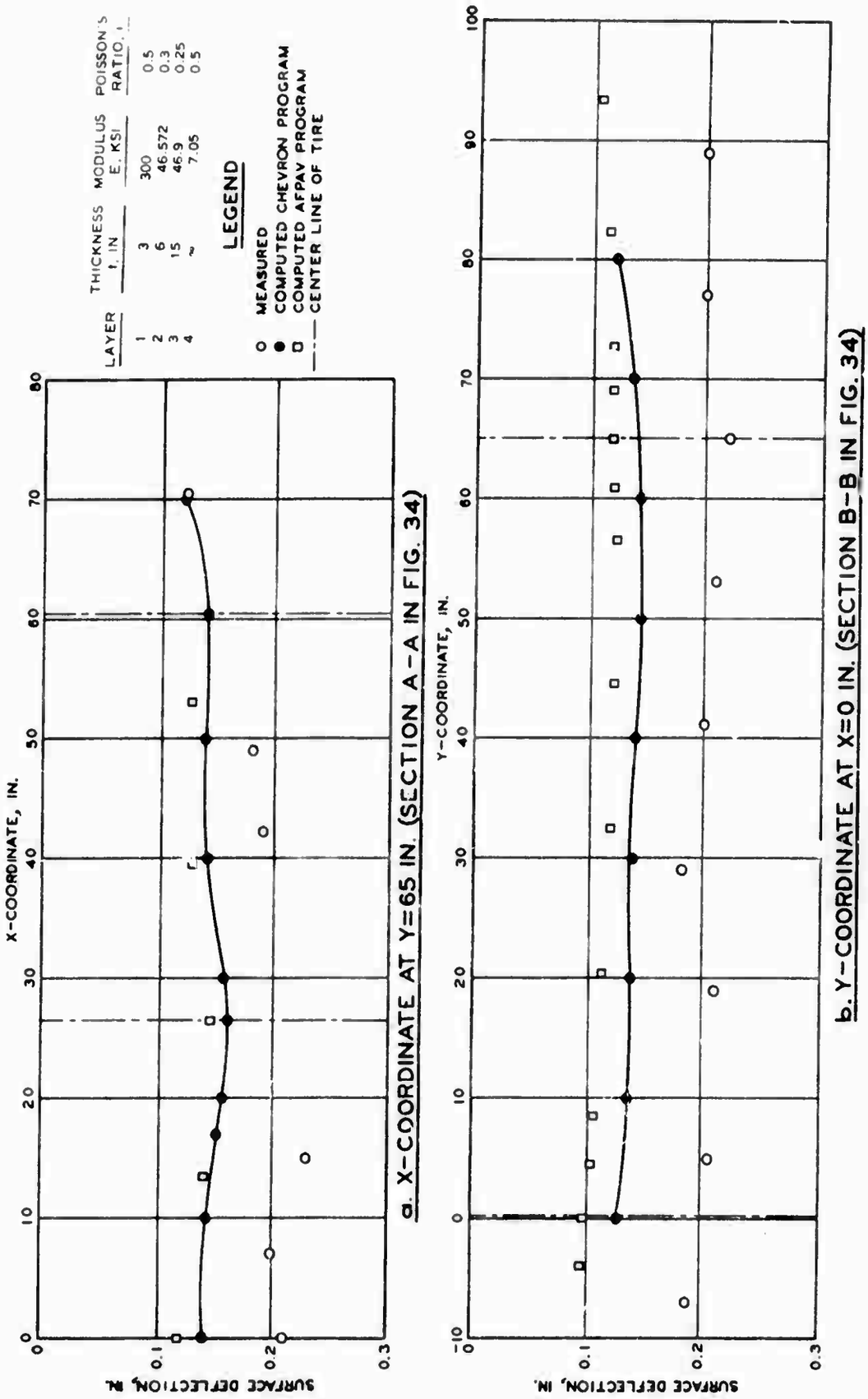

Figure 36. Measured and computed surface deflections for sections x = 0 in. and y = 65 in. for 360-kip 12-wheel assembly on item 2, structural layer test section (CHEVRON and AFPAV programs).

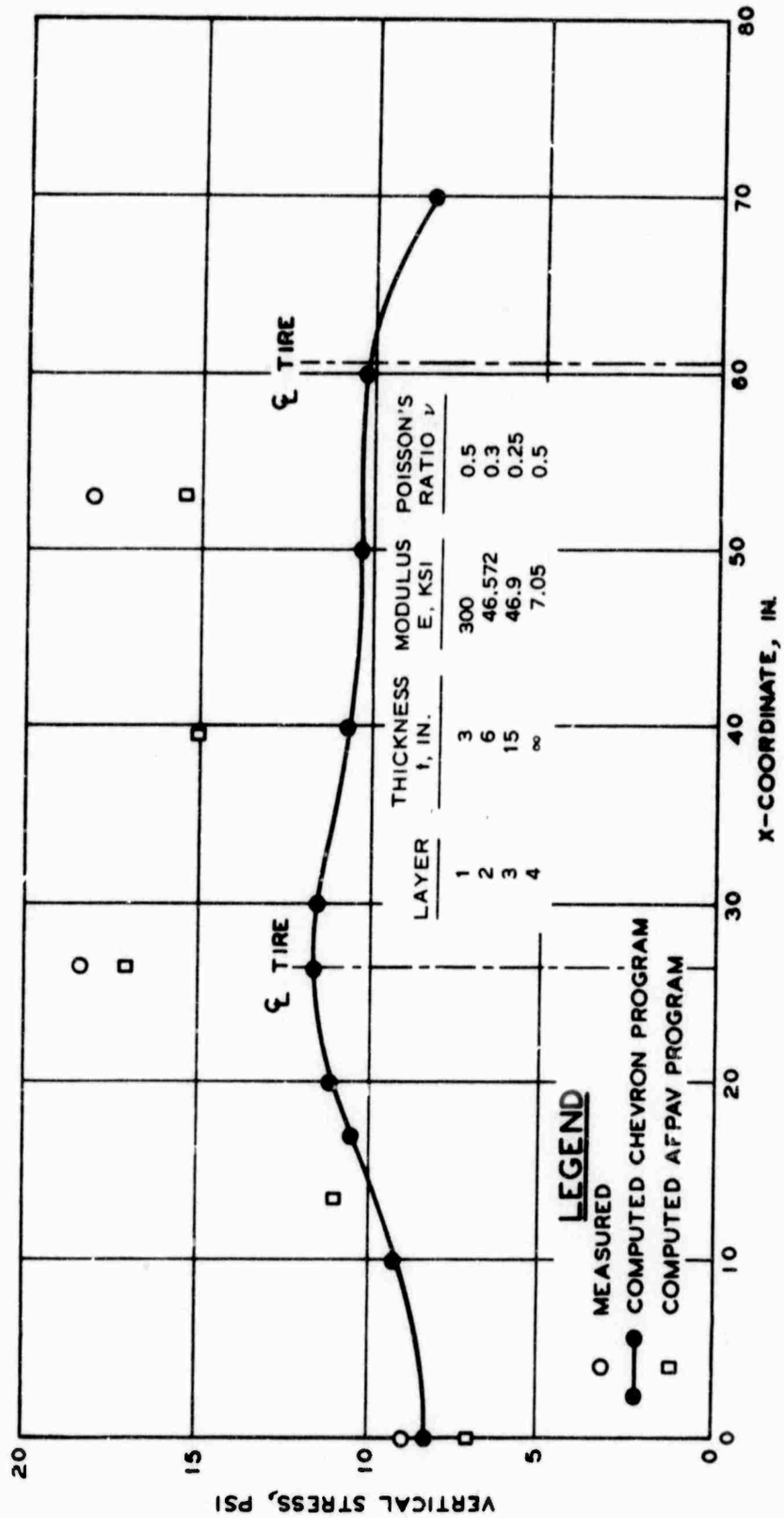

Figure 37. Measured and computed vertical stress at the top of the subgrade for x-coordinate at y = 65 in. (Section A-A in figure 35) for 360-kip 12-wheel assembly on item 2, structural layer test section (CHEVRON and AFPAV programs).

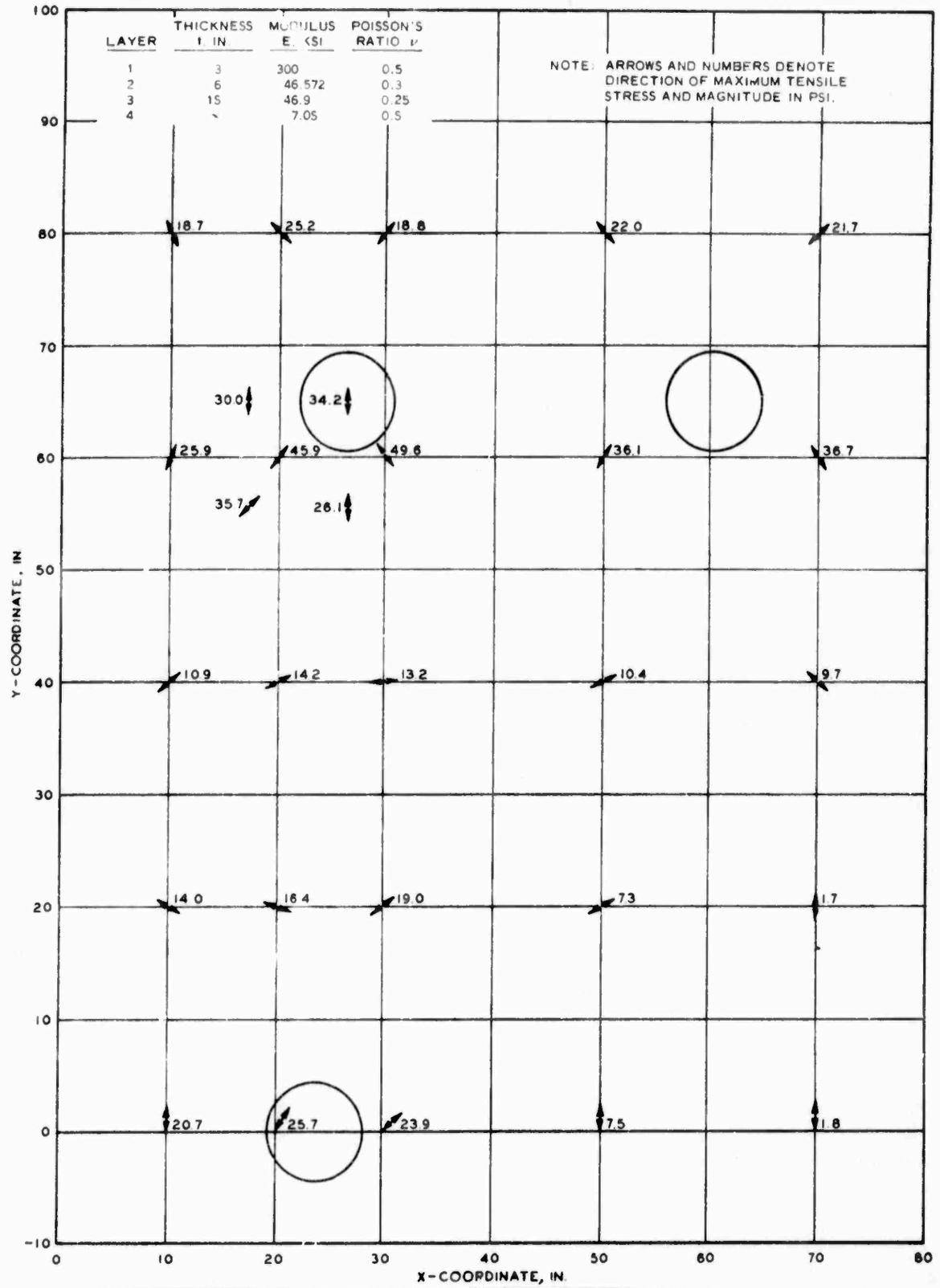

Figure 38. Computed maximum tensile stresses at bottom of stabilized layer for 360-kip 12-wheel assembly on item 2, structural layer test section (CHEVRON program).

of the stabilized material would occur but would be less severe than was anticipated for item 1.

The analysis of the single-wheel loading provided the opportunity for comparing the results of the linearly elastic analysis with the nonlinear analysis. In the nonlinear analysis, the base and the stabilized layer were considered to be nonlinear; the asphalt surfacing and the subgrade were considered to be linearly elastic and to have the same material properties as were used in the linear analysis. The base was characterized utilizing two separate functions: first, the modulus was characterized as a function of the minor principal stress by the equation $E = K_1 (\sigma_3)^{K_2}$ where $K_1 = 13{,}126$ and $K_2 = 0.55$; and the second, the modulus was characterized as a function of the first stress invariant by the equation $E = K_1 I_1^{K_2}$ where $K = 4{,}982.6$ and $K_2 = 0.45$. The values of the K's for the first and second characterizations came from work by Hicks (reference 14) and Barksdale*. The stabilized material was characterized as a function of the deviator stress and first stress invariant by the equation $E = K_1 (K_2 - \log \sigma_d) I_1^{K_3}$ where $K_1 = 1{,}372$, $K_2 = 5.07$, and $K_3 = 0.82$.

The results obtained from the two nonlinear analyses were almost identical. The surface deflection computed for the 30-kip single-wheel load utilizing the first characterization of the base was 0.082 in. as compared to 0.078 in. for the second characterization or only 5 percent difference. A comparison of the vertical distribution of stress is given in figure 39. Again it is seen that there is very little difference in the results obtained from the two methods of base characterization. No attempt was made to evaluate other

*Personal communication, Richard Barksdale to W. R. Barker, June 1971.

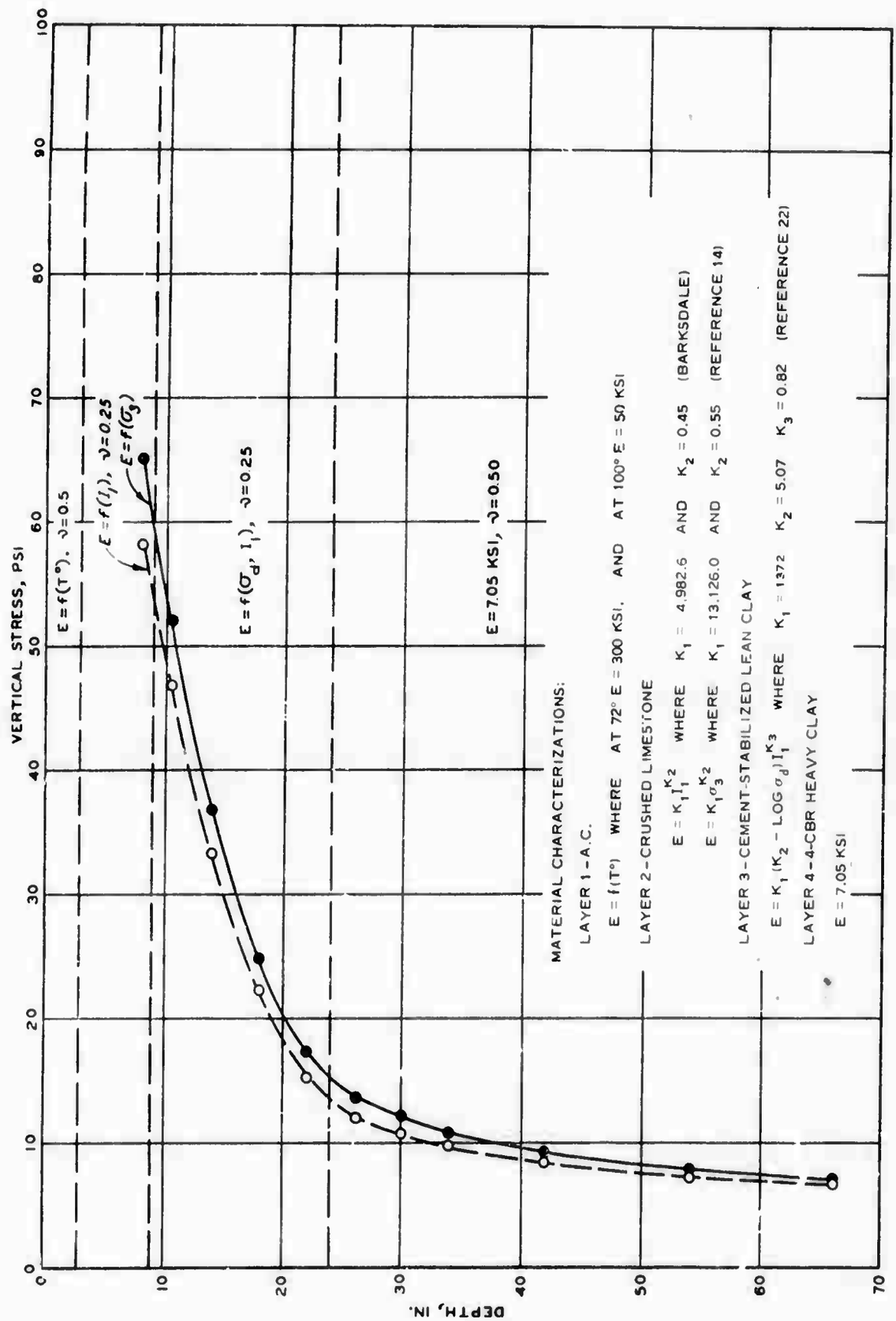

Figure 39. Computed vertical stress versus depth for 30-kip single-wheel assembly on item 2, stabilized layer test section (FEPAVE II program with various material characterizations).

methods of base characterization but this limited analysis indicated that either procedure would serve equally well.

In the comparison of the linear analysis with the nonlinear analysis, the nonlinear results from the first base characterization will be used. The first comparison is provided in figures 40 and 41, which show the surface deflection profiles for the 30- and 50-kip single-wheel loads, respectively. For both loadings, surface profiles predicted by the nonlinear analysis correlate well with the measured surface profile. Not only does the computed maximum deflection compare favorably with the measured deflection, but the shape of the computed profile matches that of the measured profile. The profiles from the linear analysis did not correlate well with the measured profile, particularly with respect to the shape of the profile.

For the 30-kip single-wheel load, the comparison of computed and measured vertical stress is provided in figures 42 and 43. Again the best agreement with measured data was obtained from nonlinear analysis. The distribution of vertical stress with depth for the 50-kip single-wheel load is given in figure 44. The relative comparisons of stresses obtained from the linear analysis with the stresses obtained from nonlinear analysis were the same for this loading as they were for the 30-kip loading; that is, the stresses from the nonlinear analysis are much greater than the stresses from the linear analysis.

The measured vertical strains and strains computed from linear analysis are shown in figures 45 and 46 for a 30-kip single-wheel load and a 360-kip 12-wheel load, respectively. As was the case in item 1, the agreement between measured and computed strains is very poor. The reason for the poor agreement in item 2 would be the same as in item 1. The modulus value of the subgrade computed from the field-measured subgrade strain and stress is approximately

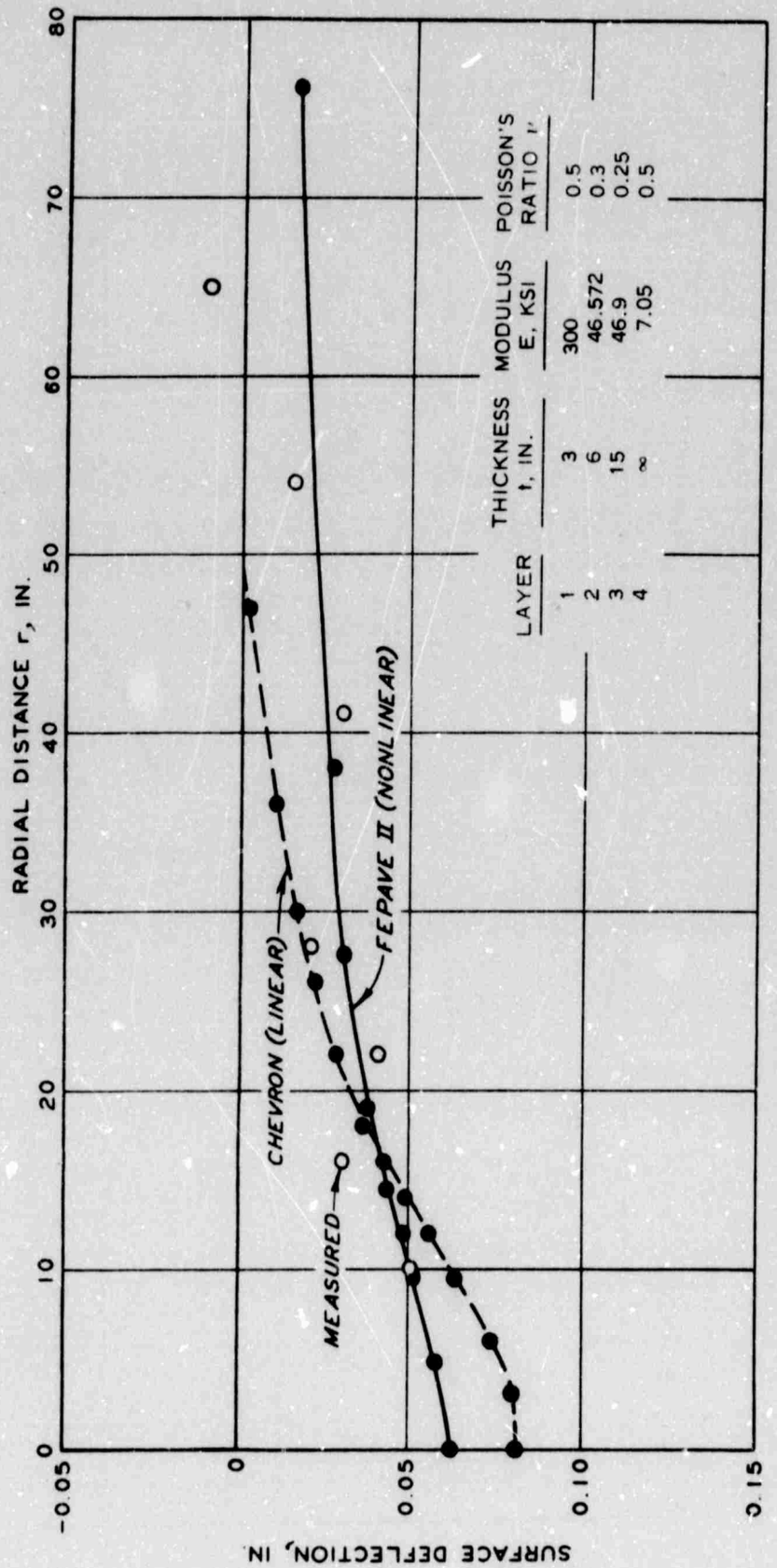

Figure 40. Measured and computed surface deflections for 30-kip single-wheel load on item 2, structural layer test section (CHEVRON and FEPAVE II programs).

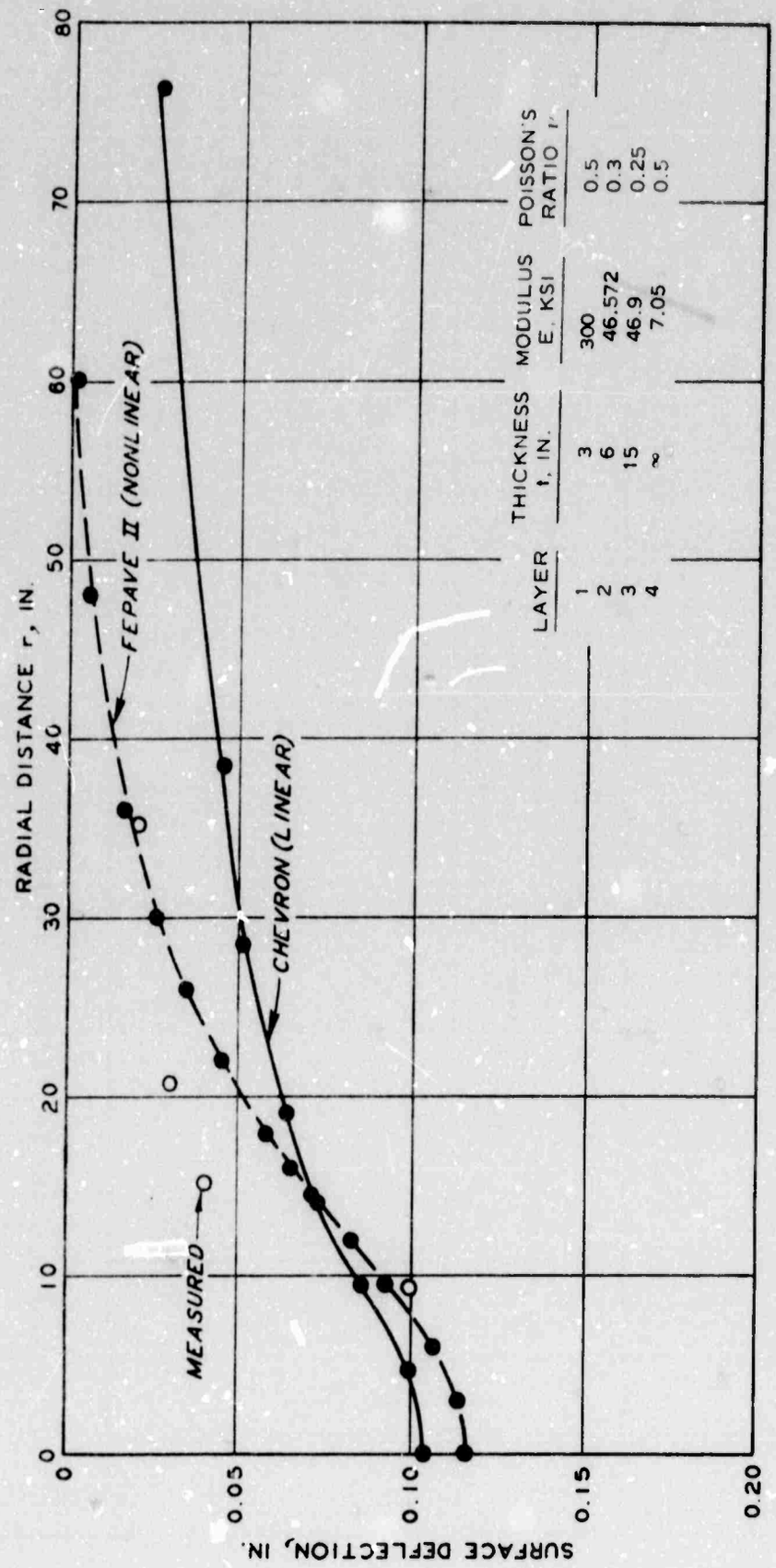

Figure 41. Measured and computed surface deflections for 50-kip single-wheel load on item 2, structural layer test section (CHEVRON and FEPAVE II programs).

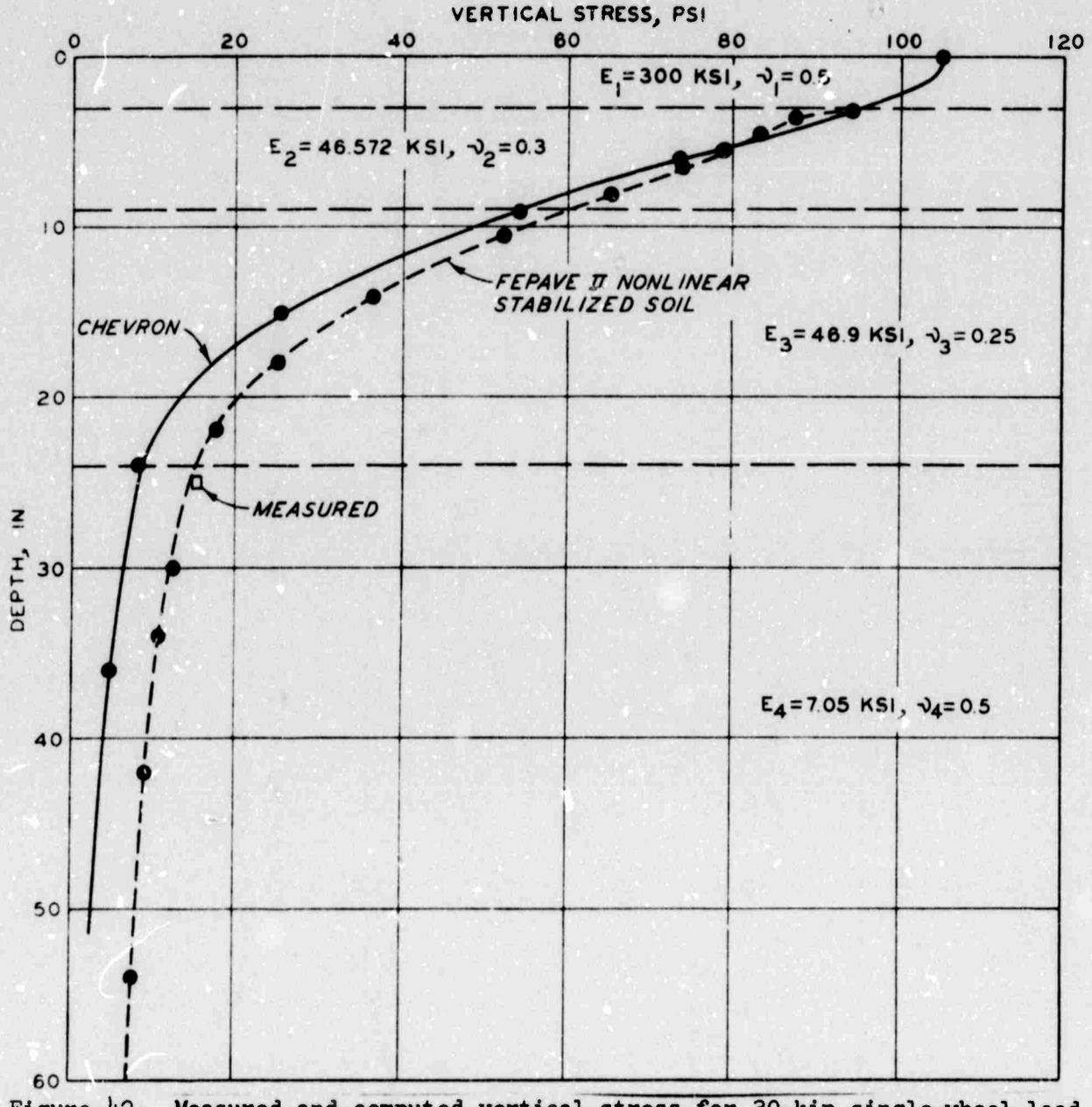

Figure 42. Measured and computed vertical stress for 30-kip single-wheel load on item 2, structural layer test section (CHEVRON and FEPAVE II programs).

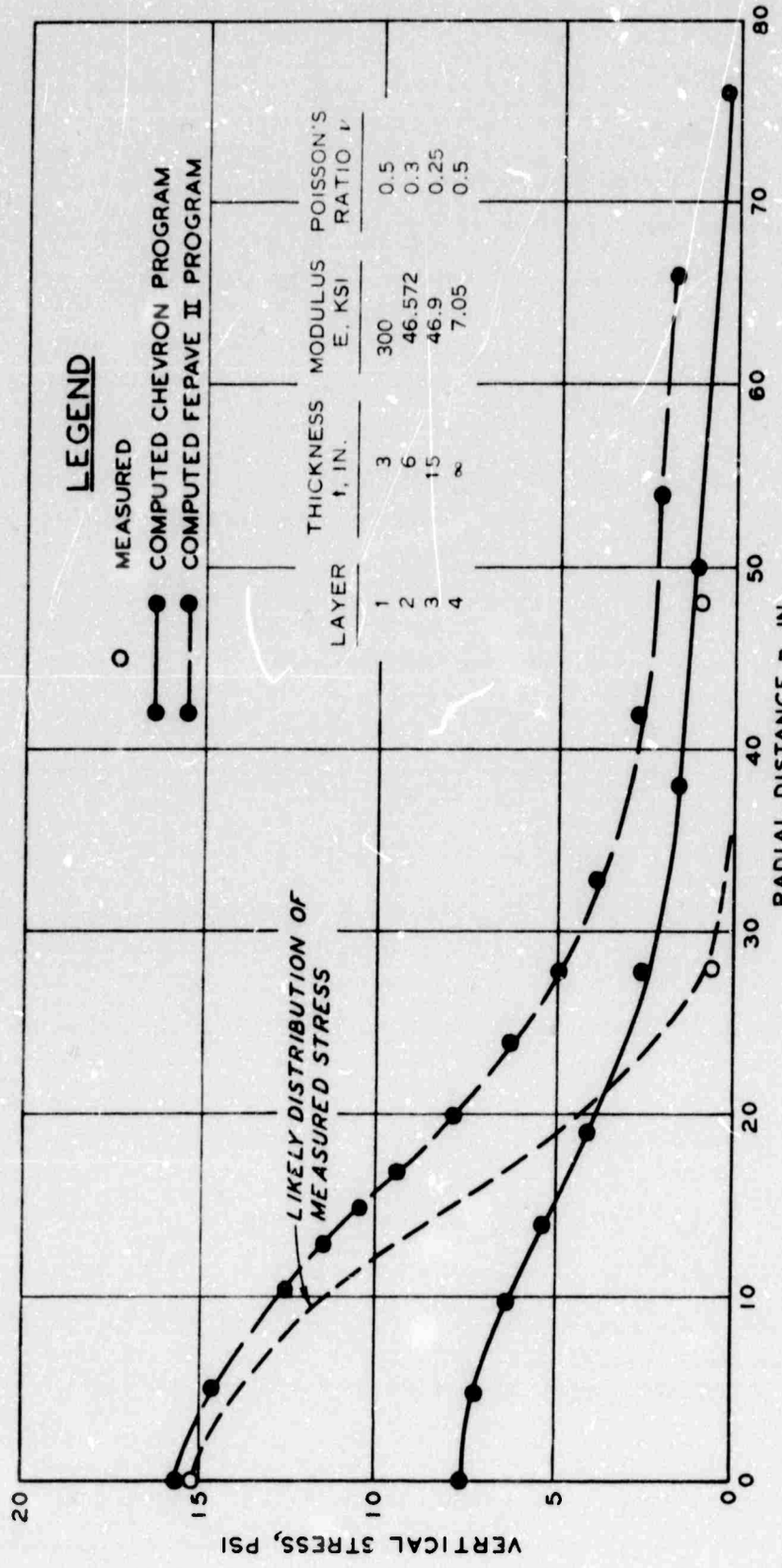

Figure 43. Measured and computed vertical stress profile at the top of the subgrade (z = 24 in.) for 30-kip single-wheel load on item 2, structural layer test section (CHEVRON and FEPAVE II programs).

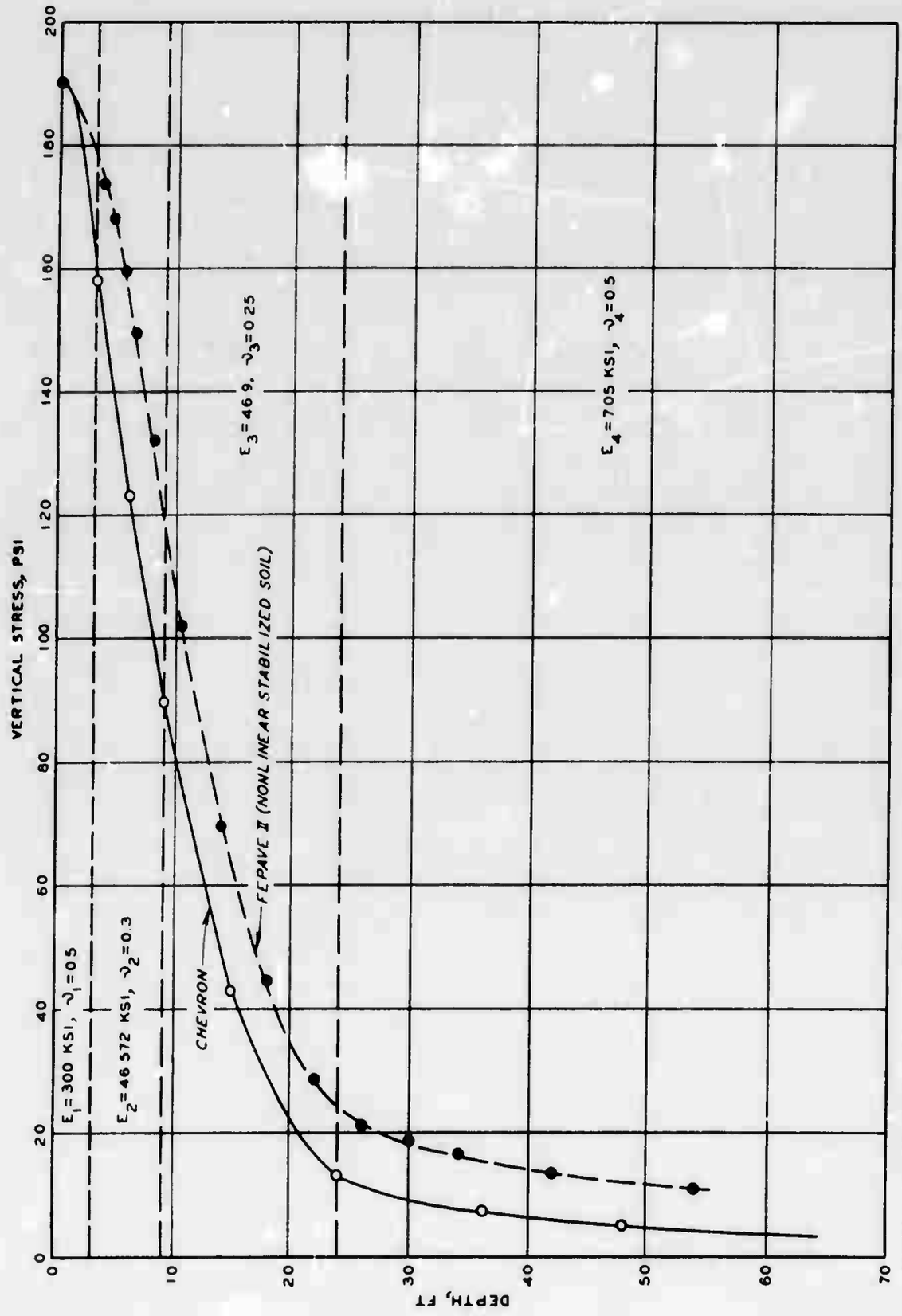

Figure 44. Computed vertical stress for 50-kip single-wheel load on item 2, structural layer test section (CHEVRON and FEPAVE II programs).

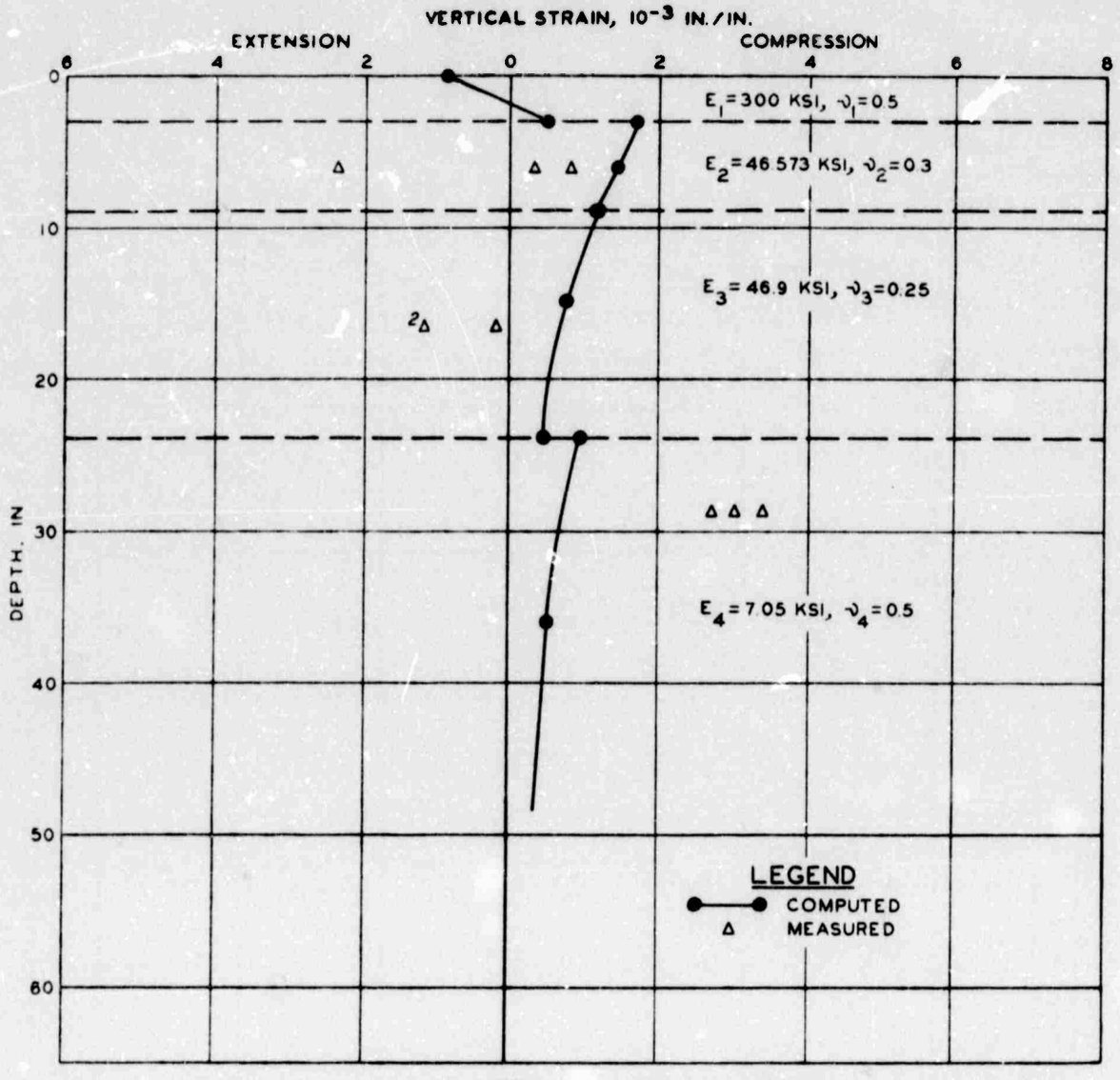

Figure 45. Computed and measured vertical stress versus depth for 30-kip single-wheel load on item 2, structural layer test section (CHEVRON program).

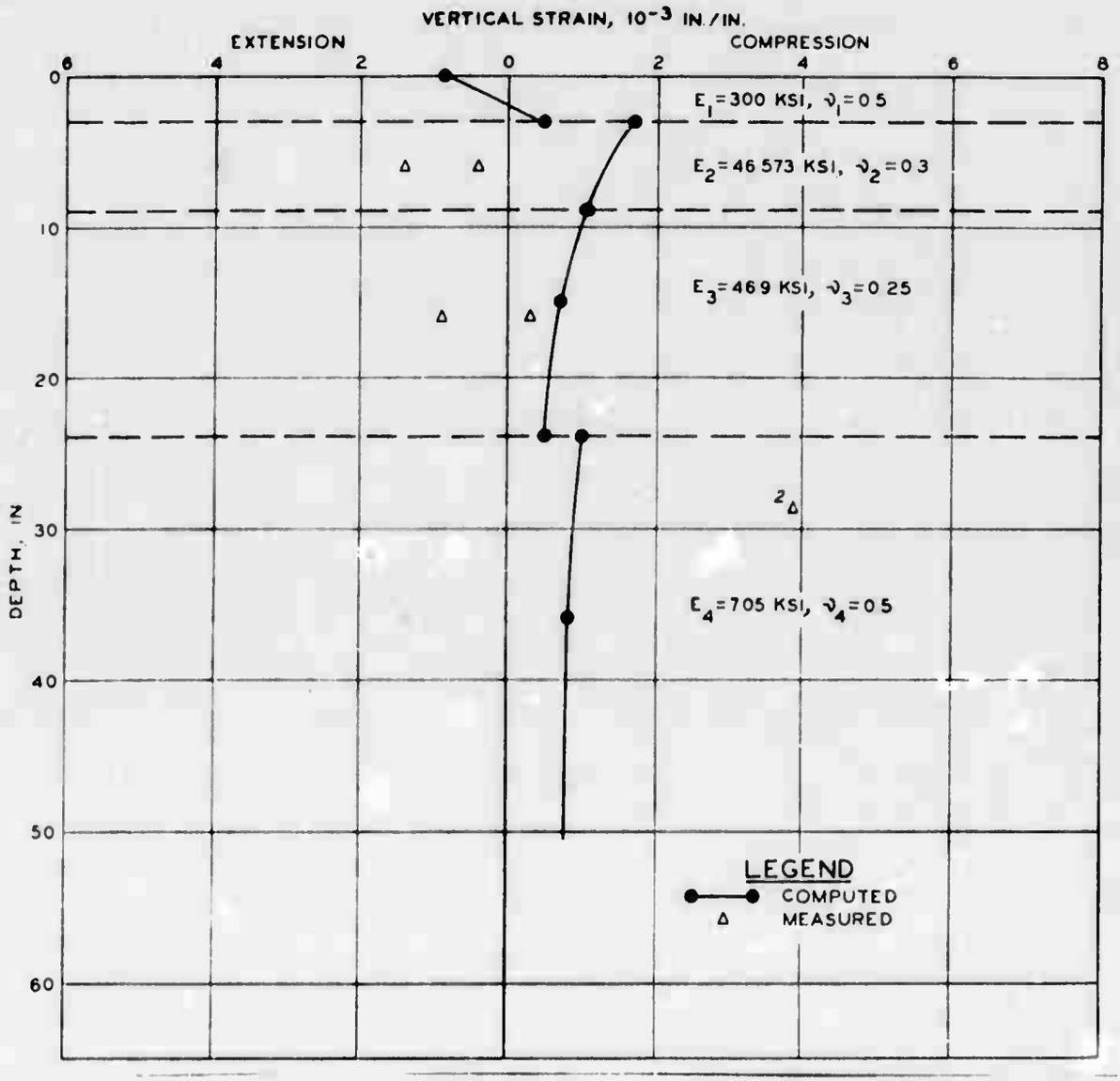

Figure 46. Computed and measured vertical stress versus depth for 360-kip 12-wheel assembly on item 2, structural layer test section (CHEVRON program)

5000 psi. This is higher than the computed subgrade modulus of item 1 but not as high as the modulus value used in the analytical analysis.

c. Item 3

The approach taken in the analysis of item 3 was to subdivide the 21 in. of crushed stone into three sublayers: the top two layers each being 6 in. in thickness and bottom layer being 9 in. in thickness. A ratio of E-moduli (i.e., the ratio of $\frac{E_4}{E_5}$, $\frac{E_3}{E_4}$, $\frac{E_2}{E_3}$) was chosen such that the tension that developed at the bottom of each layer was inconsequential. Several ratios were tried; the most promising results were obtained using a ratio of 1.2. Use of this ratio resulted in values of 8,600 psi for E_4; 10,300 psi for E_3; and 13,500 psi for E_2. For this set of modulus values, computations were made for two values of Poisson's ratio: 0.24 and 0.45. The maximum tensile stress at the bottom of the crushed limestone was 6.9 psi for a Poisson's ratio of 0.25 and 2.8 psi for a Poisson's ratio of 0.45. Thus it can be seen that the tensile stress is greatly influenced not only by the E-modulus but also by Poisson's ratio.

A summary of certain parameters for item 3 is given in table XV.

The comparison of the computed and measured surface deflection for the 30- and 75-kip single-wheel loadings is given in figure 47. This comparison indicated that the ratio of 1.2 is applicable for the 75-kip loading but not for the 30-kip loading. The comparisons of the computed and measured surface deflection for the 360-kip 12-wheel loading are shown in figures 48 and 49. In this case the agreement between computed and measured deflections was very good. Such behavior by the pavement section would certainly tend to substantiate the contention that the crushed limestone is highly nonlinear with respect to the state of stress. The distribution of vertical stress with

Table XV

Summary of Analyses of Structural Layers Test Section Item 3 Data

Assembly	Load kips	Method of Determination	Deflection in.	Subgrade	
				Vertical Stress σ_v psi	Vertical Strain ϵ_v in./in.
Single-wheel	30	CHEVRON (linear elastic)	0.15	17	0.0022
		Finite Element (nonlinear)	0.13	10	0.0012
		Measured at 0 coverages	0.06	26	0.004
	75	CHEVRON (linear elastic)	0.38	30	0.0036
		Measured at 0 coverages	0.39	-	-
Twelve-wheel	360	CHEVRON (linear elastic)	0.24	20	0.0023
		Measured at 0 coverages	0.25	25	0.0035

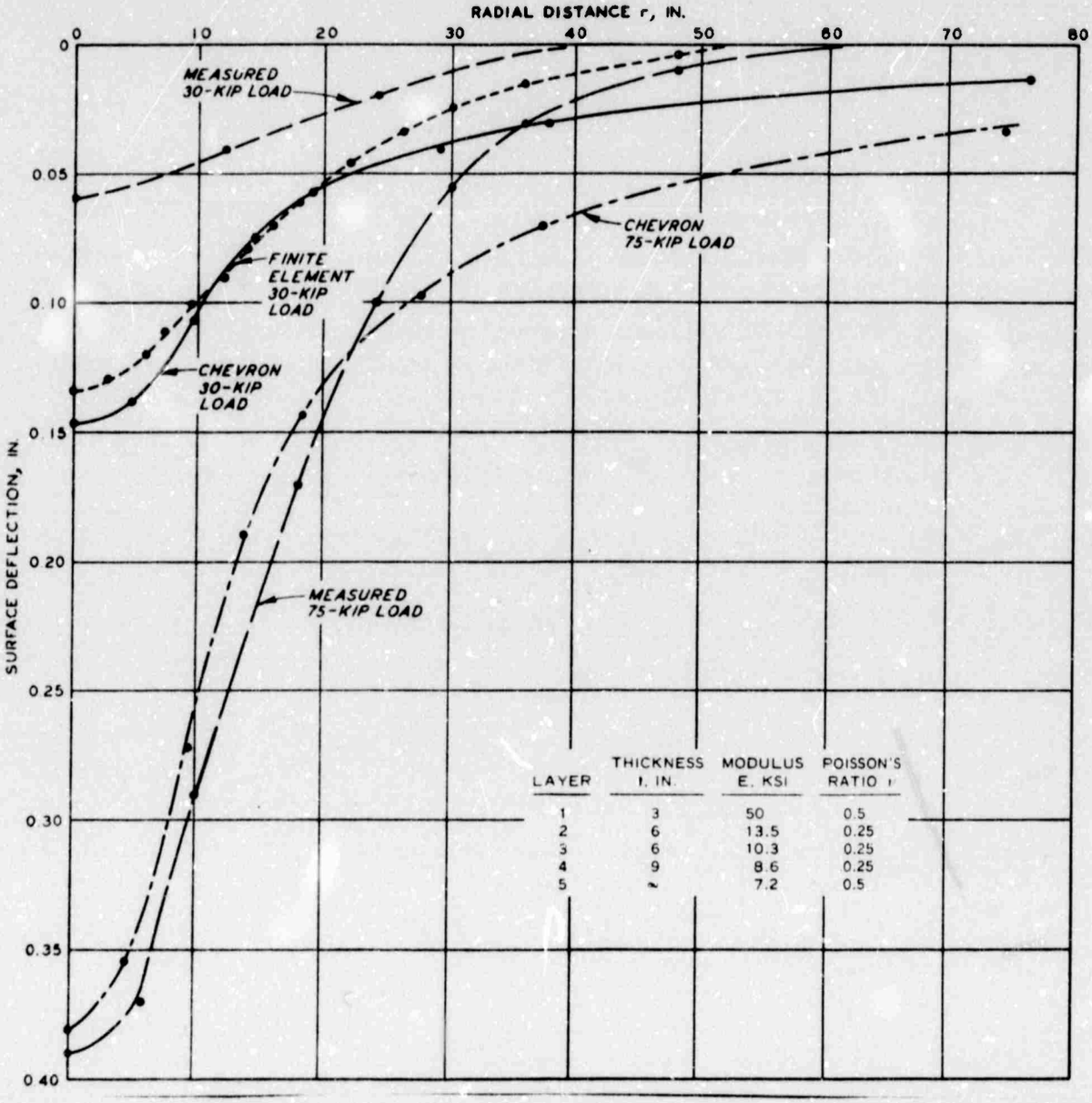

Figure 47. Measured and computed surface deflections for 30- and 75-kip single-wheel assemblies on item 3, structural layer test section (CHEVRON and finite element programs).

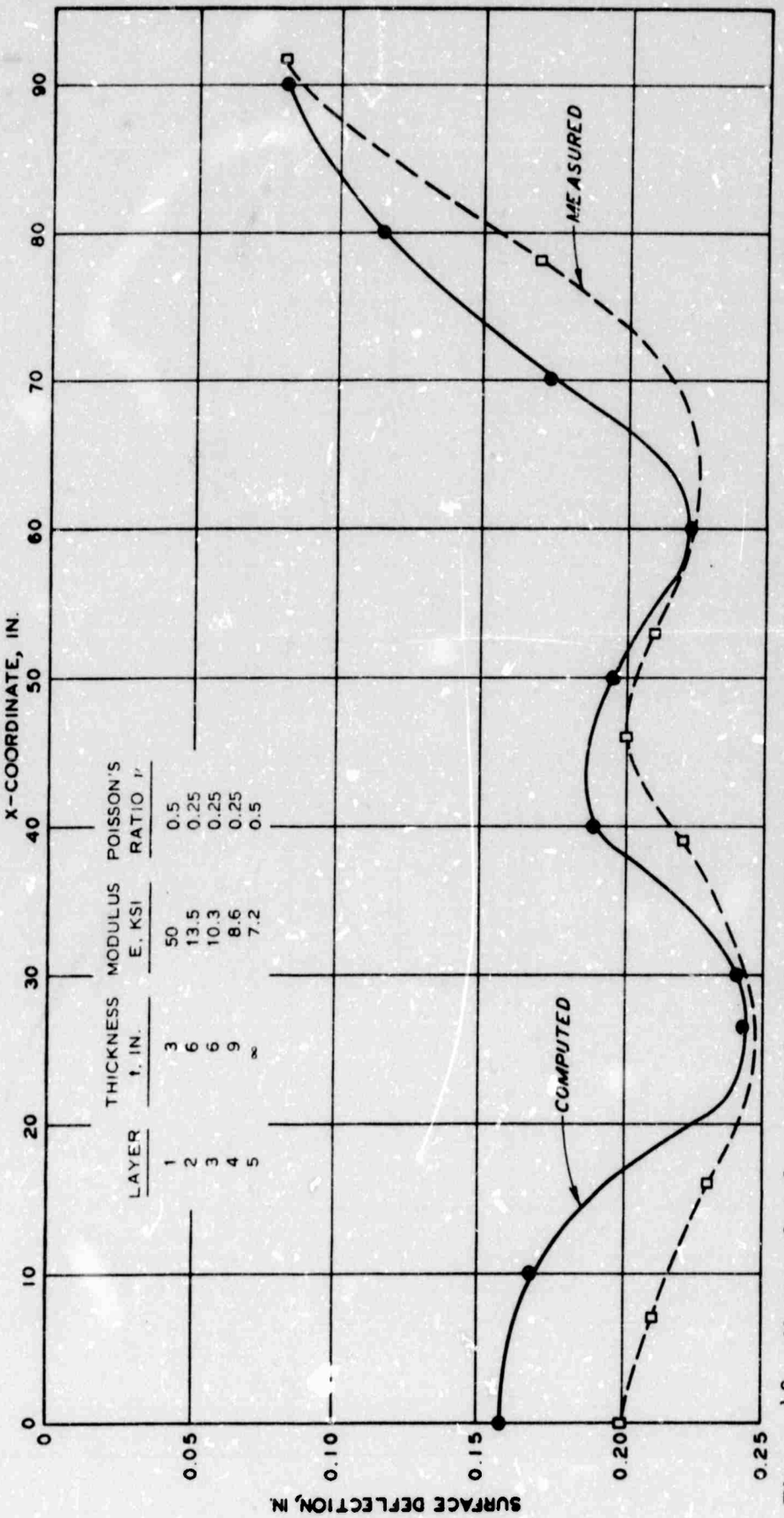

Figure 48. Measured and computed surface deflections on x-coordinate at y = 65 in. for 360-kip 12-wheel assembly on on item 3, structural layer test section (CHEVRON program).

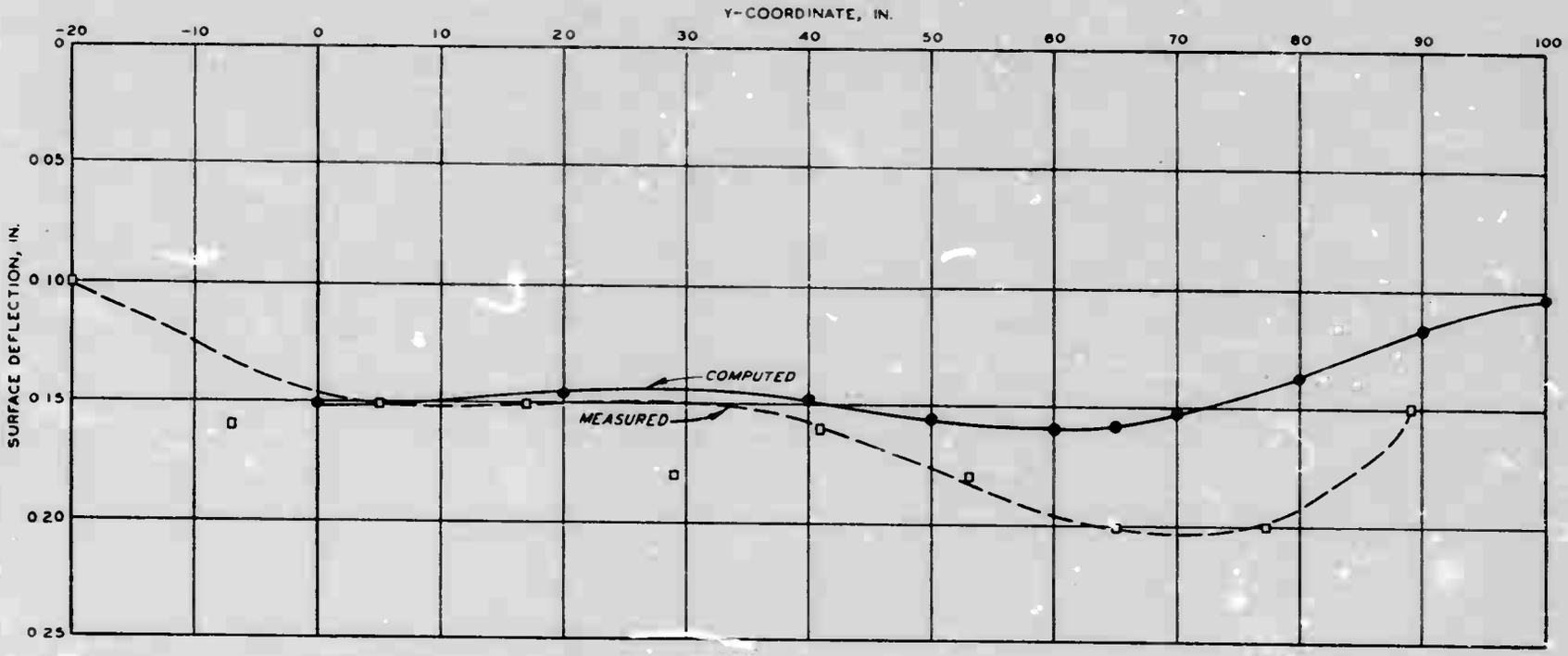

Figure 49. Measured and computed surface deflections on y-coordinate at x = 0 in. for 360-kip 12-wheel assembly on item 3, structural layer test section (CHEVRON program).

depth is given in figure 50. The measured stress for both the 30-kip single-wheel loading and 360-kip 12-wheel loading was approximately 25 psi; whereas, the computed stresses were 15 and 17 psi, respectively. The measured stress of 25 psi for item 3 is high when compared with the measured stresses of items 1 and 2 and when the relative performance of the items is considered. The high 25-psi value is probably due to over registration caused by the arching action of the granular materials over the cells.

One computer run was made for a 30-kip single-wheel loading with a finite element program in which the crushed stone was characterized as being nonlinear with respect to the confining pressure. The surface profile obtained from this run is shown in figure 47. Like the CHEVRON program, the finite element program overpredicted the surface deflection. The overestimation could result from the procedure that was employed with the program. The program uses an incremental-load technique for the nonlinear solutions with the investigator specifying the number of load increment. The number of load increments required for a satisfactory solution for a particular problem depends mainly on the characteristics of the loading and degree of nonlinearity of the materials. In the run made for item 3, the load was applied in only three load increments. Later, analysis of granular test sections revealed that the 30-kip load should be applied in at least ten load increments. Also shown was the fact that increasing the number of load increments decreased the total deflection. Thus it is expected that if the load had been applied in a greater number of load increments, the computed deflection would have agreed better with measured deformation.

The comparison of computed with measured strains in figure 51 appears much the same as the comparisons for items 1 and 2. The computed strains for the upper layers were higher than the measured strains; while in the subgrade,

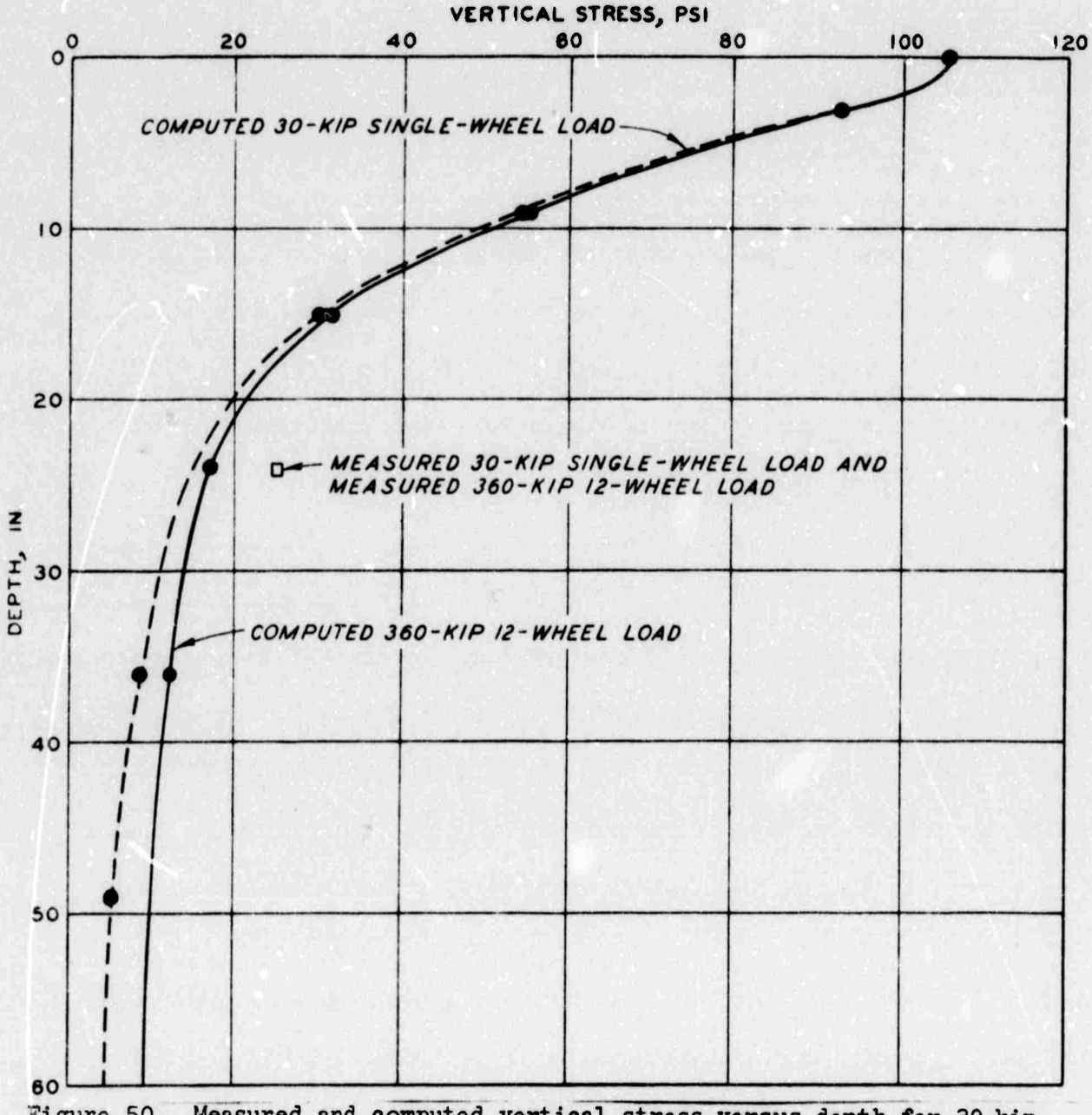

Figure 50. Measured and computed vertical stress versus depth for 30-kip single-wheel and 360-kip 12-wheel assemblies on item 3, structual layer test section (CHEVRON program).

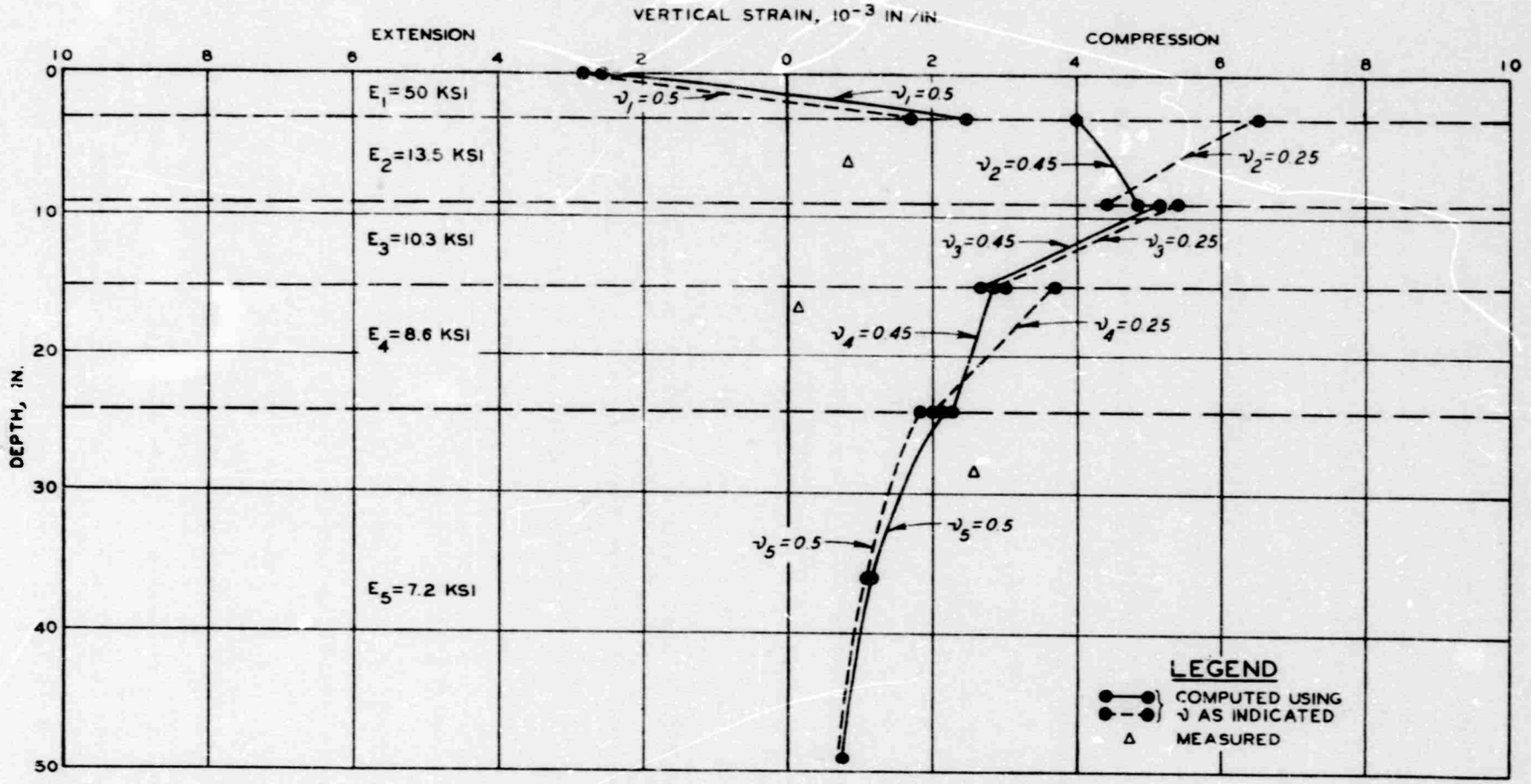

Figure 51. Measured and computed vertical strain versus depth for 30-kip single-wheel assembly on item 3, structural layer test section (CHEVRON program).

the measured strain was higher than the computed strain. If the subgrade modulus is approximated from measured stress and strain, a modulus of 10,000 psi is obtained. This is considerably higher than the moduli indicated for items 1 and 2, which would suggest that the measured stress was too large.

d. Item 4

The summary of the linearly elastic analysis for item 4 is given in table XVI.

The results of both the single-wheel and multiple-wheel analysis of item 4 indicate that the modulus of the stabilized layer was overestimated. Figure 52 presents the comparison of the computed and measured values of surface deflection and vertical stress with measure values. As can be seen, the computed surface profile is almost horizontal; whereas, the measured profile has considerable curvature. Also the computed subgrade stress was approximately 1/3 of the measured stress. The same behavior is seen in the results from the 75-kip single-wheel loading (figure 53). The surface profiles for the 360-kip multiple-wheel loading are presented in figure 54. Again the computed values did not compare favorably with the measured values. The comparison is especially poor if the configurations of the curves are used as a basis of comparison. The comparison is similar to that for the single-wheel loading, i.e., the moduli of the upper layers were overestimated.

For the 360-kip multiple-wheel loading, computed tensile stress at the bottom of the stabilized layer (94.3 psi) was very close to the tensile strength (87.3 psi) of the material. For 75-kip single-wheel, the tensile stress (138.7 psi) would cause much more distress of the pavement system.

In addition to higher tensile strength and higher modulus, item 4 had the advantage over items 1 and 2 of having a granular material as the parent material. When the material cracks due either to curing or loading, the

Table XVI

Summary of Analyses of Structural Layers Test Section Item 4 Data

Assembly	Load kips	Method of Determination	Deflection in.	Subgrade		Stabilized Layers	
				Vertical Stress σ_v psi	Vertical Strain ϵ_v in./in.	Horizontal Stress σ_H psi	Horizontal Strain ϵ_H in./in.
Single-wheel	30	CHEVRON (linear elastic)	0.033	2.6	0.0003	-55.3	-0.00013
		Measured at 0 coverages	0.04	7.3	0.002	-	-
	75	CHEVRON (linear elastic)	0.08	6.7	0.0007	-138.7	-0.00033
		Measured at 0 coverages	0.25	36	-	-	-
Twelve-wheel	360	CHEVRON (linear elastic)	0.13	6.5	0.0015	-94.3	-0.00067
		AFPAV (linear elastic)	0.10	12.3	0.002	-78	-0.00022
		Measured at 0 coverages	0.19	10.0	0.0031	-	-

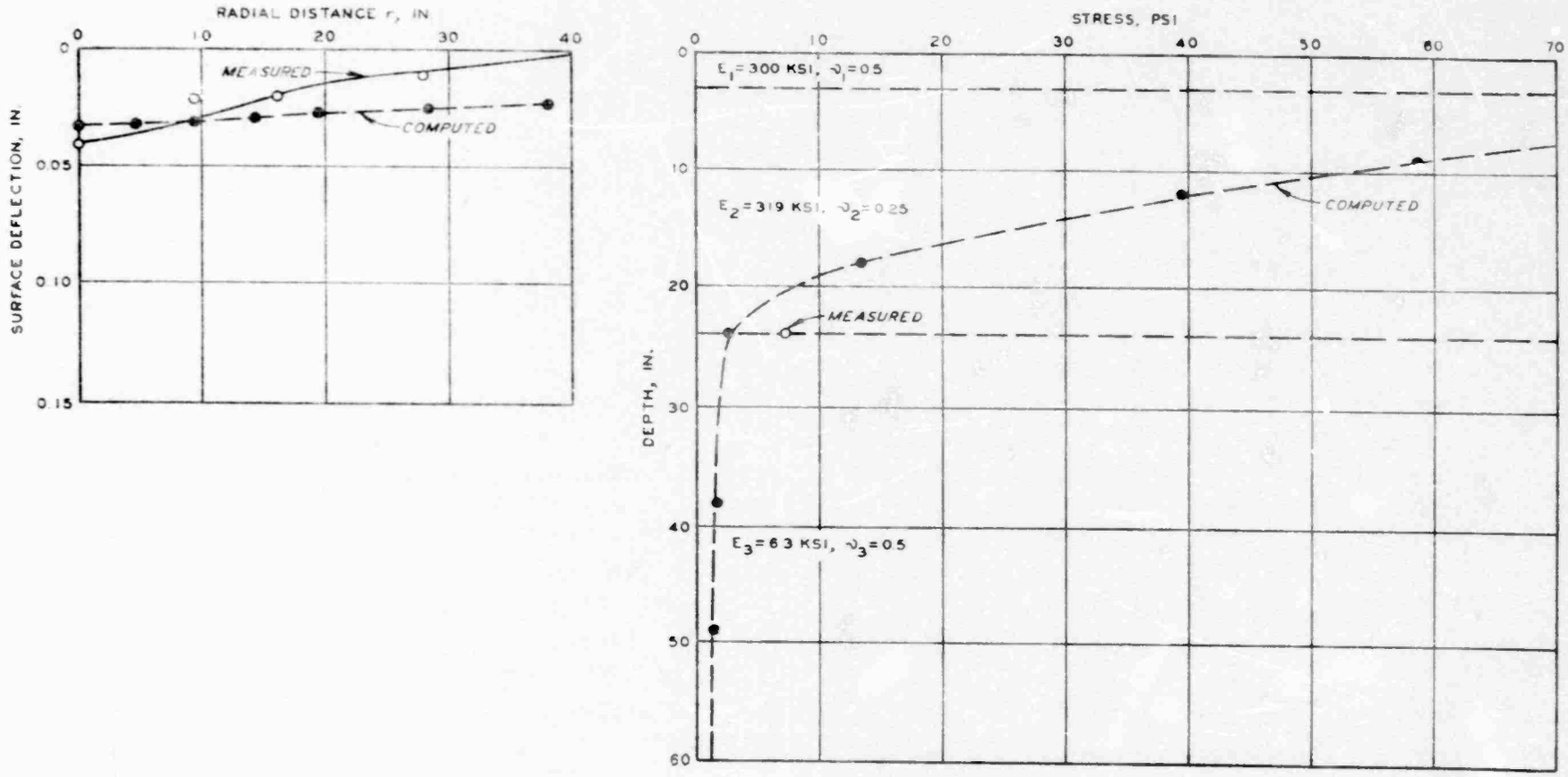

Figure 52. Measured and computed surface deflections and stress for 30-kip single-wheel assembly on item 4, structural layer test section (CHEVRON program).

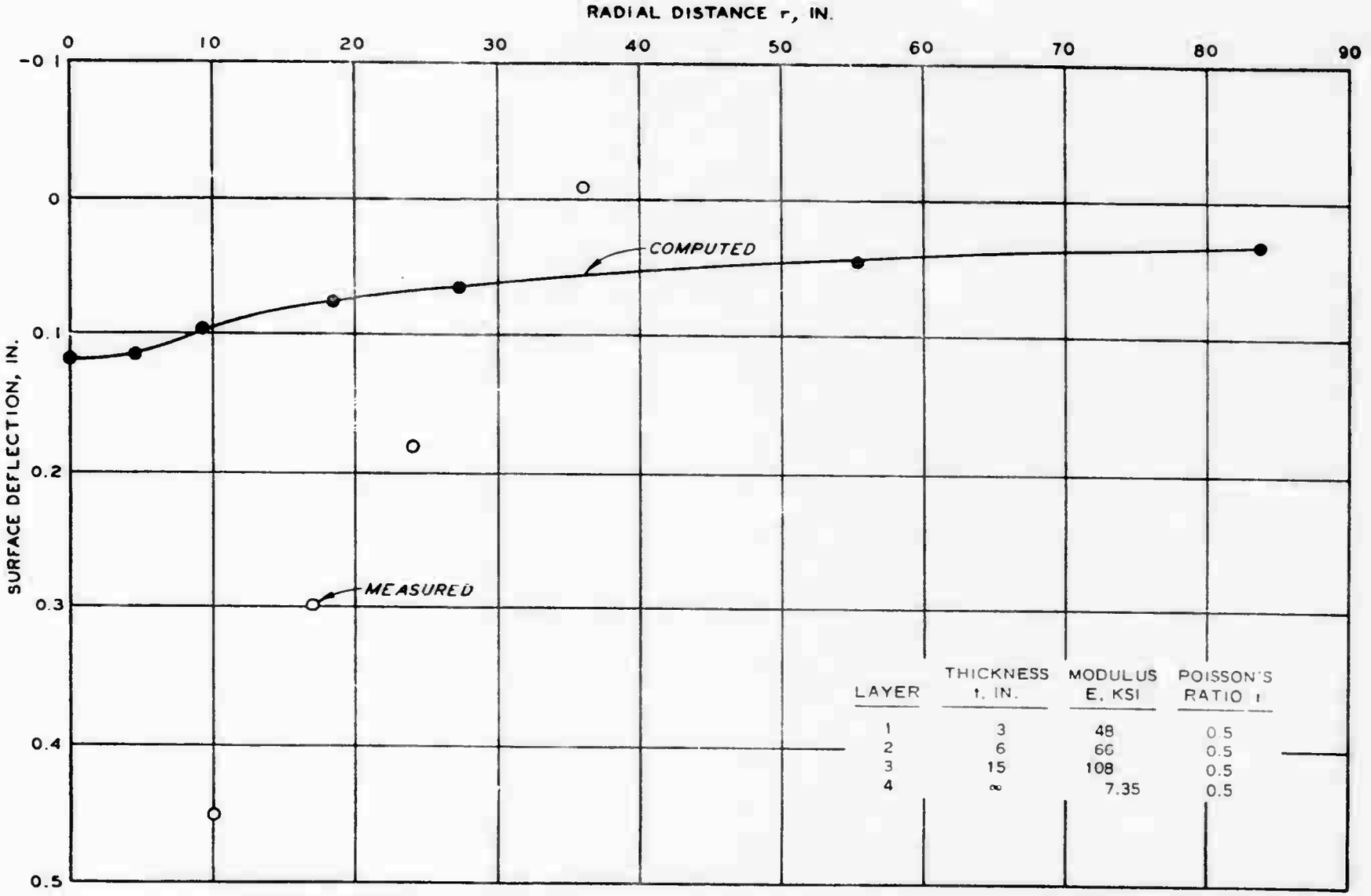

Figure 53. Measured and computed surface deflections for 75-kip single-wheel assembly on item 4, structural layer test section (CHEVRON program).

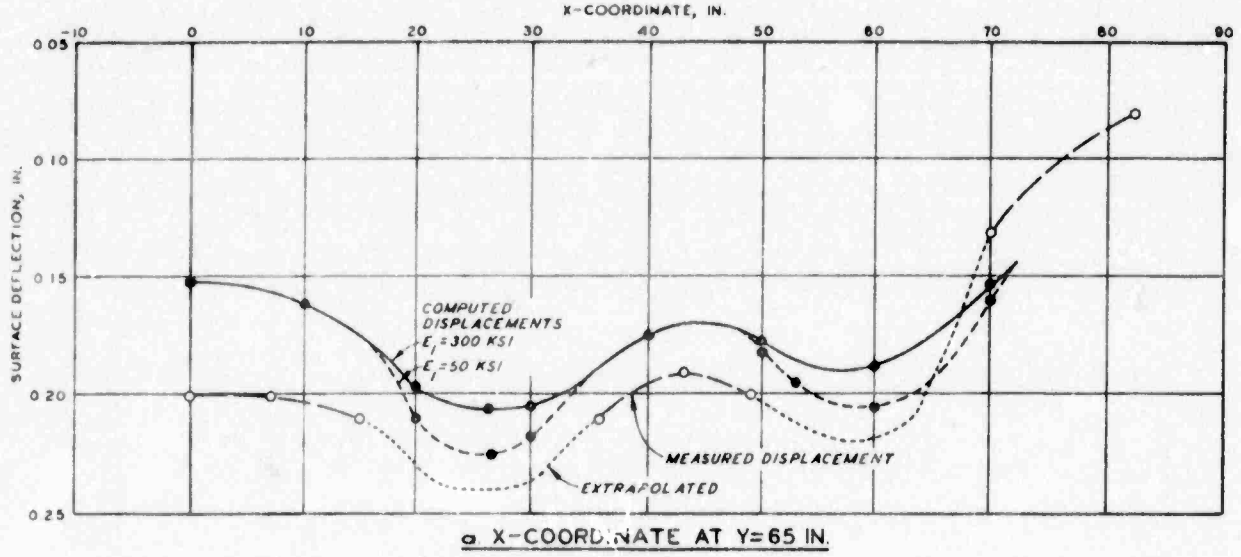

a X-COORDINATE AT Y=65 IN.

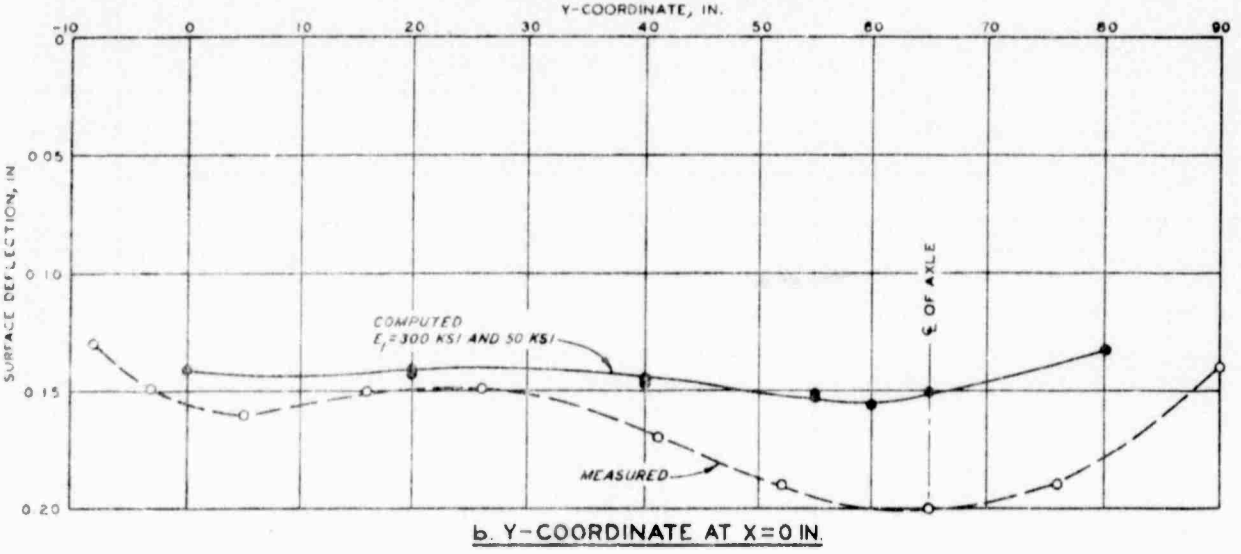

b. Y-COORDINATE AT X=0 IN.

LAYER	THICKNESS h, IN.	MODULUS E, KSI	POISSON'S RATIO μ
1	3	300 & 50	0.5
2	6	15	0.3
3	15	13.5	0.25
4	∞	7.2	0.5

Figure 54. Measured and computed surface deflections for sections x = 0 in. and y = 65 in. for 360-kip 12-wheel assembly on item 4, structural layer test section (CHEVRON and AFPAV programs).

material would continue to act as well-compacted granular material. This would give the material added strength particularly under multiple-wheel loadings, which produce high confining stresses.

The comparisons of computed strains and measured strains are presented in figures 55 and 56. The comparison of strains for this item is about the same as was discussed for items 1 and 2. The magnitudes of the strains were much smaller, but extension was again indicated by the middle set of gages. A subgrade modulus of approximately 4000 psi was indicated by the measured values of stress and strain. This is much the same as the subgrade moduli indicated in items 1 and 2.

5. CORRELATION OF PREDICTED RESPONSE WITH ACTUAL PERFORMANCE

Although predicted response as determined by linear analysis does not correlate particularly well with measured response, the linear elastic theory yields results that are correlatable with performance and that are presently being used as a basis for pavement design. The most frequently used design parameters are surface deflection, tensile stress/strain at the bottom of the asphalt surfacing, and stress/strain at the top of the subgrade. In this study, the parameters of vertical stress and strain at the top of the subgrade, surface deflections, and the ratio of tensile strength with tensile stress at the bottom of the stabilized layer were plotted against coverages. These plots were used to determine if a correlation existed between the computed parameter and the actual performance. Actual performance of the items included in the analysis is shown in table XVII.

a. Subgrade Stress and Strain

The first parameter to be considered is the vertical stress and strain at the top of the subgrade. Since, in the case of the test sections analyzed, the subgrades were all constructed to have approximately the same strength and

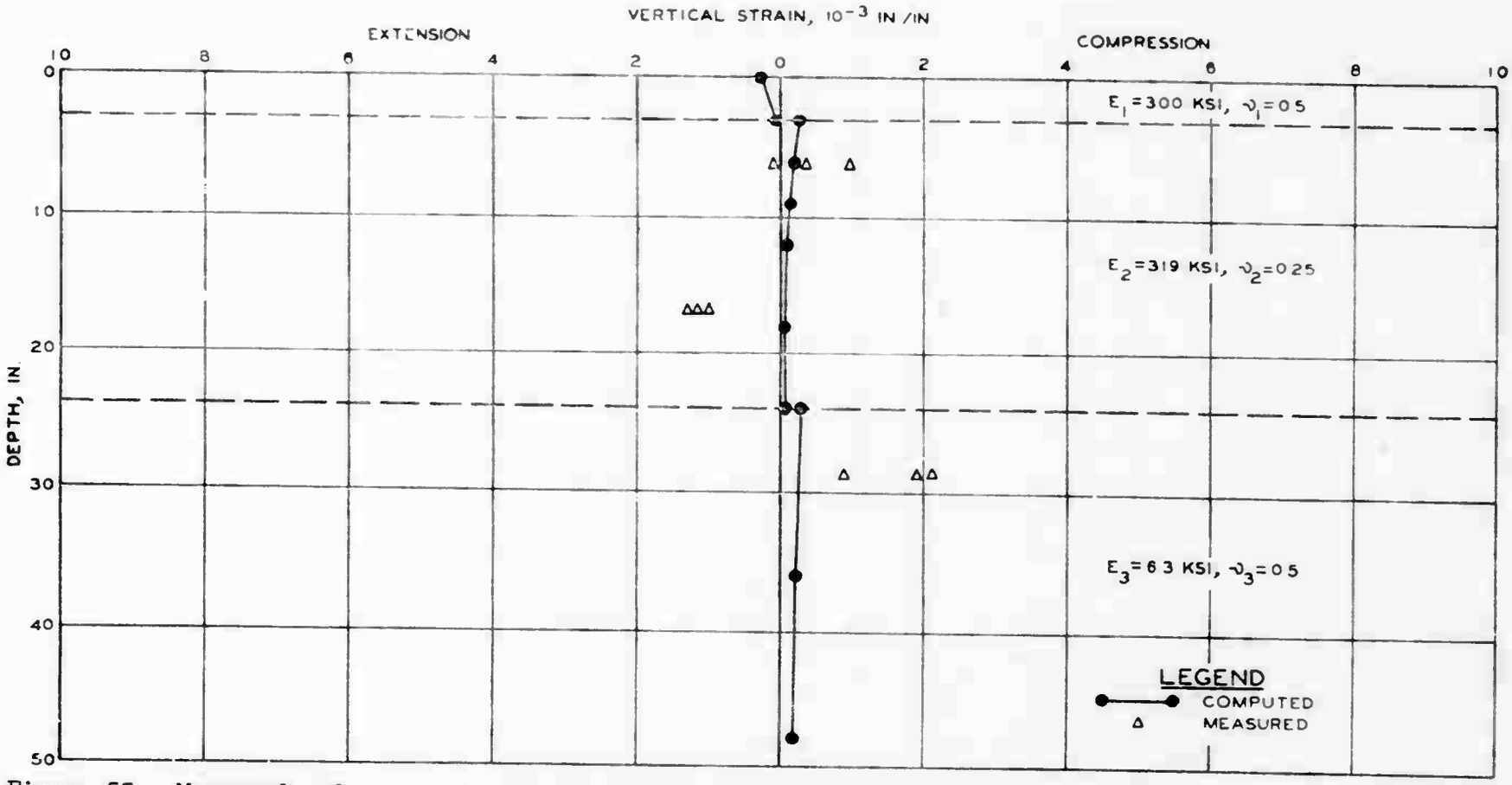

Figure 55. Measured and computed vertical strain versus depth for 30-kip single-wheel assembly on item 4, structural layer test section (CHEVRON program).

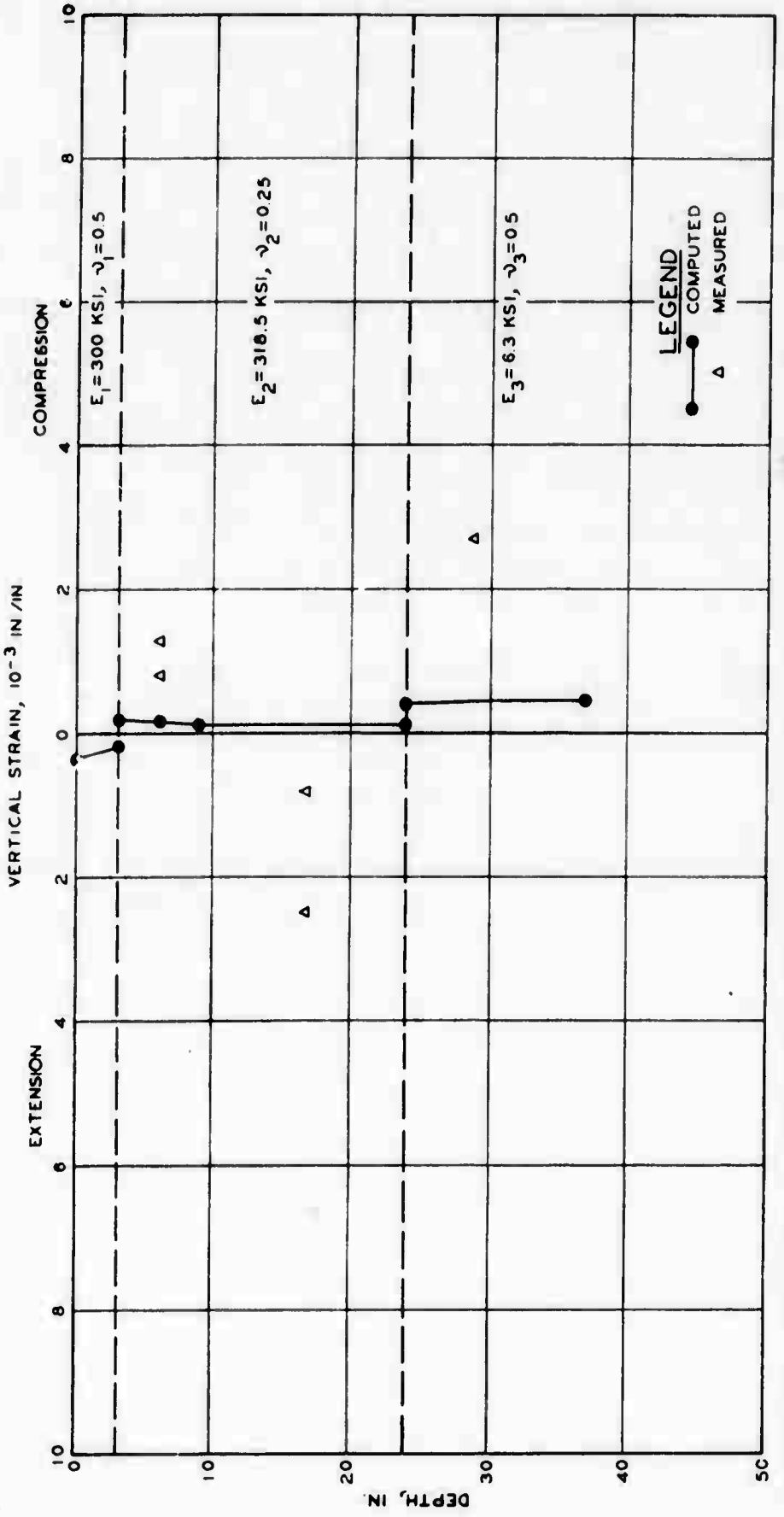

Figure 56. Measured and computed strain versus depth for 360-kip 12-wheel assembly on item 4, structural layer test section (CHEVRON program).

Table XVII

Performance of Pavements Included in Analysis

Test Section	Item	Assembly Type	Load Kips	Coverages to Failure
MWHGL	1	Single-wheel	30	120
			50	6
	2	Single-wheel	30	450+*
			50	200
	3	Single-wheel	75	18
Bituminous Base Course Study	1	Single-wheel	75	6
		12-wheel	360	98
	2	Single-wheel	75	8
		12-wheel	360	425
	3	Single-wheel	75	100
		12-wheel	360	2,198
	4	Single-wheel	75	100
		12-wheel	360	734
Structural Layers Study	1	Single-wheel	50	40
		12-wheel	360	198
	2	Single-wheel	50	120
		12-wheel	360	1,871
	3	Single-wheel	75	50
		12-wheel	360	5,037
	4	Single-wheel	75	120
		12-wheel	360	10,406+*

*Traffic stopped at indicated coverage level; no failure occurred.

since the subgrade was considered to be linearly elastic, the subgrade stress and subgrade strain can be considered almost analogous. The relationship between the stress imposed by the 12-wheel 360-kip load and the number of coverages to failure can be seen in figure 57. The vertical stresses for single-wheel loadings are presented in figures 58 and 59 for the stabilized and MWHGL test sections, respectively. From these plots, it is possible to conclude that a relationship does exist between vertical stress at the top of the subgrade and coverages.

The curves shown in figures 58 and 59 are estimates of the existing relationship. For the reasons previously stated, a similar relationship would exist between subgrade strains and coverages. The relationships shown for the CHEVRON analysis indicate that for a 5000-coverage level, the vertical stress due to a single tire must be kept below approximately 7.5 psi and below approximately 9.5 psi due to the multiple wheels. Considering the modulus of the subgrade to be 6000 psi, these stress values would correspond to strain values of approximately 1.25×10^{-3} in./in. and 1.58×10^{-3} in./in., respectively.

In reference 12, Edwards and Valkering reported use of a limiting subgrade strain value of 1.03×10^{-3} in./in. in the design of airfield pavements, while Witczak used a limiting subgrade strain value of 1.55×10^{-3} in./in. (reference 27). Although the subgrade strain values appear to be in very close agreement, it should be remembered that earlier it was pointed out that the layered analysis was underestimating the subgrade stresses and strains. Thus although these values of strain may be used for design purposes, they are lower than the actual strains that will be produced by traffic loadings. The stress value picked from the curve correlating the nonlinear results with performance (figure 59) is 13.5 psi, which is considerably higher than the tolerable maximum of 7.5 psi indicated by the CHEVRON analyses. This stress

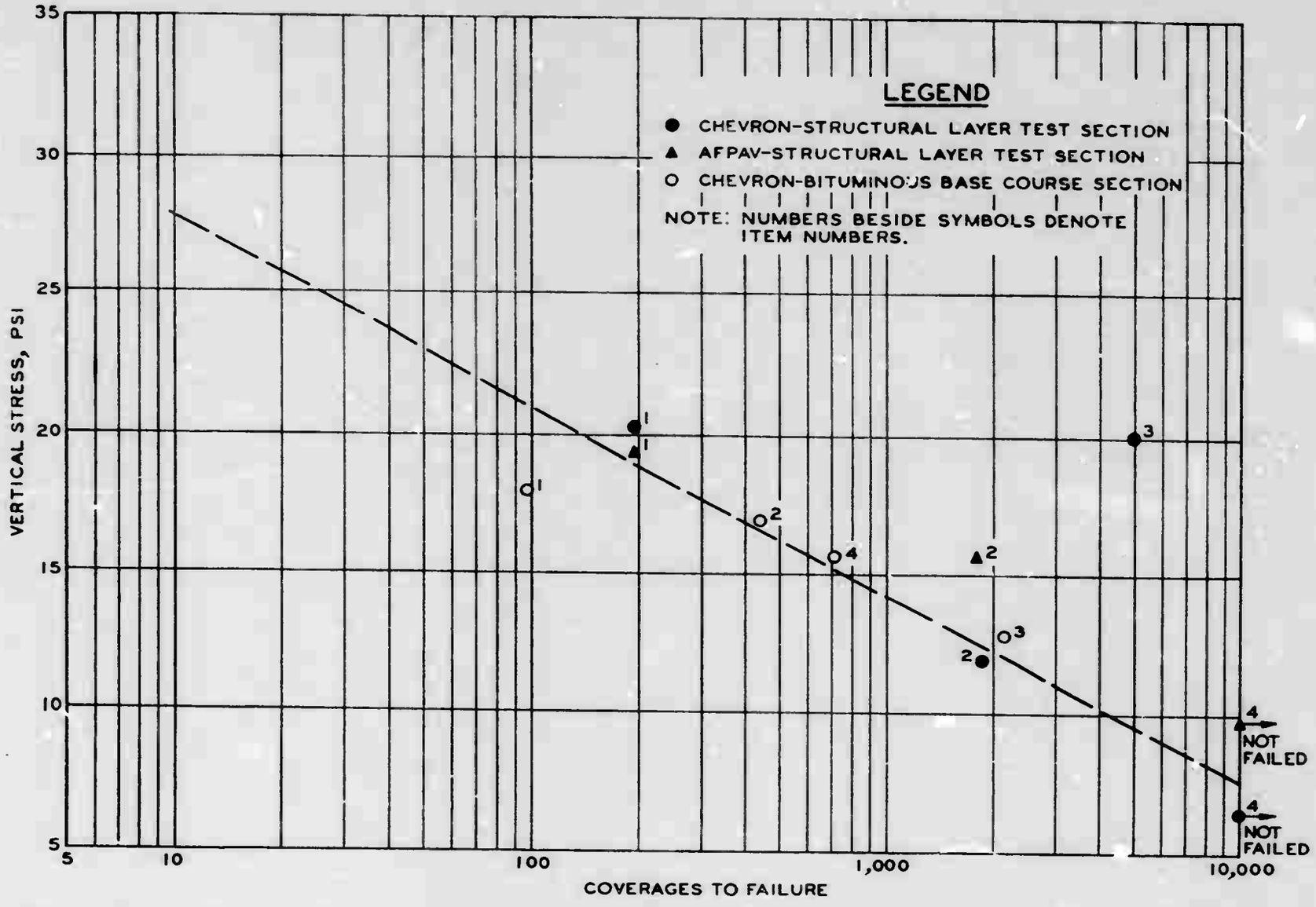

Figure 57. Computed vertical stress imposed on subgrade versus coverages to failure for 12-wheel 360-kip load on stabilized test sections.

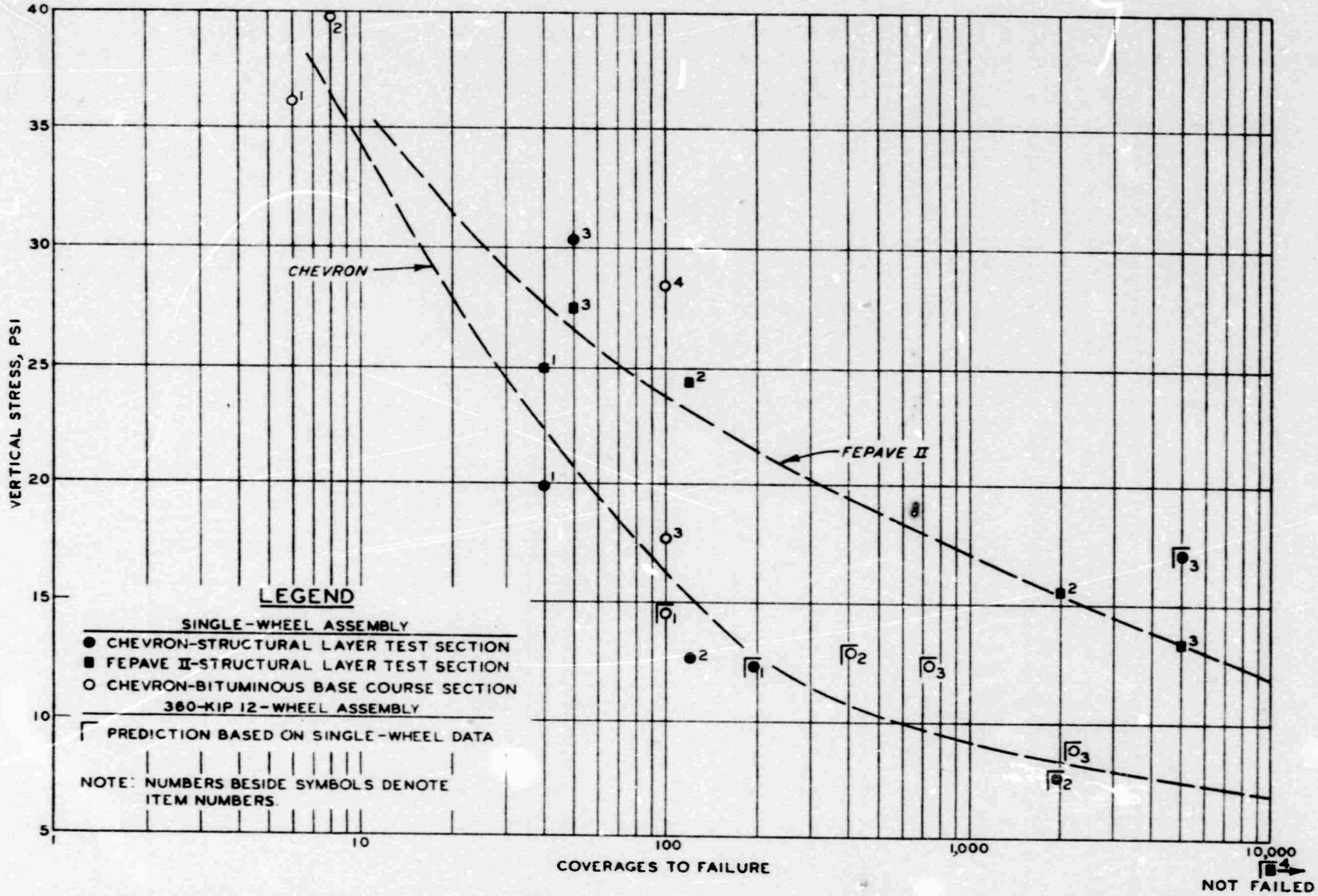

Figure 58. Computed vertical stress imposed on subgrade versus coverages to failure for single- and 12-wheel assemblies on stabilized test sections.

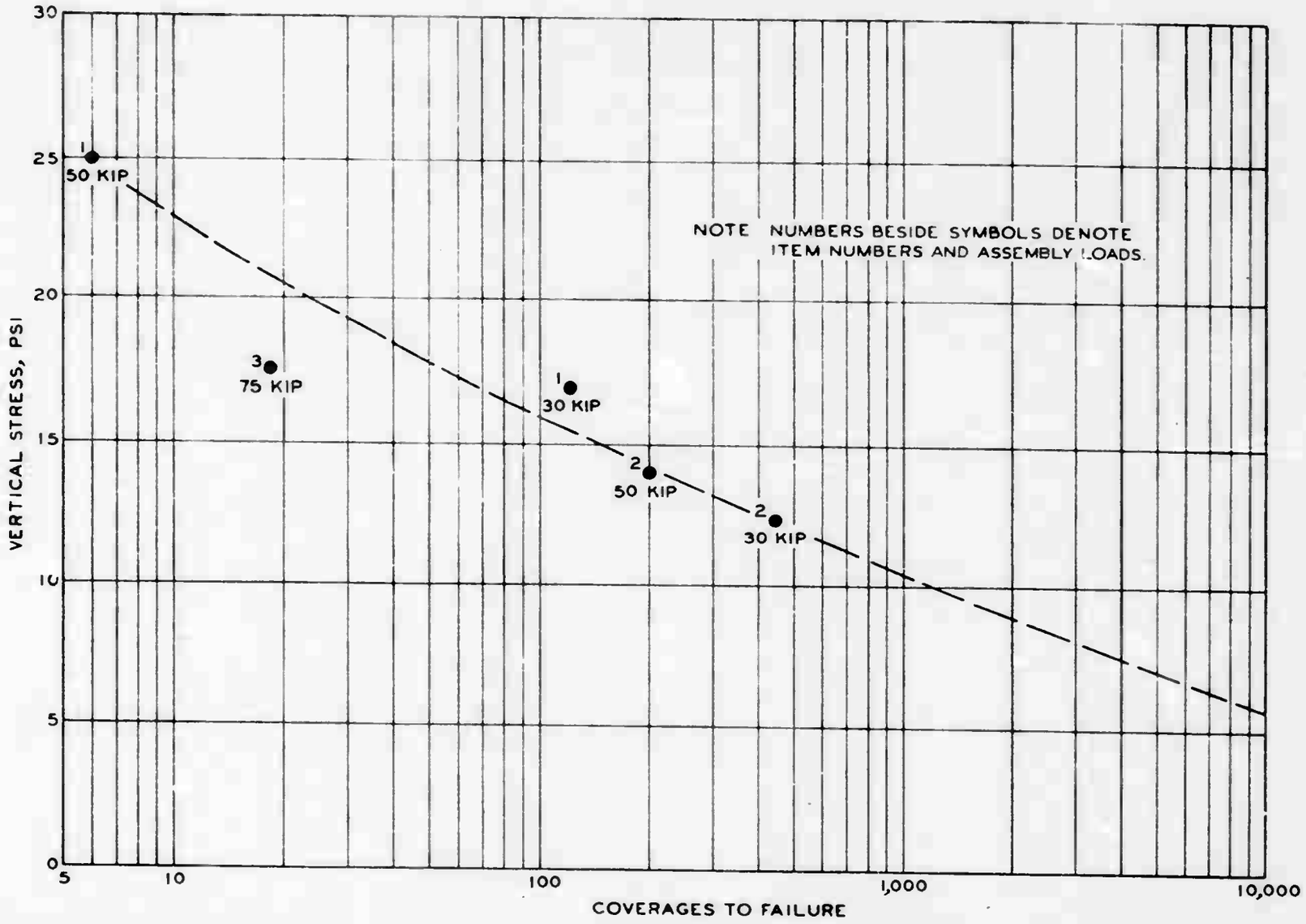

Figure 59. Computed vertical stress imposed on subgrade versus coverages to failure for single-wheel assemblies on MWHGL test section (FEPAVE II program).

level would give a strain value of 2.25×10^{-3}, which would more nearly approximate the actual behavior of the pavement system.

For stabilized material, which is considered to act as a structural element similar to a beam, the relationship between the tensile strength of the material and the tensile stress developed under loading has been considered to have considerable influence on the pavement performance. One method of indicating this influence is by plotting the ratio obtained by dividing the tensile strength by the tensile stress versus the coverages (figure 60). With the exception of the 360-kip loading of item 4 of the structural layer test section, the ratios shown in the figure appear to have definite relationship with coverages. The fact that the parent material of item 4 is granular would be the reason for the deviation from the relationship shown by the other test sections.

b. Surface Deflection

The other frequently used parameter is the surface deflection. The plot of predicted surface deflections of the stabilized sections under a single-wheel load versus coverages to failure for both single- and 12-wheel loads is presented in figure 61, and a similar plot for deflections under a 12-wheel load is presented in figure 62. Figure 63 shows predicted surface deflections for the MWHGL test section under a single-wheel load. Considering all of the assumptions made in analysis, the surface deflections indicate surprisingly good correlation with performance.

Surface deflection reflects the distress of all the pavement components and thus would tend to correlate with performance regardless of the failure mechanism. The present Navy method of pavement design uses the deflection of a 30-in.-diam plate as the basis for design (reference 28). The

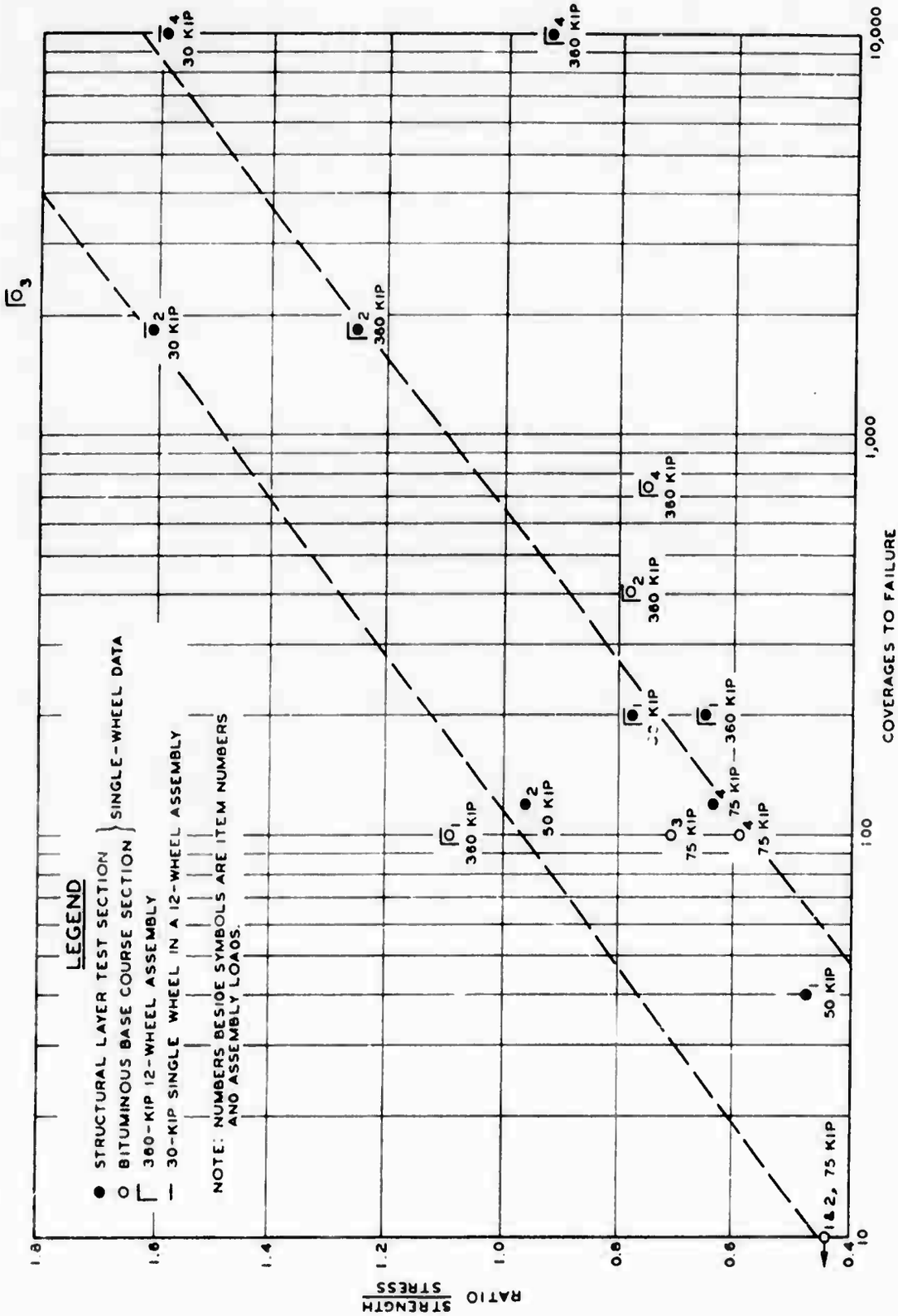

Figure 60. Strength-stress ratio versus coverages to failure for stabilized test sections.

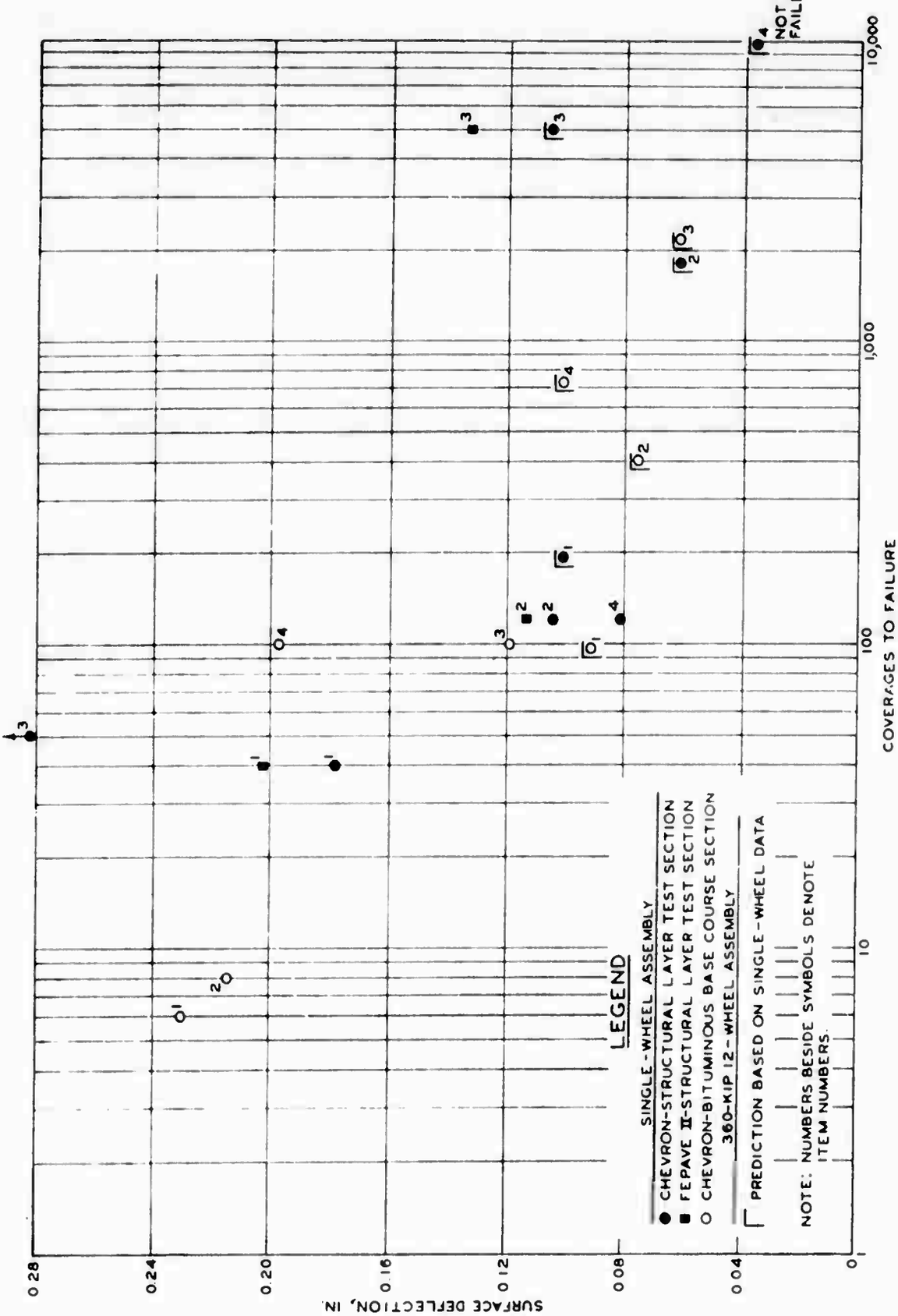

Figure 61. Computed surface deflection versus coverages to failure for single- and 12-wheel assemblies on stabilized test sections.

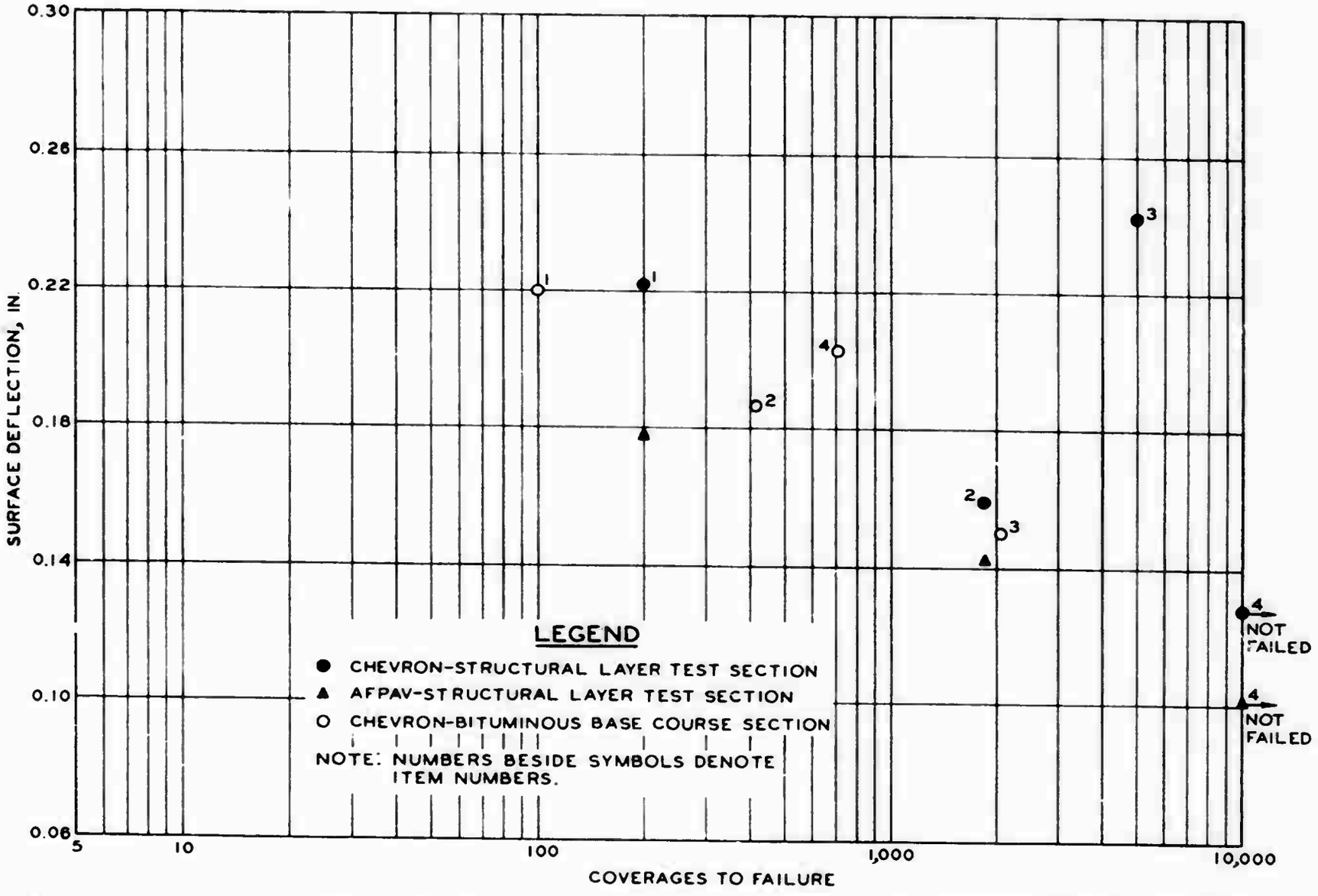

Figure 62. Computed surface deflections versus coverages to failure for 12-wheel 360-kip assembly on stabilized test sections.

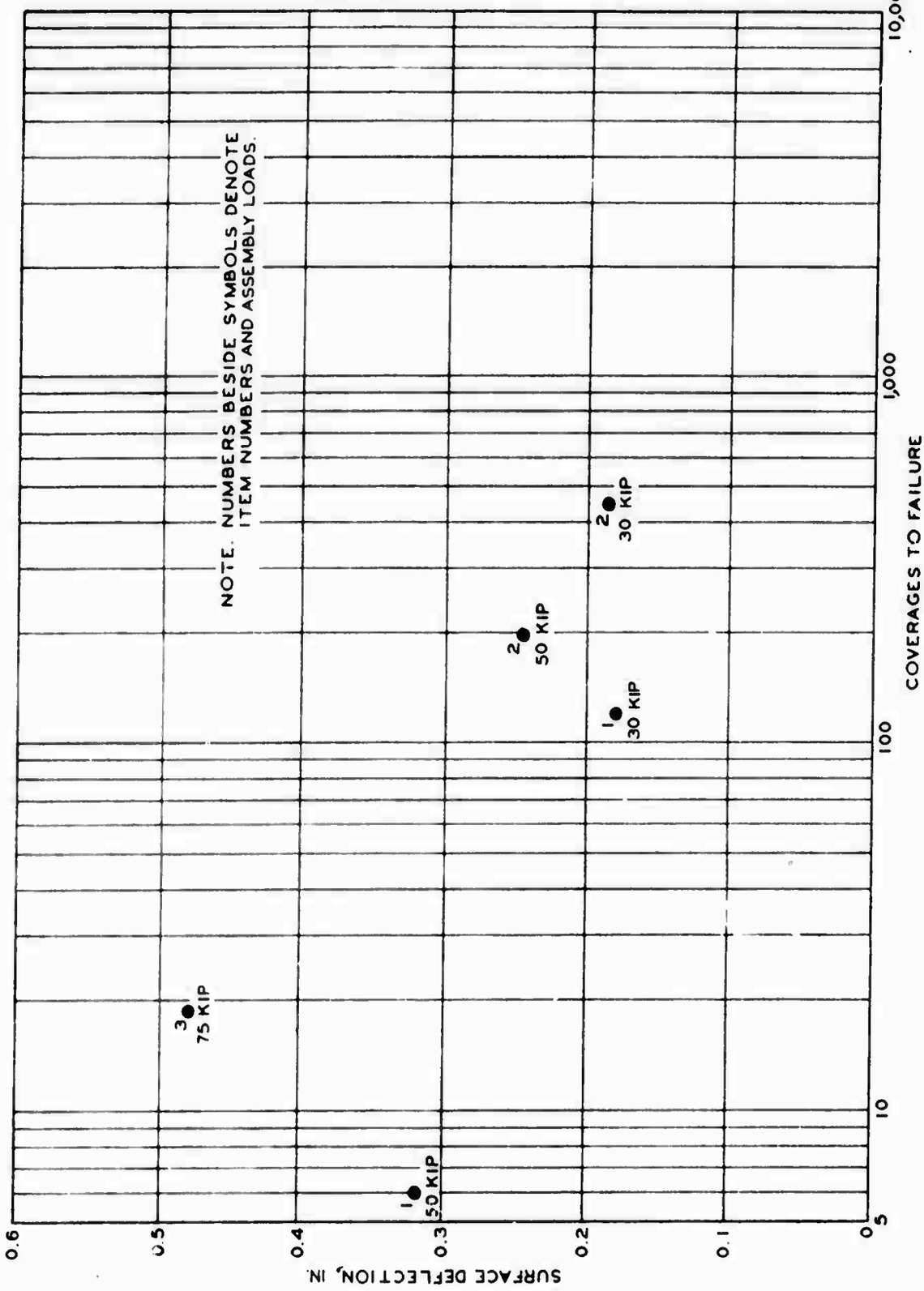

Figure 63. Surface deflections versus coverages to failure for single-wheel assemblies on MWHGL test section (FEPAVE II program).

system requires a pavement thickness sufficient to limit the surface deflection to 0.2 in. The correlation shown for the single-wheel load on the stabilized material would indicate a much smaller limiting surface deflection. For the conventional pavement section, the limiting surface deflection would be somewhat larger than for the stabilized section but still not as large as 0.2 in. It should be kept in mind that the diameter of the tire contact area used in the analysis was in the order of 19 in. and thus would produce more pavement distress per unit deflection than would a 30-in.-diam tire, as represented by the plate used for the Navy design. The 12-wheel 360-kip load produces deflections that come still closer to the 0.2-in. criterion. Thus it would seem that the resulting limiting deflection is going to be highly dependent on tire and gear characteristics. Even with this restriction, the indication is that the surface deflection is a parameter that may be used in the prediction of pavement performance.

6. DISCUSSION OF RESULTS

The approach taken in this investigation was to develop a method by which a pavement structure employing stabilizer layers could be evaluated in terms of performance. The measured response was obtained from test sections constructed and tested at WES. This analysis was attempted without extensive laboratory testing of the material that made up the pavement systems. Thus, the analysis technique employed was one utilizing the simplest of material properties i.e., one employing linear elastic theory. For this reason, the primary tool chosen for the analysis was a computer program (CHEVRON program) that used the Burmister solution of a linearly elastic layered system. A limited amount of work was accomplished utilizing the finite element technique. Because the primary material characterizations were assumed on the basis of the characterizations for similar materials reported in the literature rather

than on laboratory tests of the actual materials, the full analysis capabilities of this technique were not exploited.

The results of the linearly elastic analysis did not agree well with the measured data, but this was not totally unexpected. For the stabilized section, the layered theory tended to underestimate the surface deflections and the subgrade stresses and strains. Even though the computed parameters did not agree with the measured data, a definite correlation was shown to exist between the computed parameters and pavement performance (figures 57-63). The parameters can form the basis for a method of designing pavement systems utilizing structural layers, such as is presented in Appendix II. Since the computed pavement response does not agree with the actual pavement response, the correlations become empirical in nature and thus are valid only for the particular method of analysis used in determining the correlation. This is not to say the values presented cannot be used for design, but that they must be used with caution.

The importance of this study was not in the values computed but in the trends that were indicated. The first and most important indication is that the theoretical approach to pavement design is a valid approach. The theoretical approach offers a procedure by which pavement response and performance can be evaluated regardless of the materials used in the pavement structure. The second indication is the degree of nonlinearity of the material behavior under aircraft loading. This nonlinearity extends in the horizontal direction as well as in vertical direction. Because of this material nonlinearity, the linearly elastic solution fails to simulate actual pavement response. The nonlinear finite elements technique is a tool by which the nonlinear material characteristic can be used and the indication is that much better response simulation is obtained from the nonlinear solutions. Nonlinear axisymmetric

finite element programs that are capable of simulating single-wheel loadings of pavement systems are readily available. One simulation of multiple-wheel loading requires the use of a three-dimensional (3D) analysis program. The AFPAV finite element solution used in this study is capable of linear analysis only and is not suitable for nonlinear analysis. The most promising multiple-wheel analysis is the 3D finite element program. The adaptation of the 3D finite program for nonlinear analysis is a relative new development but one which has been employed successfully to simulate pavement response. Computer storage capacity and costs may still preclude extensive use of nonlinear 3D finite element programs in pavement analysis, but it is expected that with time, the combination of advanced computer technology and more efficient codes will provide a usable tool for pavement analysis. As an interim procedure, it is felt that the nonlinear response of pavement systems to single-wheel loadings could be correlated to pavement performance and could serve as an excellent design tool.

The study brought to light the importance of the material characterization. The material characterization for pavement systems is made especially difficult by factors inherent with both pavement materials and loadings. The properties of the materials are highly dependent on the state of stress, stress history, rate of loading, and environmental conditions. The types of loading include static loadings, slowly moving loads, rapidly moving loads, and dynamic loads caused by landing gear vibrations. As an added complication, these loads are applied in some random distribution across the pavement surface. These complications are reflected in the measured data by the unexplained pattern of strains, the concentration of stresses and strains under the tires, the differences in parameters measured at different times, the consolidation-type deformations, and the plastic subgrade deformations.

One very significant observation made from the measured data is a conditioning of the soil at a point due to loadings directly over the point, then a deconditioning of the soil due to loadings a short distance from the point. This type of behavior greatly increases the magnitude of the repeated stresses and strains and decreases the life of the pavement. The implication in this behavior is that the stress history is of major importance and that tests for characterizing the material must realistically simulate not only the state of stress but also the stress history. Thus it would appear that much work is necessary for developing laboratory tests and procedures that will furnish the necessary material characterizations to be used in the nonlinear analysis of pavement systems.

SECTION V

CONCLUSIONS AND RECOMMENDATIONS

1. CONCLUSIONS

The conclusions reached as a result of this study are:

a. For the test sections at WES, there is a correlation between computed parameters and pavement performance. This correlation can be used as a basis for developing design methods for pavement systems having similar structural layers.

b. The performance of pavement systems employing structural layers is influenced by the stress-strain relationship and the tensile strength of the stabilized material. Thus the structural benefit of the layers can be evaluated by evaluating these material properties.

c. The linearly elastic analysis utilizing modulus values from the indirect tensile test does not adequately simulate the behavior of all pavement systems employing stabilized layers. The simulation was better for the lime- and cement-stabilized lean clay than for the cement-stabilized clay gravel or the asphalt-stabilized material. The primary cause of the disagreement in the case of the stabilized gravel was the stress-dependent stress-strain relation of the parent material and in the case of asphalt material, time- and temperature-dependent stress-strain relationship of the asphalt.

d. The behavior of the buckshot clay is nonlinear with respect to deviator stress. At the stress levels obtained in the test sections, the secant modulus is less than one-half the modulus indicated by the relationship of 1500 times CBR.

e. Because of the highly nonlinear nature of the pavement materials, the most promising technique for simulating the pavement behavior is the nonlinear finite element technique. For single-wheel analysis, programs are readily available; for multiple-wheel analysis, some interim procedure must be devised until the nonlinear 3D finite element programs are fully developed.

f. This same nonlinearity requires the development of sophisticated laboratory testing equipment and techniques that more nearly simulate field conditions than the tests now being conducted. The area of material characterization is the area where maximum effort should now be applied.

2. RECOMMENDATIONS

The study clearly demonstrates the need for basic research in the area of pavement behavior. As a result of the study the following recommendations are made:

a. The study of the WES test sections should be continued with emphasis placed on use of nonlinear finite element analysis.

b. Work should be pursued on the development of tests and techniques for adequately characterizing the pavement materials. Emphasis should be placed on the state of stress, stress history, and environmental factors.

c. The correlations derived in this study should be checked against the performance of the pavement systems.

d. New test sections should be considered where the primary purpose of the test sections would be to verify the theoretical approach to pavement design. Small-scale tests could be utilized as part of the verification process.

e. Further investigation should be given the explained development of extension in the stabilized layers as the pavement was loaded. In future test

sections particular attention should be given to vertical strains in the stabilized materials.

APPENDIX I: STRESS AND STRAIN MEASUREMENTS MADE DURING STATIC LOADING OF STRUCTURAL LAYERS TEST SECTION

Stress and strain sensors were used to monitor the behavior of the static loading of structural layers test section. The data from these tests, used in the analyses described in the main text, are presented in Tables I-1 through I-4. Figure I-1 shows the coordinate systems referenced in the tables.

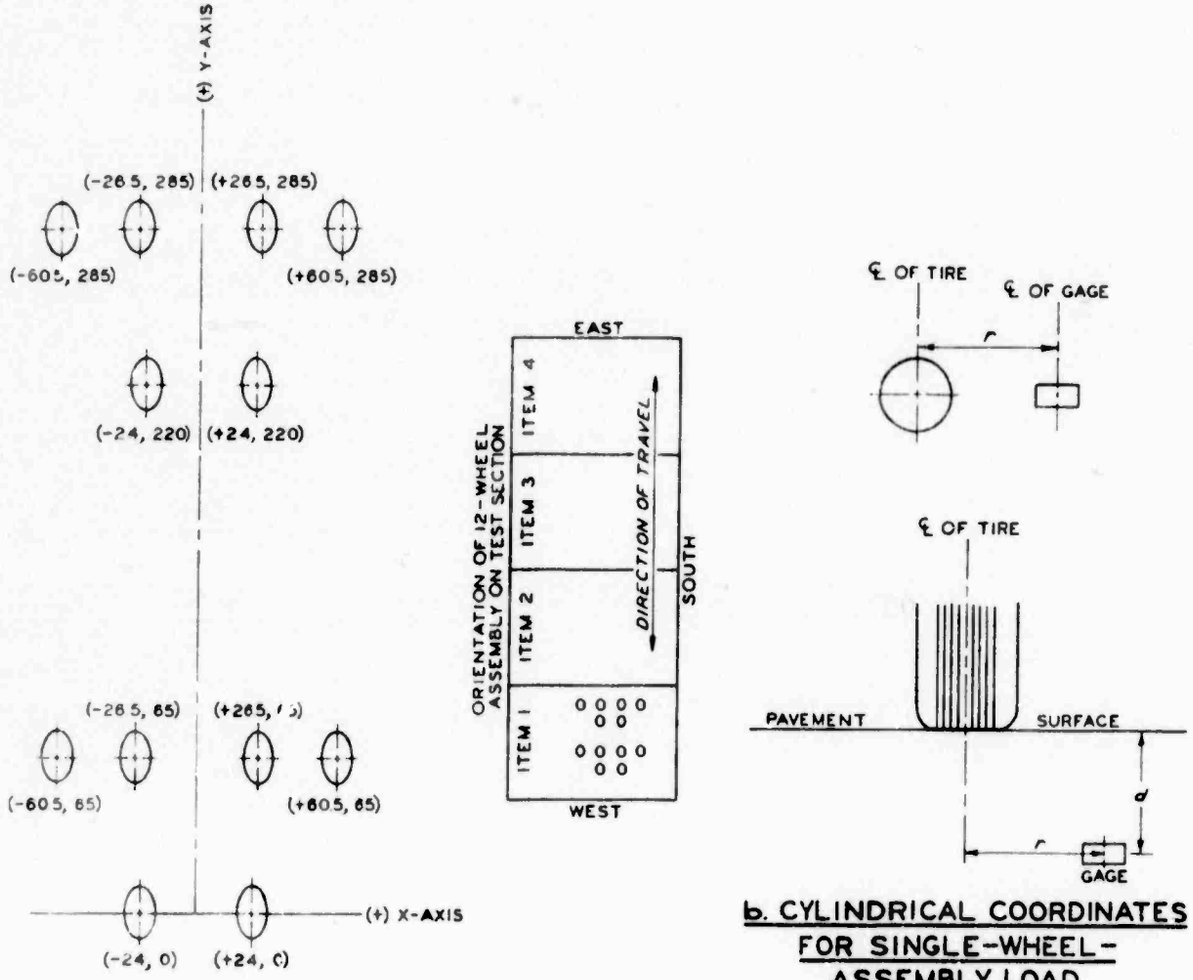

a. X-Y AXES FOR 12-WHEEL-ASSEMBLY LOAD

b. CYLINDRICAL COORDINATES FOR SINGLE-WHEEL-ASSEMBLY LOAD

Figure I-1. Coordinate systems for 12-wheel and single-wheel assemblies.

Table I-1

Stress Data for Single-Wheel Assembly Tests

Item	Coverages	Assembly Gross Load Kips	Assembly Location Coordinates, in.* r	Assembly Location Coordinates, in.* d	Stress σ_v psi
1	0	30	0	24	18.1
			26.5	24	0.8
			48	24	- 0.2
2	0	30	0	24	15.3
			26.5	24	0.7
			48	24	1.0
3	0	30	0	24	25.8
			26.5	24	0
			48	24	1.0
4	0	30	0	24	7.3
			26.5	24	0.5
			48	24	0.8
4	After 10,000 coverages, 12-wheel 360-kip load	50	0	24	31.0
			13.25	24	26.5
			26.50	24	11.5
			39.75	24	3.0
			53.00	24	0.5
		60	0	24	30.0
			13.25	24	22.0
			26.50	24	8.5
			39.75	24	2.3
			53.00	24	0.3
		75	0	24	36.0
			13.25	24	29.0
			26.50	24	12.0
			39.75	24	1.5
			53.00	24	0.3

* Coordinates are shown in figure I-1.

Table I-2

Strain Data for Single-Wheel Assembly Tests

Item	Coverages	Gross Load Kips	Assembly Location Coordinates, in.* r	d	Reading No.	Strain, in./in.** ε_v	ε_r	ε_t
1	0	30	26.5	6	1	-0.0039	-	-
			26.5	16.5	2	+0.0066	-	-
			26.5	28.5	3	+0.0050	-	-
			0	6	4	+0.0021	-	-
			0	16.5	5	-0.0011	-	-
			0	28.5	6	+0.0056	-	-
			53.0	6	7	0	-	-
			53.0	16.5	8	-0.0008	-	-
			53.0	28.5	9	0	-	-
			0	6	10	+0.0035	-	-
			0	16.5	11	0	-	-
			0	28.5	12	+0.0052	-	-
			26.5	6	13	+0.0041	-	-
			26.5	16.5	14	+0.0070	-	-
			26.5	28.5	15	+0.0075	-	-
			0	6	16	No reading	-	-
			0	16.5	17	-0.0013	-	-
			0	28.5	18	+0.0083	-	-
			53.0	6	19	+0.001	-	-
			53.0	16.5	20	-0.002	-	-
			53.0	28.5	21	+0.007	-	-
2	0	30	26.5	6	22	-0.009	-	-
			26.5	16.5	23	-0.0018	-	-
			26.5	28.5	24	+0.0001	-	-
			0	6	25	+0.0003	-	-
			0	16.5	26	-0.0012	-	-
			0	28.5	27	+0.0027	-	-
			53.0	6	28	-0.0001	-	-
			53.0	16.5	29	-0.0007	-	-
			53.0	28.5	30	+0.0001	-	-
			0	6	31	-0.0024	-	-
			0	16.5	32	-0.0002	-	-
			0	28.5	33	+0.0034	-	-
			0	16.5	34	-0.0003	-	-
			0	28.5	35	+0.0039	-	-
			26.5	16.5	36	-0.0006	-	-
			26.5	28.5	37	+0.0015	-	-
			26.5	16.5	38	-0.0014	-	-
			26.5	28.5	39	+0.0002	-	-
			26.5	6	40	-0.0006	-	-

Table I-2 (Cont'd)

Item	Coverages	Gross Load Kips	Assembly Location Coordinates, in.* r	d	Reading No.	Strain, in./in.** ε_v	ε_r	ε_t
2	0	30	26.5	16.5	41	-0.0011	-	-
			26.5	28.5	42	+0.0017	-	-
			53.0	6	43	0	-	-
			53.0	16.5	44	-0.0003	-	-
			53.0	28.5	45	0	-	-
			0	6	46	+0.0008	-	-
			0	16.5	47	-0.0012	-	-
			0	28.5	48	+0.0030	-	-
			26.5	16.5	49	-	+0.0020	-
			0	16.5	50	-	-0.0003	-
			53.0	16.5	51	-	-0.0004	-
			0	16.5	52	-	-0.0004	-
			0	28.5	53	-	-0.0010	-
			26.5	28.5	54	-	0	-
			26.5	28.5	55	-	0	-
			0	28.5	56	-	-	-0.0011
			26.5	28.5	57	-	-	-0.0003
			26.5	28.5	58	-	-	0
3	0	30	26.5	6	59	-0.0016	-	-
			26.5	16.5	60	-0.0014	-	-
			26.5	28.5	61	-0.0020	-	-
			0	6	62	+0.0008	-	-
			0	16.5	63	+0.0001	-	-
			0	28.5	64	+0.0029	-	-
			53.0	6	65	-0.001	-	-
			53.0	16.5	66	-0.007	-	-
			53.0	28.5	67	-0.002	-	-
			0	6	68	+0.0016	-	-
			0	16.5	69	+0.0006	-	-
			0	28.5	70	+0.0034	-	-
			26.5	6	71	+0.0002	-	-
			26.5	16.5	72	-0.0004	-	-
			26.5	28.5	73	+0.0011	-	-
			53.0	6	74	+0.0001	-	-
			53.0	16.5	75	0	-	-
			53.0	28.5	76	+0.0002	-	-
			0	6	77	+0.0006	-	-
			0	16.5	78	+0.0006	-	-
			0	28.5	79	-0.0060	-	-
4	0	30	26.5	6	80	-0.0009	-	-
			26.5	16.5	81	-0.0013	-	-
			26.5	28.5	82	+0.0006	-	-
			0	6	83	-0.0001	-	-

Table I-2 (Cont'd)

Item	Coverages	Gross Load Kips	Assembly Location Coordinates, in.* r	d	Reading No.	Strain, in./in.** ε_v	ε_r	ε_t
-	0	30	0	16.5	84	-0.0012	-	-
			0	28.5	85	+0.0019	-	-
			53.0	6	86	+0.0011	-	-
			53.0	16.5	87	-0.0006	-	-
			53.0	28.5	88	+0.0005	-	-
			0	6	89	+0.0010	-	-
			0	16.5	90	-0.0010	-	-
			0	28.5	91	+0.0009	-	-
			0	28.5	92	+0.0021	-	-
			26.5	28.5	93	+0.0008	-	-
			26.5	28.5	94	+0.0003	-	-
			26.5	6	95	0	-	-
			26.5	16.5	96	-0.0002	-	-
			53.0	6.0	97	0	-	-
			53.0	16.5	98	0	-	-
			0	6	99	+0.0003	-	-
			0	16.5	100	-0.0013	-	-
			26.5	16.5	101	-	-0.0002	-
			0	16.5	102	-	-0.0005	-
			53.0	16.5	103	-	0	-
			0	16.5	104	-	-0.0004	-
			0	28.5	105	-	-0.0006	-
			26.5	28.5	106	-	-0.0004	-
			26.5	28.5	107	-	0	-
			26.5	16.5	108	-	-	-0.0011
			0	16.5	109	-	-	-0.0007
			53.0	16.5	110	-	-	-0.0002
			0	16.5	111	-	-	0
			0	28.5	112	-	-	-0.0007
			26.5	28.5	113	-	-	-0.0002
			26.5	28.5	114	-	-	+0.0047
4	After 10,000 coverages 12-wheel 30-kip load	50	0	6	1	+0.0022	-	-
			0	6	2	+0.0013	-	-
			0	16.5	3	-0.0016	-	-
			0	16.5	4	-0.0014	-	-
			0	28.5	5	+0.0053	-	-
			0	28.5	6	+0.0058	-	-
			26.5	6	7	-0.0003	-	-
			26.5	6	8	-0.0020	-	-
			26.5	16.5	9	-0.0012	-	-
			26.5	16.5	10	-0.0020	-	-
			26.5	28.5	11	+0.0014	-	-
			26.5	28.5	12	+0.0008	-	-
			26.5	28.5	13	+0.0020	-	-
			53.0	6	14	-0.0003	-	-

Table I-2 (Cont'd)

Item	Coverages	Gross Load Kips	Assembly Location Coordinates, in.* r	d	Reading No.	Strain, in./in.** ε_v	ε_r	ε_t
4	After 10,000 coverages 12-wheel 360-kip load	50	53.0	6	15	-0.0011	-	-
			53.0	16.5	16	-0.0013	-	-
			53.0	16.5	17	-0.0011	-	-
			53.0	28.5	18	-0.0001	-	-
			0	16.5	19	-	-0.0009	-
			26.5	16.5	20	-	-0.0010	-
			53.0	16.5	21	-	-0.0010	-
			0	28.5	22	-	-0.0002	-
			26.5	28.5	23	-	-0.0015	-
			53.0	28.5	24	-	-0.0001	-
			0	16.5	25	-	-	-0.0007
			26.5	16.5	26	-	-	-0.0009
			53.0	16.5	27	-	-	-0.0002
			0	28.5	28	-	-	-0.0014
			26.5	28.5	29	-	-	-0.0021
			53.0	28.5	30	-	-	-0.0003
		60	0	6	1	+0.0036	-	-
			0	6	2	+0.0018	-	-
			0	16.5	3	-0.0012	-	-
			0	16.5	4	-0.0011	-	-
			0	28.5	5	+0.0059	-	-
			0	28.5	6	+0.0081	-	-
			26.5	6	7	-0.0011	-	-
			26.5	6	8	-0.0021	-	-
			26.5	16.5	9	-0.0016	-	-
			26.5	16.5	10	-0.0021	-	-
			26.5	28.5	11	+0.0023	-	-
			26.5	28.5	12	+0.0008	-	-
			26.5	28.5	13	+0.0026	-	-
			53.0	6	14	-0.0008	-	-
			53.0	6	15	-0.0005	-	-
			53.0	16.5	16	-0.0013	-	-
			53.0	16.5	17	-0.0010	-	-
			53.0	28.5	18	0	-	-
			0	16.5	19	-	-0.0018	-
			26.5	16.5	20	-	-0.0012	-
			53.0	16.5	21	-	-0.0014	-
			0	28.5	22	-	-0.0004	-
			26.5	28.5	23	-	-0.0018	-
			53.0	28.5	24	-	0	-
			0	16.5	25	-	-	-0.0015
			26.5	16.5	26	-	-	-0.0001
			53.0	16.5	27	-	-	-0.0005
			0	28.5	28	-	-	-0.0011

Table I-2 (Cont'd)

Item	Coverages	Gross Load Kips	Assembly Location Coordinates, in.* r	d	Reading No.	Strain, in./in.** ε_v	ε_r	ε_t
4	After 10,000 coverages	60	26.5	28.5	29	-	-	-0.0029
			53.0	28.5	30	-	-	-0.0009
	12-wheel	75	0	6	1	+0.0024	-	-
	360-kip load		0	6	2	+0.0015	-	-
			0	16.5	3	-0.0018	-	-
			0	16.5	4	-0.0011	-	-
			0	28.5	5	+0.0057	-	-
			0	28.5	6	+0.0072	-	-
			26.5	6	7	-0.0014	-	-
			26.5	6	8	-0.0015	-	-
			26.5	16.5	9	-0.0018	-	-
			26.5	16.5	10	-0.0019	-	-
			26.5	28.5	11	+0.0025	-	-
			26.5	28.5	12	+0.0012	-	-
			26.5	28.5	13	+0.0026	-	-
			53.0	6	14	-0.0002	-	-
			53.0	6	15	-0.0003	-	-
			53.0	16.5	16	-0.0012	-	-
			53.0	16.5	17	-0.0009	-	-
			53.0	28.5	18	+0.0001	-	-
			0	16.5	19	-	-0.0018	-
			26.5	16.5	20	-	-0.0010	-
			53.0	16.5	21	-	-0.0010	-
			0	28.5	22	-	+0.0001	-
			26.5	28.5	23	-	-0.0018	-
			53.0	28.5	24	-	-0.0004	-
			0	16.5	25	-	-	-0.0011
			26.5	16.5	26	-	-	-0.0003
			53.0	16.5	27	-	-	-0.0006
			0	28.5	28	-	-	-0.0012
			26.5	28.5	29	-	-	-0.0022
			53.0	28.5	30	-	-	-0.0003

* Coordinates are shown in figure I-1.

** ε_v, ε_r, ε_t represent orientation of strain measurement in vertical, radial, and tangential directions, respectively, as related to cylindrical coordinate system. Readings preceded by minus sign represent extension. Readings preceded by plus sign represent compresion.

Table I-3

Stress Data for 12-Wheel 360-Kip Assembly Tests

Item	Coverages	Assembly Location Coordinates, in.* x	y	z	Stress σ_v psi
1	0	0	65	24	6.5
		26.5	65	24	20.4
		53.0	65	24	17.8
		26.5	113	24	0.9
	96	26.5	65	24	27.3
		26.5	113	24	2.8
	201	26.5	65	24	24.2
		26.5	113	24	1.1
2	0	0	65	24	9.0
		26.5	65	24	18.4
		53.0	65	24	18.2
		26.5	113	24	1.9
	96	26.5	65	24	23.4
		26.5	113	24	1.6
	1327	26.5	65	24	12.4
		26.5	113	24	2.0
3	0	0	65	24	6.5
		26.5	65	24	24.9
		53.0	65	24	18.5
		26.5	113	24	-0.8
	96	26.5	65	24	29.6
		26.5	113	24	1.2
	1515	26.5	65	24	30.2
		26.5	113	24	0.9
	5000	26.5	65	24	27.0
		26.5	113	24	1.0
4	0	0	65	24	7.3
		26.5	65	24	10.0
		53.0	65	24	7.3
		26.5	113	24	1.8

1 of 2 pages

Table I-3 (Cont'd)

Item	Coverages	Assembly Location Coordinates, in.* x	y	z	Stress σ_v psi
4	96	26.5	65	24	14.8
		26.5	113	24	2.2
	1515	26.5	65	24	16.2
		26.5	113	24	1.3
	5000	26.5	65	24	18.4
		26.5	113	24	2.5

* Coordinates are shown in figure I-1.

Table I-4

Strain Data for 12-Wheel 360-Kip Assembly Tests

Item	Coverages	Assembly Location Coordination, in.* x	y	z	Strain, in./in.** ε_v	ε_{x-x}	ε_{y-y}
1	0	-26.5	65	6	+0.0035		
				16.5	0		
				28.5	+0.0054		
		+26.5	65	6	NR		
				16.5	-0.0030		
				28.5	-0.0065		
		0	65	6	-0.0021		
				16.5	-0.0006		
				28.5	+0.0029		
		53.0	65	6	-0.0020		
				16.5	-0.0012		
				28.5	+0.0069		
	96	-26.5	65	6	+0.0022		
				16.5	+0.0019		
				28.5	+0.0069		
		+26.5	65	6	+0.0054		
				16.5	+0.0004		
				28.5	+0.0069		
	200	-26.5	65	6	+0.0028		
				16.5	+0.0012		
				28.5	+0.0166		
		+26.5	65	6	NR		
				16.5	+0.0016		
				28.5	+0.0038		
2	0	-26.5	65	6	-0.0016		
				16.5	+0.0003		
				28.5	+0.0039		
		+26.5	65	6	-0.0004		
				16.5	-0.0009		
				28.5	+0.0039		
		0	65	6	NR		
				16.5	-0.0007		
				28.5	+0.0020		
		0	65	6	-0.0042		
				16.5	+0.0001		
				28.5	+0.0021		
		53.0	65	6	-0.0018		
				16.5	+0.0003		
				28.5	+0.0039		
		+26.5	65	6	NR		
				16.5	-0.0004		
				28.5	+0.0037		

Table I-4 (Cont'd)

Item	Coverages	Assembly Location Coordination, in.* x	y	z	Strain, in./in.** ε_v	ε_{x-x}	ε_{y-y}
2	96	-26.5	65	6	-0.0059		
				16.5	+0.0003		
				28.5	+0.0043		
		+26.5	65	6	-0.0024		
				16.5	+0.0010		
				28.5	+0.0051		
		0	65	6	NR		
				16.5	-0.0004		
				28.5	+0.0024		
	1327	-26.5	65	6.	-0.0327		
				16.5	-0.0056		
				28.5	-0.0001		
		+26.5	65	6	-0.0097		
				16.5	-0.0060		
				28.5	-0.0003		
		0	65	6	NR		
				16.5	-0.0066		
				28.5	-0.0005		
	0	-26.5	65	6		NR	
				16.5		-0.0001	
				28.5		--	
		0	65	6		--	
				16.5		--	
				28.5		-0.0001	
		0	65	6		--	
				16.5		-0.0006	
				28.5		--	
		26.5	65	6		--	
				16.5		--	
				28.5		-0.0007	
	96	-26.5	65	6		--	
				16.5		-0.0004	
				28.5		--	
		0	65	6		--	
				16.5		--	
				28.5		+0.0004	
	1327	-26.5	65	6		--	
				16.5		-0.0062	
				28.5		--	
		0	65	6		--	
				16.5		--	
				28.5		-0.0024	
	0	0	65	6		--	--
				16.5			--
				28.5			-0.0004

Table I-4 (Cont'd)

Item	Coverages	Assembly Location Coordination, in.* x	y	z	Strain, in./in.** ε_v	ε_{x-x}	ε_{y-y}
2	0	+26.5	65	6			--
				16.5			--
				28.5			-0.0013
	96	0	65	6			--
				16.5			--
				28.5			-0.0012
	1327	0	65	6			--
				16.5			--
				28.5			-0.0051
3	0	-26.5	65	6	-0.0010		
				16.5	+0.0003		
				28.5	+0.0026		
		+26.5	65	6	0		
				16.5	+0.0003		
				28.5	+0.0050		
		0	65	6	-0.0002		
				16.5	+0.0008		
				28.5	+0.0005		
		53.0	65	6	-0.0004		
				16.5	+0.0005		
				28.5	+0.0059		
	96	-26.5	65	6	-0.0002		
				16.5	+0.0011		
				28.5	+0.0026		
		+26.5	65	6	-0.0008		
				16.5	+0.0003		
				28.5	+0.0051		
	1515	-26.5	65	6	-0.0115		
				16.5	-0.0069		
				28.5	-0.0101		
		26.5	65	6	-0.0037		
				16.5	-0.0037		
				28.5	0		
	5000	-26.5	65	6	-0.0004		
				16.5	0		
				28.5	+0.0025		
		+26.5	65	6	NR		
				16.5	0		
				28.5	+0.0035		
4	0	-26.5	65	6	+0.0013		
				16.5	-0.0025		
				28.5	+0.0031		
		+26.5	65	6	+0.0008		
				16.5	-0.008		
				28.5	--		

Table I-4 (Cont'd)

Item	Coverages	Assembly Location Coordination, in.* x	y	z	Strain, in./in.** ε_v	ε_{x-x}	ε_{y-y}
4	0	0	65	6	--		
				16.5	--		
				28.5	+0.0021		
		0	65	6	-0.0021		
				16.5	-0.0017		
				28.5	+0.0014		
		53.0	65	6	-0.0027		
				16.5	-0.0014		
				28.5	--		
		+26.5	65	6	--		
				16.5	--		
				28.5	+0.0018		
	96	-26.5	65	6	+0.0151		
				16.5	+0.0051		
				28.5	+0.0101		
		+26.5	65	6	+0.0133		
				16.5	+0.0069		
				28.5	--		
		0	65	6	--		
				16.5	--		
				28.5	+0.0124		
	1515	-26.5	65	6	-0.0005		
				16.5	-0.0013		
				28.5	+0.0018		
		+26.5	65	6	+0.0001		
				16.5	-0.0007		
				28.5	--		
		0	65	6	--		
				16.5	--		
				28.5	+0.0005		
	5000	-26.5	65	6	+0.0006		
				16.5	-0.0004		
				28.5	+0.0024		
		+26.5	65	6	+0.0003		
				16.5	-0.0012		
				28.5	--		
		0	65	6	--		
				16.5	--		
				28.5	+0.0008		
	10,000	-26.5	65	6	+0.0006		
				16.5	-0.0007		
				28.5	+0.0020		
		+26.5	65	6	+0.0003		
				16.5	-0.0012		
				28.5	--		

Table I-4 (Cont'd)

Item	Coverages	Assembly Location Coordination, in.* x	y	z	Strain, in./in.** ε_v	ε_{x-x}	ε_{y-y}
4	10,000	0	65	6	--		
				16.5	--		
				28.5	+0.0011		
	0	-26.5	65	16.5		-0.0007	
				28.5		--	
		0	65	16.5		--	
				28.5		+0.0001	
		0	65	16.5		-0.0015	
				28.5			
		+26.5	65	16.5		--	
				28.5		-0.0021	
	96	-26.5	65	16.5		+0.0072	
				28.5		--	
		0	65	16.5		--	
				28.5		+0.0072	
	1515	-26.5	65	16.5		+0.0037	
				28.5		--	
		0	65	16.5		--	
				28.5		-0.0035	
	5000	-26.5	65	16.5		-0.0008	
				28.5		--	
		0	65	16.5		--	
				28.5		0	
	10,000	-26.5	65	16.5		-0.0010	
				28.5		--	
		0	65	16.5		--	
				28.5		0	
	0	-26.5	65	16.5			-0.0002
				28.5			
		0	65	16.5			
				28.5			-0.0003
		0	65	16.5			-0.0019
				28.5			--
		+26.5	65	16.5			--
				28.5			-0.0031
	96	-26.5	65	16.5			+0.0076
				28.5			--
		0	65	16.5			--
				28.5			+0.0076
	1515	-26.5	65	16.5			-0.0048
				28.5			--
		0	65	16.5			--
				28.5			-0.0052

Table I-4 (Concl'd)

Item	Coverages	Assembly Location Coordination, in.* x	y	z	Strain, in./in.** ε_v	ε_{x-x}	ε_{y-y}
4	5,000	-26.5	65	16.5			-0.0006
				28.5			--
		0	65	16.5			--
				28.5			-0.0005
	10,000	-26.5	65	16.5			-0.0004
				28.5			--
		0	65	16.5			--
				28.5			-0.0003

* Coordinates are shown in figure I-I.

** Subscripts refer to rectangular coordinate system shown in figure I-I. Readings preceded by minus sign represent extension. Readings preceded by plus sign represent compression. NR equals no reading.

APPENDIX II: EXAMPLE OF DESIGN PROCEDURE FOR THREE-LAYER FLEXIBLE PAVEMENTS INVOLVING STABILIZED PAVEMENTS

1. DESIGN PROCEDURE

The design procedure presented herein is based on two computed response parameters - surface deformation and vertical stress at the top of the subgrade. The correlations between these two parameters and performance are based on the data presented in figures II-1 and II-2, which were figures 58 and 61 of the main text of this report. The data on which the correlations were based were somewhat limited in scope; therefore, extension of the design procedure into other areas should be approached with caution.

Basically the procedure calls for initially determining the material properties of the pavement section and computing the vertical subgrade stress and surface deformation due to the load of a single wheel of the design aircraft. The parameters are then related to predicted performance using the criteria presented in figures II-3 and II-4.

The procedure consists of five base steps as follows.

(1) The total section thickness for the desired service life is estimated using conventional criteria.

(2) The modulus of elasticity and Poisson's ratios of the materials in the three different layers above the subgrade are determined. The modulus and Poisson's ratio of asphaltic concrete can be estimated on the basis of anticipated temperature and a static loading condition. The modulus of the stabilized material should be determined utilizing results of split tensile tests on representative samples of the material. Poisson's ratio for most stabilized material may be assumed to be 0.3 or 0.35. The modulus of the subgrade in psi can be estimated by use of the expression: $E = 1500 \times \overline{CBR}$.

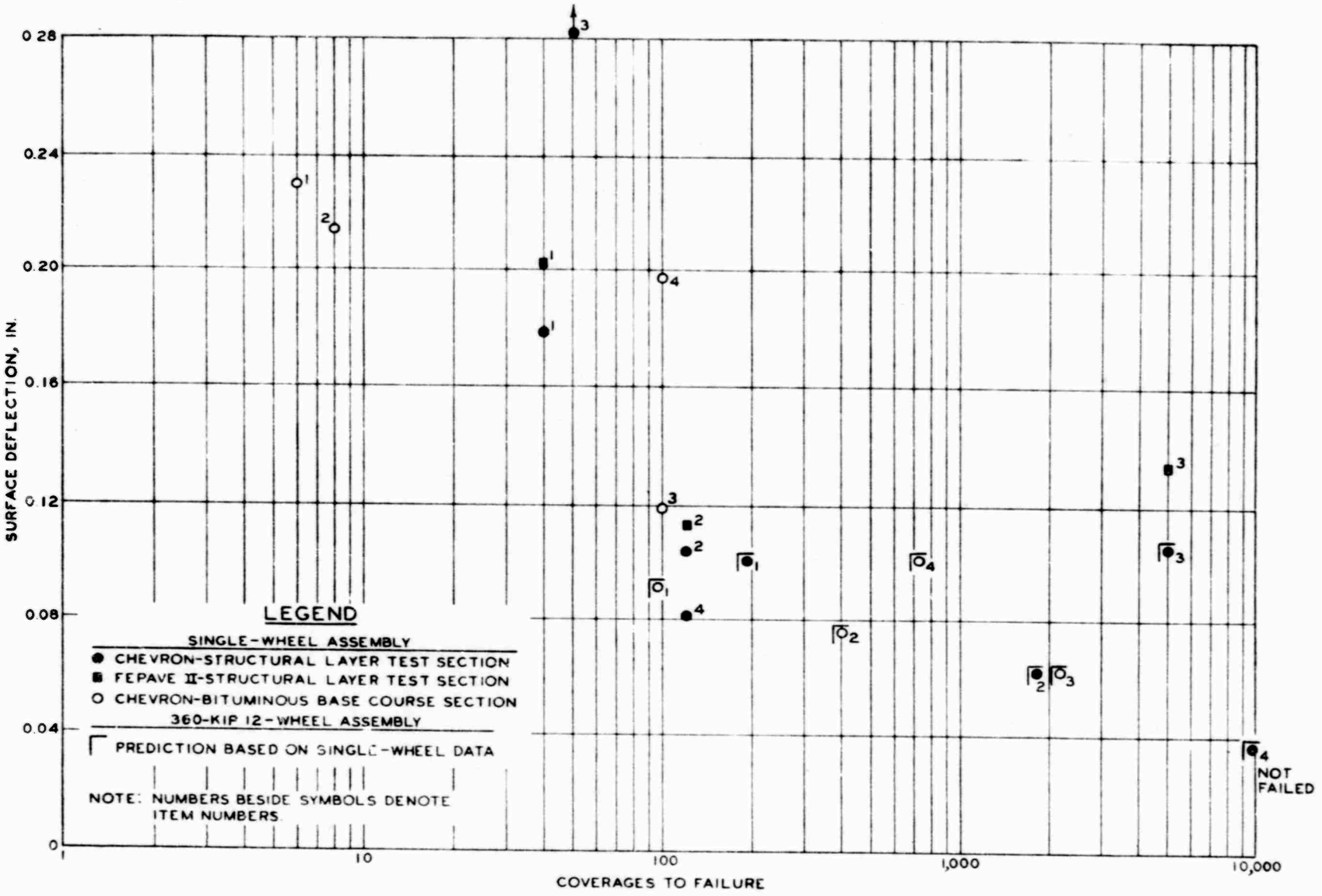

Figure II-1. Computed vertical stress imposed on subgrade versus coverages to failure for single- and 12-wheel assemblies on stabilized test sections.

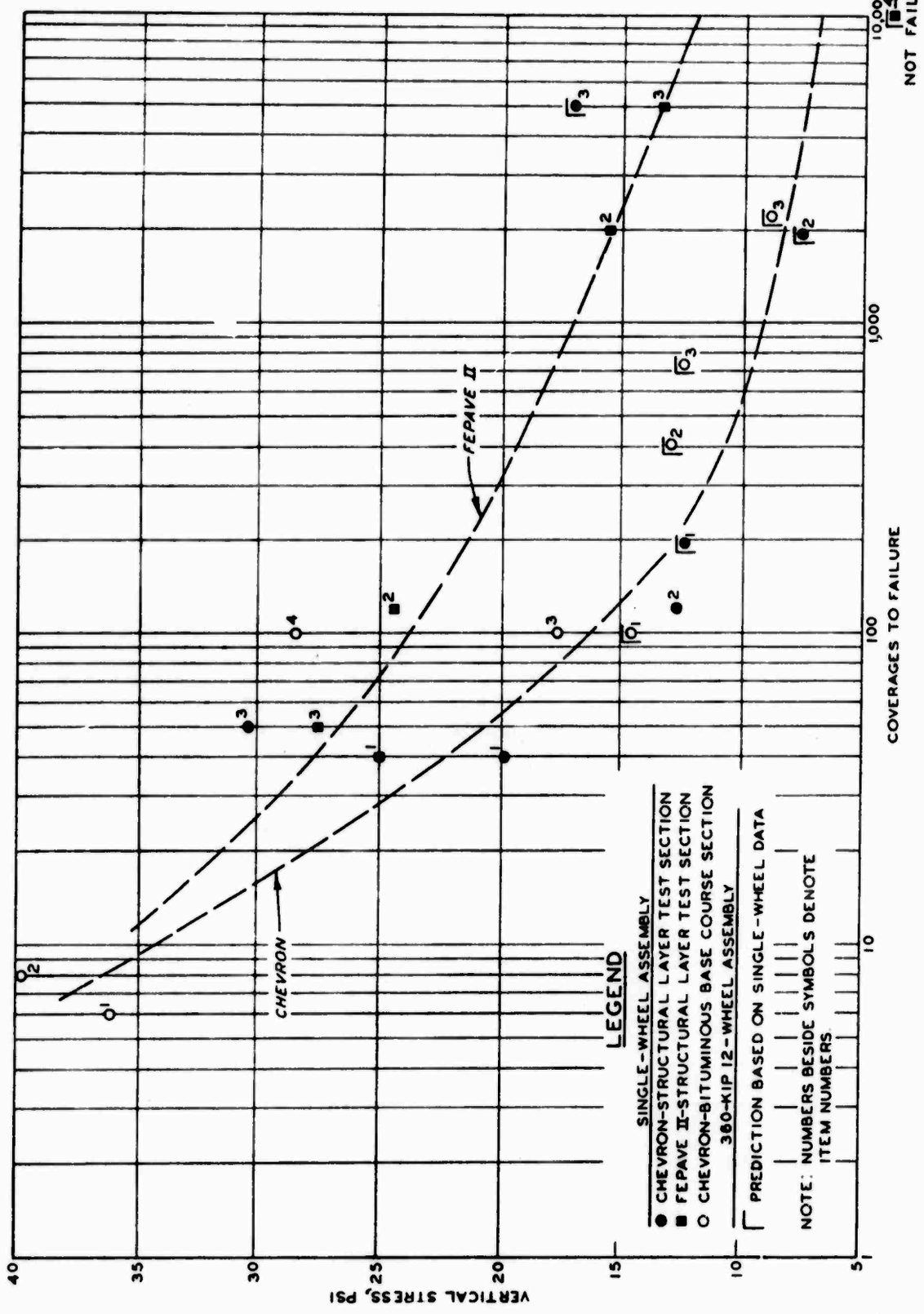

Figure II-2. Computed surface deflection versus coverages to failure for single- and 12-wheel assemblies on stabilized test sections.

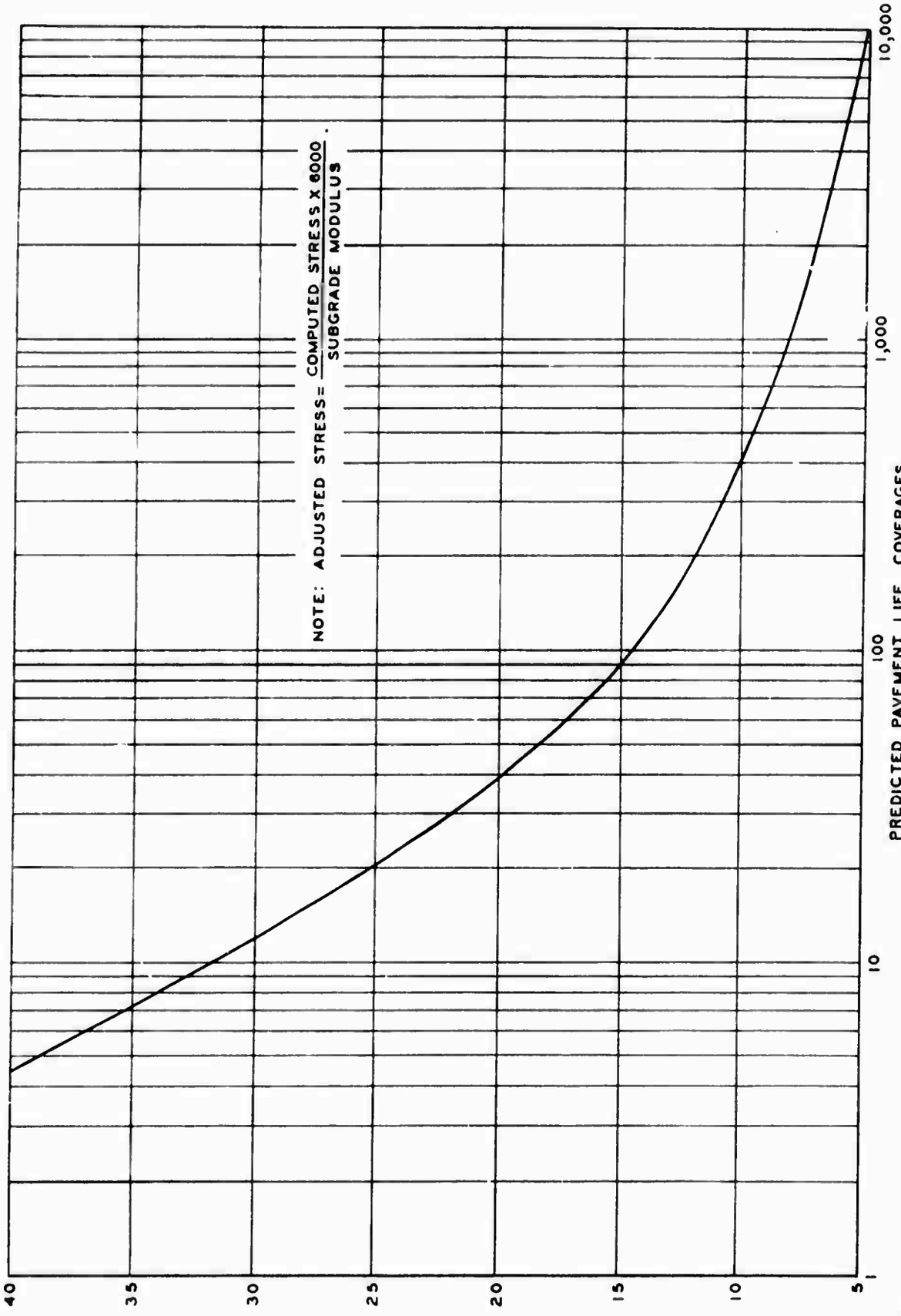

Figure II-3. Adjusted computed stress at top of subgrade versus predicted pavement life in coverages for the load of a single wheel of the C-5A aircraft.

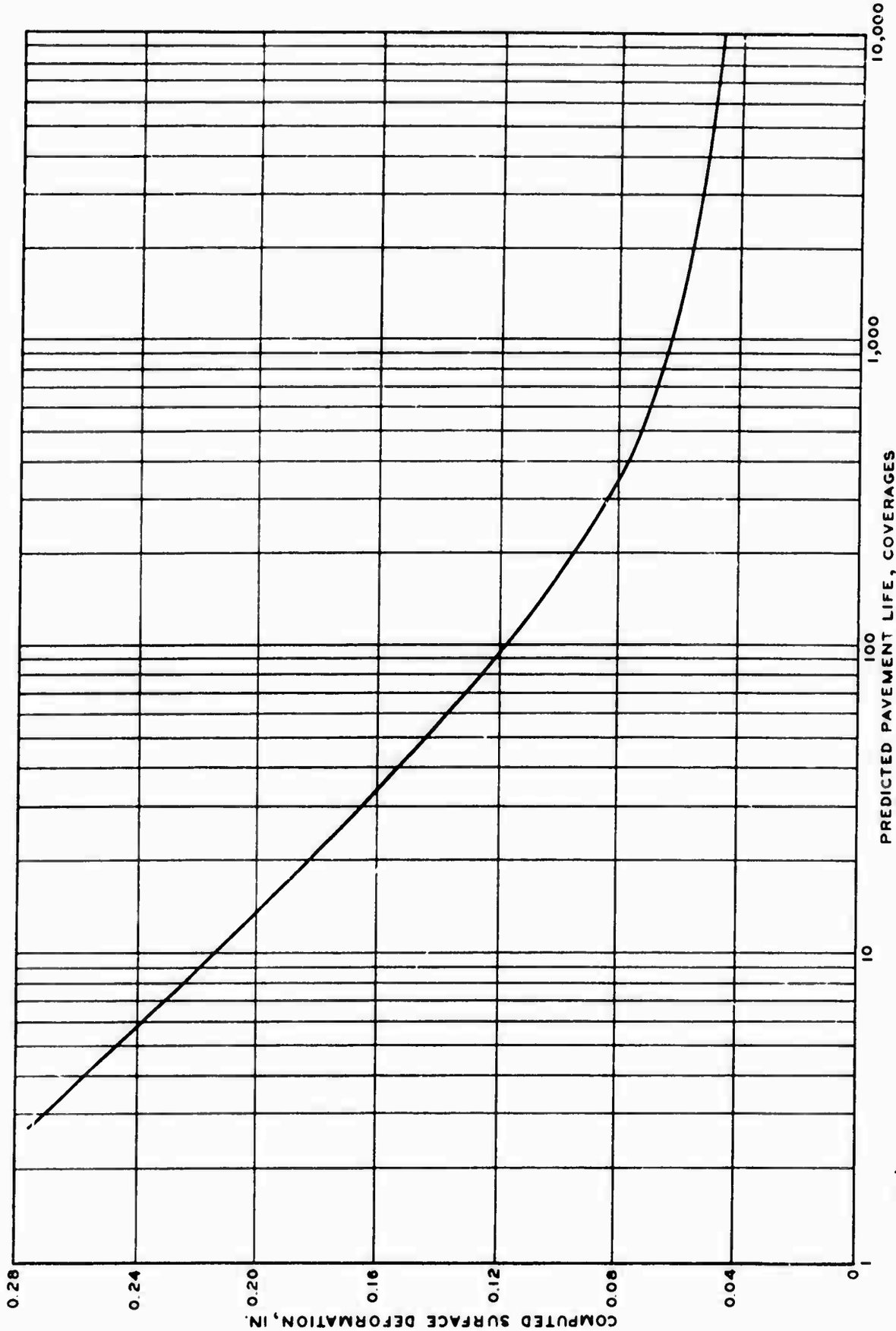

Figure II-4. Computed surface deformation versus predicted pavement life in coverages for the load of a single wheel of the C-5A aircraft.

Poisson's ratio for the subgrade may be assumed. For a saturated subgrade, Poisson's ratio would be approximately 0.5.

(3) Using the estimated section thickness and material properties, the surface deflection and vertical stress at the top of subgrade under the loading of a single wheel of the design aircraft assembly can then be computed by the layered elastic theory.

(4) The surface deformation can be related directly to pavement service life in terms of coverages using the correlation shown in figure II-4. The vertical stress at the top of the subgrade must be adjusted for the difference in the modulus value of the subgrade on which the correlation is based and the value of the subgrade modulus for the pavement being designed. The adjustment is made by multiplying the computed vertical stress times the following factor: $\frac{6000}{\text{actual subgrade modulus}}$. The adjusted vertical stress is then related to coverage through the correlation in figure II-3.

The lower of the two coverage levels will be the predicted life of the section being analyzed.

(5) If the predicted pavement life is not within the bounds of the desired life of the pavement system (or ±3%), then the thickness is adjusted and the process is repeated. The process may require several iterations to obtain a pavement thickness having a predicted service life within the bounds desired life of the pavement systems.

2. LIMITATIONS

In the design of pavement systems incorporating stabilized layers, the ratio of the tensile strength of the stabilized material to the tensile stress developed in the pavement systems is considered to be an important parameter influencing the performance of the pavement system. The procedure presented does not consider this parameter in the prediction of pavement life. This is

due to lack of correlation shown in the test data between the ratio of strength to stress and pavement performance. Even though no correlation can be given at this time, the ratio of the tensile strength to stress should be computed and compared to the plot shown in figure 60 of the main text.

It should also be noted that the foregoing procedure is based on somewhat limited test data. The principal test data considered were obtained from three different test pavements with approximately consistent subgrade strength (≈ 4 CBR), which were trafficked under two different loadings. Also, the design system uses the response of the pavement to a single wheel to predict pavement life under multiple-wheel traffic. This appears to work satisfactorily for the C-5A gear but has not been verified for other assemblies.

3. EXAMPLE DESIGN PROBLEM

a. Problem

The example problem is to determine the required thickness of a pavement having a cement-stabilized clay gravel base to sustain 5000 coverages of a B-52 aircraft. The surface material is 3 in. of asphaltic concrete. The material properties assumed in the example are shown in table II-1 and the aircraft assembly data in table II-2.

TABLE II-1

TYPICAL MATERIAL PROPERTIES

Description	Thickness in.	Rated CBR	Estimated Modulus psi	Estimated Poisson's Ratio
Asphaltic Concrete	3	-	50,000	0.5
Cement-Stabilized Clay Gravel	To be Determined	-	150,000	0.3
Soft Clay	144	3.3	5,000	0.5
Stiff Clay	144	6.7	10,000	0.5
Clay Shales	-	-	900,000	0.5

TABLE II-2

B-52 AIRCRAFT CHARACTERISTICS

Type Assembly	Twin - Twin
Assembly Load, kips	240
Tire Load, kips	60
Contact Area, $in.^2$	285
Contact Pressure, psi	210.53
Load Radius, in.	9.52

The material properties shown for the asphaltic concrete are what might be expected for a 3-in. surfacing for an airfield in a hot climate. The material properties for the stabilized material are representative for a cement-stabilized clay gravel.

b. Solution

The conventional design for this situation would specify approximately 68 in. of material above the subgrade. If an equivalency of 2 is assumed for the stabilized material, then the required thickness would be in order of 34 in. or more of pavement. Using this starting point, analyses of three initial sections were conducted utilizing the CHEVRON computer program. The subgrade stress and surface deformation were computed and related to coverages through the correlations shown in figures II-3 and II-4. The results from the analysis are given in table II-3.

TABLE II-3

DESIGN ANALYSIS - CHEVRON COMPUTER PROGRAM

Thickness Above Subgrade, in.	29	32	36
Stress at Top of Subgrade, psi	6.14	4.76	3.84
Adjusted Stress, psi	7.35	5.72	4.60
Coverages (From figure II-3)	1,800	5,000	10,000
Surface Deformation, in.	0.0669	0.0592	0.0539
Coverages (From figure II-4)	700	1,200	2,000

From the results of these analyses, it is seen that a much thicker pavement section would be required. To obtain a new estimate of the required thickness, the critical thicknesses were plotted against coverages as shown in figure II-5. The plot was projected to 5000 coverages and a new estimated thickness of 43 in. obtained.

Repeating the analysis for pavement thicknesses of 43 and 45 in., it was determined based on the surface deflection correlation that the pavement sections would sustain 4800 and 6000 coverages, respectively.

The tensile stress at the bottom of the stabilized material due to loading by one twin-twin assembly was estimated to be less than 45 psi for either of the two thicknesses. The estimate was made by superposition of the computed tangential stresses. Thus, the tensile strength is more than twice the developed tensile stress. From figure 60 of the main text, it can be seen that a strength to stress ratio of 2 would be more than adequate.

Based on the analysis, material thickness of 45 in. above the subgrade would provide the required pavement life. This design procedure then essentially substitutes 43 in. of cement-stabilized clay gravel for 65 in. of granular base and subbase material.

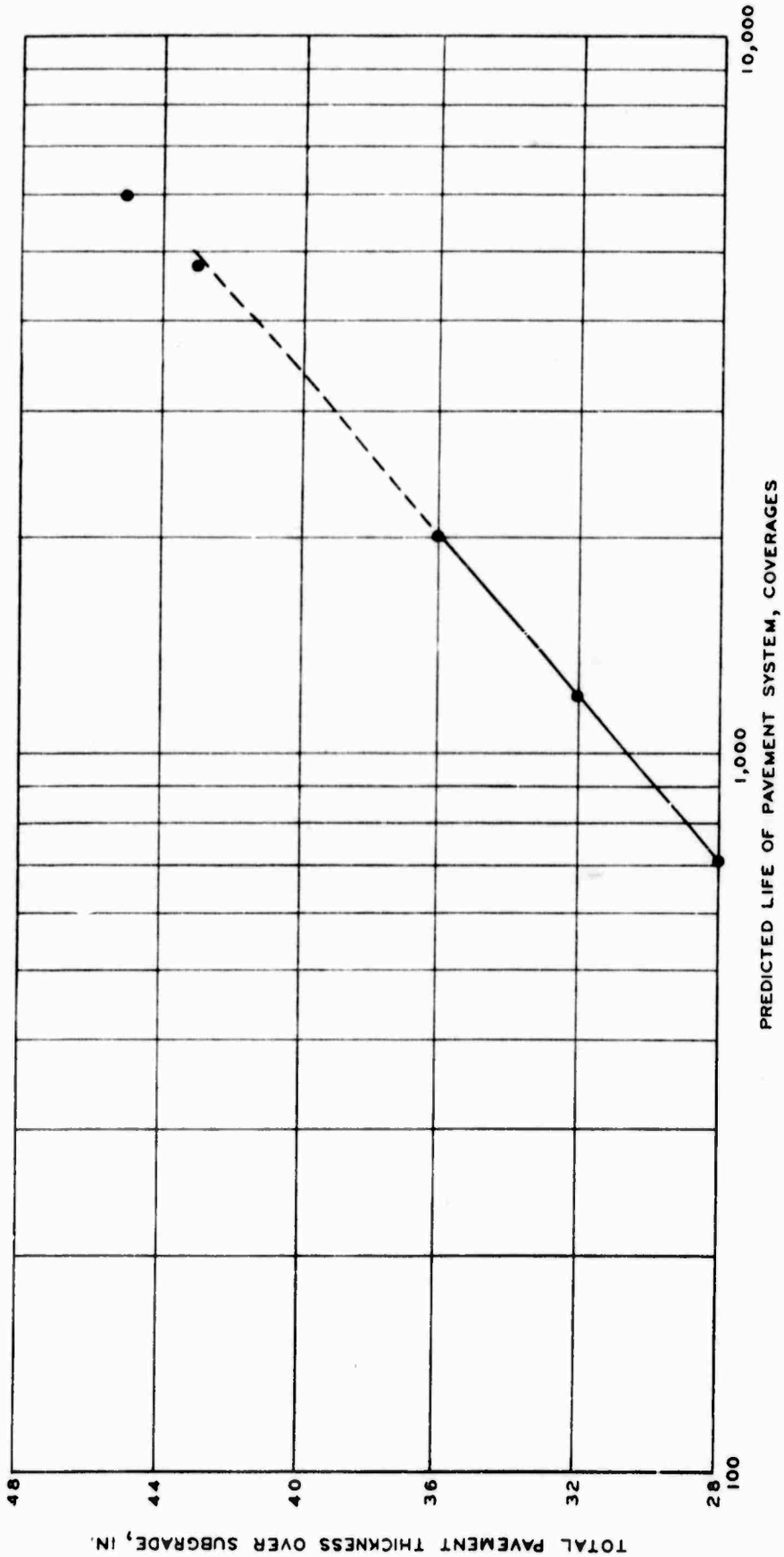

Figure II-5. Critical thicknesses determined by CHEVRON program versus coverages.

REFERENCES

1. Peutz, M. G. F.; Jones, A.; van Kempten, H. P.; Layered Systems Under Normal Surface Loads, Computer Program, Koninklijke/Shell Laboratorium, Amsterdam, Holland.

2. Michelow, J.; Analysis of Stresses and Displacements in an N-Layered Elastic System Under a Load Uniformly Distributed on a Circular Area, Computer Program, California Research Corporation, Richmond, Calif., September 1963.

3. Ahlvin, R. G., et al.; Multiple-Wheel Heavy Gear Load Pavement Tests, Vol I-IV, Technical Report S-71-17, U. S. Army Engineer Waterways Experiment Station, CE, Vicksburg, Miss., November 1971.

4. Burns, C. D.; Ledbetter, R. H.; Grau, R. W.; Study of Behavior of Bituminous-Stabilized Layers, Miscellaneous Paper (in publication), U. S. Army Engineer Waterways Experiment Station, CE, Vicksburg, Miss.

5. Grau, R. W.; Evaluation of Structural Layers in Flexible Pavement, Miscellaneous Paper (in publication), U. S. Army Engineer Waterways Experiment Station, CE, Vicksburg, Miss.

6. Department of the Army, CE, Office, Chief of Engineers; Guide Specifications for Military Construction, Bituminous Binder and Surface Courses for Airfields, Heliports, and Tank Roads (Central-Plant Hot-Mix), CE-807.22, Washington, D. C., October 1959.

7. Department of the Army, CE, Office, Chief of Engineers; Guide Specifications for Military Construction, Graded-Crushed Aggregate Base Course, CE-807.07, Washington, D. C., January 1969.

8. Department of the Army, CE, Office, Chief of Engineers; Guide Specifications for Military Construction, Subbase Course, CE-807.02, Washington, D. C., January 1968.

9. Wilson, E. L.; "Structural Analysis of Axi-Symmetric Solids," Journal of the American Institute of Aeronautics, December 1965.

10. Pichumani, R.; Theoretical Analysis of Airfield Pavement Structures, Technical Report AFWL-TR-71-26, Air Force Weapons Laboratory, Kirtland Air Force Base, N. Mex., July 1971.

11. Izatt, J. O.; Lettier, J. A.; Taylor, C. A.; The Shell Group Methods for Thickness Design of Asphalt Pavement, Shell Oil Company, January 1968.

12. Edwards, J. M.; Valkering, C. P.; Structural Design of Asphalt Pavements for Heavy Aircraft, Shell International Petroleum Company Limited, London.

13. Kasianchuk, D. A.; Fatigue Considerations in the Design of Asphalt Concrete Pavements, PhD Dissertation, University of California, 1968.

14. Hicks, R. G.; Factors Influencing the Resilient Properties of Granular Materials, PhD Dissertation, University of California, 1970.

15. Monismith, C. L.; Epps, J. A.; Kasianchuk, D. A.; Asphalt Mixture Behavior in Repeated Flexure, Report No. TE 68-8 to the Materials and Research Department, Division of Highways, State of California, 1969.

16. Dunlap, W. A.; A Report on a Mathematical Model Describing the Deformation Characteristics of Granular Materials, TR Report No. 1, Project 2-8-62-27, Texas Highway Department.

17. Duncan, J. M.; Monismith, C. L.; Wilson, E. L., Finite Element Analyses of Pavements, Highway Research Record No. 228, pp. 18-33, 1968.

18. Epps, J. A.; Influence of Mixture Variables on the Flexural Fatigue and Tensile Properties of Asphalt Concrete, PhD Dissertation, University of California, 1968.

19. Hudson, W. R.; Kennedy, T. W.; An Indirect Tensile Test for Stabilized Materials, Research Report 98-1, Center for Highway Research, University of Texas, Austin, Texas, January 1968.

20. Hadley, W. O.; Hudson, W. R.; Kennedy, T. W.; An Evaluation of Factors Affecting the Tensile Properties of Asphalt-Treated Materials, Research Report 98-2, Center For Highway Research, University of Texas, Austin Texas, March 1969.

21. Hondros, G., "The Evaluation of Poisson's Ratio and the Modulus of Materials of a Low Tensile Resistance by the Brazilian (Indirect Tensile) Test with Particular Reference to Concrete," Australian Journal of Applied Science, Vol. 10, No. 3, p. 243, September 1959.

22. Wang, M. C.; Mitchell, J. K.; Monismith, C. L.; Behavior of Stabilized Soils Under Repeated Loading, Contract Report No. 3-145, Report No. 4, U. S. Army Engineer Waterways Experiment Station, CE, Vicksburg, Miss., 1970.

23. Heukelom, W.; Foster, C. R.; "Dynamic Testing of Pavements," Journal of Soil Mechanics and Foundations Division, ASCE, 1960.

24. Peattie, K. P.; "A Fundamental Approach to the Design of Flexible Pavements," Conference Proceedings, Structural Design of Asphalt Pavements, University of Michigan, 1962.

25. Mitchell, J. K.; Chih-Kang Shen; Monismith, C. L.; Behavior of Stabilized Soils Under Repeated Loading, Contract Report No. 3-145, Report No. 1, U. S. Army Engineer Waterways Experiment Station, CE, Vicksburg, Miss., 1965.

26. Hadala, P. F.; Dynamic Bearing Capacity of Soils, Report 4 - Investigation of a Dimensionless Load-Displacement Relation for Footings on Clay, Technical Report 3-599, U. S. Army Engineer Waterways Experiment Station, CE, Vicksburg, Miss., June 1965.

27. Witczak, M. W.; Design of Full-Depth Asphalt Pavements, to be presented at the Third International Conference on the Structural Design of Asphalt Pavements, London, England, September 1972.

28. U. S. Naval Civil Engineering Laboratory; Rational Pavement Evaluation - Review of Present Technology, AFWL-TR-69-9, Air Force Weapons Laboratory, Kirtland AFB, N. Mex., October 1969.

29. Palmerton, J. B.; "Application of Three-Dimensional Finite Element Analysis," Proceedings of Symposium on Application of the Finite Elements Method in Geotechnical Engineering, held at the U. S. Army Engineer Waterways Experiment Station, CE, Vicksburg, Miss., 1-4 May 1972.